

Some pages of this thesis may have been removed for copyright restrictions.

If you have discovered material in Aston Research Explorer which is unlawful e.g. breaches copyright, (either yours or that of a third party) or any other law, including but not limited to those relating to patent, trademark, confidentiality, data protection, obscenity, defamation, libel, then please read our [Takedown policy](#) and contact the service immediately (openaccess@aston.ac.uk)

MODELLING AND CONTROL OF A
HYBRID STEPPING MOTOR

GRAHAM RICHARD BARBER B.Sc.

SUBMITTED FOR THE DEGREE OF
DOCTOR OF PHILOSOPHY

THE UNIVERSITY OF ASTON IN BIRMINGHAM
DEPARTMENT OF ELECTRICAL AND ELECTRONIC ENGINEERING

DECEMBER 1980

MODELLING AND CONTROL OF A HYBRID STEPPING MOTOR

Graham Richard Barber

Doctor of Philosophy 1980

Summary

The integration of a microprocessor and a medium power stepper motor in one control system brings together two quite different disciplines. Various methods of interfacing are examined and the problems involved in both hardware and software manipulation are investigated. Microprocessor open-loop control of the stepper motor is considered. The possible advantages of microprocessor closed-loop control are examined and the development of a system is detailed. The system uses position feedback to initiate each motor step. Results of the dynamic response of the system are presented and its performance discussed.

Applications of the static torque characteristic of the stepper motor are considered followed by a review of methods of predicting the characteristic. This shows that accurate results are possible only when the effects of magnetic saturation are avoided or when the machine is available for magnetic circuit tests to be carried out. A new method of predicting the static torque characteristic is explained in detail. The method described uses the machine geometry and the magnetic characteristics of the iron types used in the machine. From this information the permeance of each iron component of the machine is calculated and by using the equivalent magnetic circuit of the machine, the total torque produced is predicted.

It is shown how this new method is implemented on a digital computer and how the model may be used to investigate further aspects of the stepper motor in addition to the static torque.

Indexing Terms

MODELLING, STEPPING MOTORS, TORQUE,
MICROPROCESSOR CONTROL, REAL TIME SYSTEMS.

LIST OF CONTENTS

	PAGE
1. INTRODUCTION	
1.1 STEPPING MOTORS	1
1.2 DRIVE CIRCUIT	5
1.3 MICROPROCESSOR CONTROL	9
1.4 STATIC TORQUE CHARACTERISTIC	10
2. MICROPROCESSOR CONTROL	
2.1 INTRODUCTION	12
2.2 POSSIBLE METHODS OF DRIVING THE STEPPER MOTOR	
2.2.1 INTRODUCTION	14
2.2.2 MICROSTEPPING	15
2.2.3 MICROPROCESSOR CONTROLLERS	17
2.2.4 CONCLUSIONS	23
2.3 RECORDING POSITION INFORMATION	23
2.4 ASPECTS OF MICROPROCESSOR TECHNOLOGY RELEVANT TO STEPPER MOTOR CONTROL	27
2.5 OPEN-LOOP CONTROL	
2.5.1 INTRODUCTION	29
2.5.2 HARDWARE DESIGN	31
2.5.3 SOFTWARE DESIGN	32
2.5.4 RESULTS	41
2.5.5 CONCLUSIONS	45
2.6 CLOSED-LOOP CONTROL	
2.6.1 INTRODUCTION	46
2.6.2 INPUT OF POSITION DATA	47
2.6.3 BOOK KEEPING CLOSED-LOOP CONTROL	54
2.6.4 CLOSED-LOOP STEP CONTROL	56

	PAGE
2.6.5 RESULTS	58
2.6.6 CONCLUSIONS	63
2.7 CONCLUSIONS	64
3. STATIC TORQUE DISPLACEMENT CHARACTERISTIC	
3.1 INTRODUCTION	66
3.2 METHODS OF PREDICTING THE STATIC TORQUE CHARACTERISTIC	
3.2.1 INTRODUCTION	70
3.2.2 METHODS NEGLECTING MAGNETIC SATURATION	71
3.2.3 METHODS WHICH CONSIDER MAGNETIC SATURATION	76
3.3 THE EQUIVALENT MAGNETIC CIRCUIT OF THE MOTOR	
3.3.1 INTRODUCTION	79
3.3.2 PERMEANCE OF THE AIR GAP	85
3.3.3 PERMEANCE OF THE IRON COMPONENTS	95
3.3.4 COMPARISON OF SINGLE PHASE AND DOUBLE PHASE EXCITATION	103
3.3.5 CONCLUSIONS	103
3.4 PREDICTION OF THE STATIC TORQUE DISPLACEMENT CHARACTERISTIC	
3.4.1 DEVELOPMENT OF THE TORQUE EQUATION	105
3.4.2 DEVELOPMENT OF THE ALGORITHM	107
3.4.3 THE STATIC TORQUE PROGRAMME	112
3.4.4 RESULTS OF THE STATIC TORQUE PROGRAMME	116
3.5 DISCUSSION	
3.5.1 SIMPLIFICATION OF THE MODEL	125
3.5.2 EXTENSIONS TO THE USE OF THE MODEL	130

	PAGE
3.5.3 THE DYNAMIC TORQUE CHARACTERISTIC	137
3.5.4 SINGLE STEP RESPONSE	141
3.6 CONCLUSION	145
APPENDIX	147
REFERENCES	150

LIST OF TABLES

		PAGE
TABLE	2.1 Winding excitation for 2 phase clockwise rotation	14
	2.2 Winding excitation for 2 phase anticlockwise rotation	15
	2.3 Winding excitation for half step mode clockwise rotation.	16
	2.4 Step rate from register value	40
	2.5 Single step response natural frequencies	42
	3.1 Normalised tooth permeance coefficients	91
	3.2 Pole permeance coefficients	94
	3.3 Rotor flux path dimensions	125
	3.4 Permeance coefficients for saturated tooth profiles	129
	3.5 Permeance coefficients for alternative stator design	134
	3.6 Two phase single step response time current and position.	139

LIST OF ILLUSTRATIONS

FIGURE		PAGE
1.1	Chopped Voltage Waveforms	7
1.2	Bilevel Voltage Waveforms	8
1.3	Full Bridge Switching Circuit	9
2.1	The Minimum Hardware M.P.U. System of Step Motor Control	18
2.2	The System with the Sequence Generator Implemented in Hardware	18
2.3	Motor Control System with External Count and Rate Registers	22
2.4	Incremented Encoder Output	24
2.5	Reading Digital Encoder by Time Increments	26
2.6	Reading Digital Encoder by Position Increments	26
2.7	Programme: Continuous Stepping	33
2.8	Flow Diagram of Continuous Stepping Programme	34
2.9	Programme: Real Time Clock Service Routine	37
2.10	Programme: External Register Service Routine	39
2.11	Curve of Step Rate Against Register Value	40
2.12	Single Step Response at Various Currents	43
2.13	Multistep Response Open Loop at 44 s.p.s.	44
2.14	Multistep Response Open Loop at 94 s.p.s.	44
2.15	Algorithm for Gray to Binary Conversion	50
2.16	Programme: Gray to Binary Conversion	51
2.17	Hardware Gray to Binary Conversion	52
2.18	Programme: Read Position Via Hardware Decoder	54
2.19	Flow Diagram of Bookkeeping Closed-Loop Control	55
2.20	Dynamic Response 1 Ampere	59
2.21	Dynamic Response 5 Ampere	60

FIGURE		PAGE
2.22	Dynamic Response Various Currents	61
2.23	Loaded and Unloaded Response 1.5 Ampere	61
2.24	Loaded and Unloaded Response 5 Ampere	62
2.25	Comparison of Step Rates	62
3.1	Typical Static Torque Characteristic and its Approximations	67
3.2	One Stepping Cycle	68
3.3	Torque Characteristic for 3A Two Phase using Justice's Model	77
3.4	Torque Characteristic for 7A Two Phase using Justice's Model	77
3.5	H.D. Chai's Approximation to a Hyperbolic Tangent	78
3.6	The Construction of the Hybrid Vernier Stepper Motor	80
3.7	The Sixteen Limb Equivalent Magnetic Circuit	82
3.8	The Eight Limb Equivalent Magnetic Circuit	83
3.9	Permeance Against Angle Characteristic	88
3.10	Rectangular Approximation to Tooth Profile	89
3.11	Semi-Circular Approximation to Tooth Profile	92
3.12	Air Gap Profile for One Pole	92
3.13	B-H Curve for Both Stator and Rotor Iron Types	97
3.14	Permeance-Flux Characteristic for the Stator Components	98
3.15	Permeance-Flux Characteristic for the Rotor Components	98
3.16	Extreme Permeance-Flux Characteristics for Rotor Components.	99

FIGURE		PAGE
3.17	Demagnetisation Curve for Alcomax III	101
3.18	Permeance-Flux Characteristic for the Permanent Magnet	102
3.19	Flux Path for Two Phase Excitation	104
3.20	Flux Path for Single Phase Excitation	104
3.21	Series to Parallel Conversion for One Limb	108
3.22	Eight Parallel Limb Equivalent Magnetic Circuit	109
3.23	Summed Parallel Limb Equivalent Magnetic Circuit	109
3.24	Series Equivalent Magnetic Circuit	110
3.25	Flow Diagram of the Static Torque Programme	115
3.26	Static Torque Characteristic Prediction 2 Phase 0.5A	118
3.27	Static Torque Characteristic Prediction 2 Phase 1.0A	118
3.28	Static Torque Characteristic Prediction 2 Phase 3.0A	119
3.29	Static Torque Characteristic Prediction 2 Phase 6.0A	119
3.30	Static Torque Characteristic Prediction 2 Phase 7.0A	120
3.31	Holding Torque Characteristic for 2 Phase Excitation	121
3.32	Static Torque Characteristic Prediction Single Phase 0.5A	122
3.33	Static Torque Characteristic Prediction Single Phase 3.0A	122
3.34	Static Torque Characteristic Prediction Single Phase 7.0A	123

FIGURE	PAGE
3.35 Holding Torque Characteristic for Single Phase Excitation	123
3.36 Static Torque Characteristic Prediction 2 Phase 3A using Extreme Values of Rotor Permeance	124
3.37 Static Torque Characteristic Prediction 2 Phase 7A using Extreme Values of Rotor Permeance .	124
3.38 Simplified Equivalent Magnetic Circuit using Pa to Represent all the Non-linear Permeances	127
3.39 Approximation of Magnetic Saturation by Varying Tooth Profile	129
3.40 Static Torque Characteristic Prediction 2 Phase 3A using Tooth Profiles 1 and 3.	131
3.41 Static Torque Characteristic Prediction 2 Phase 7A using Tooth Profiles 1 and 3	131
3.42 Variation of Flux over One Cycle	133
3.43 Static Torque Characteristic Prediction 2 Phase 3A for Alternative Pole Design	135
3.44 Static Torque Characteristic Prediction 2 Phase 7A for Alternative Pole Design	135
3.45 Static Torque Characteristic Prediction 2 Phase 3A using Air Gap Permeances Calculated by the Straight-Line-Arc and Conformal Transformation Methods	136
3.46 Static Torque Characteristic Prediction 2 Phase 7A using Air Gap Permeances Calculated by the Straight-Line-Arc and Conformal Transformation Methods	136
3.47 Two Phase, Single Step Time Current Curve	138

FIGURE		PAGE
3.48	Two Phase, 6A Single Step Response	138
3.49	The Dynamic Torque Characteristic	140
3.50	Single Phase, 6A Single Step Response	143
3.51	Control System Representation of the Stepper Motor	144

ACKNOWLEDGEMENTS

I would like to thank Dr. R. C. Johnson for his guidance and assistance throughout the project and Dr. M. Justice for discussion and data supplied. I would also like to acknowledge the technical support given by Mr. W. Harper and his staff.

Financial support was given by The U.K. Science Research Council and the Alfred Herbert Machine Tool Company.

CHAPTER ONE

INTRODUCTION

1.1 STEPPING MOTORS

A stepping motor, as its name suggests, is an incremental device, which in common with other motors may be a linear or rotory machine for converting power into a controllable form of motion. The stepper motor is excited by a series of applied voltages or currents. Each change of state in the sequence produces an increment of position. At each increment the motor is latched, either mechanically or magnetically and under normal operating conditions each change of state of the applied voltage or current produces one and only one increment of position. When this condition is not true the motor is said to be "out of synchronism". Most stepping motors can operate in a bidirectional manner by altering the input sequence.

The basic groups of stepping devices are:-

1. Solenoid and Ratchet
2. Electro Mechanical
3. Variable Reluctance (V.R.)
4. Permanent Magnet (P.M.)
5. Hybrid (combining V.R. and P.M.)

It is the latter three of these which are of interest in this work. V.R. motors are usually 3 phase machines and may consist of one or more stacks. Step sizes are in the

order of 15 degrees and hence they are used for large distance movement where good acceleration is required. P.M. motors generally produce greater torque than V.R. motors but have more inertia associated with their own rotors. Their main feature is the magnet mounted radially on the rotor. Hybrid motors use a permanent magnet mounted axially on the rotor and are usually of the Vernier type, having many teeth on the rotor in order to reduce step size to less than 2 degrees. These motors are used where precise position stepping is required.

The machine used as the basis for the work presented in this thesis is of the hybrid type and is described in detail in subsequent chapters. However many of the conclusions discussed may be equally applied to other types of stepper motors, particularly the V.R. and P.M. types.

One of the first uses of stepping motors was by the Royal Navy in the 1930's. However, as a position control device, stepper motors were not as fast or as accurate as d.c. servo systems. It was as a result of the 1960s 'Digital Electronics Revolution' that stepper motors began to substantially improve in performance. By this time d.c. servos were well developed and had acquired the confidence of industry. Therefore it was mainly the new techniques which employed stepper motors rather than replacing the conventional control systems. With present day technology stepper motor systems are to be found in many small and medium power applications. Paper tape readers, Man-made

satellites, electronic typewriters and copying machines are just a few examples.

Stepper motor systems have many advantages over the d.c. servos and conventional motor systems, a few are listed below, followed by some of the less attractive features.

ADVANTAGES

1. Stepper motors may be used as open-loop devices.
2. The motor may be held stationary with considerable holding torque.
3. The stepper motor is essentially a digital machine and hence readily interfaces to digital electronic circuits.
4. Stalling the stepper motor does not result in dangerous over currents.
5. Stepper motors are bidirectional.
6. Stepper motors provide rapid acceleration.
7. Stepper motors may be used in speed or position control systems.
8. The motor has no position drift when stationary.
9. There is no accumulative error associated with the stepper motor, it may therefore be used for position control over many revolutions.

DISADVANTAGES

1. Maximum start and stop rates are below the true maximum speed.
2. The size of the step increment is fixed.
3. Stepper motors have low efficiency.
4. Each step has overshoot associated with it.
5. Large inertia loads cause problems with stepping.
6. Good control requires complex control circuits.

As a general introduction to the subject, the five opening papers of the Conference on Stepping Motors and Systems (Leeds 1974) give a comprehensive explanation of the operation of stepper motors.

In the first paper Morreale and Irani⁽¹⁾ explore most of the known variations of step motors with explanations of their operation. Kent⁽²⁾ in the second paper studies in detail the variable reluctance stepper motor and Nijdam and King⁽³⁾ explain the permanent magnet type of motor. In the fourth paper Kordik and Senica⁽⁴⁾ make a more practical assessment of the application and selection of step motors. Finally Spracklan⁽⁵⁾ attempts to standardise the terminology and test data for step motors. However this last paper should be considered in conjunction with Biscoe and Mills's paper⁽⁶⁾ on the same subject.

One point which may cause some confusion is the manner in which the term 'pulse' is freely used by many authors. An electrical pulse applied to a solenoid and ratchet device has a well defined response, in that the solenoid will activate and then deactivate at the end of the pulse. The response however, when an electrical pulse is applied directly to a rotary stepper motor, depends upon its state and the polarity of the applied pulse. Applying pulses directly to the motor is not the normal method of operation but instead pulses are applied to some form of sequencing device, which in turn applies known continuous currents to the appropriate windings of the motor.

1.2 DRIVE CIRCUIT

The overall performance of a stepping motor system is influenced, to a considerable extent, by the type of drive circuit employed to control the applied voltages. Almost all drive circuits used today consist of only solid state devices, most using transistors to control the motor current, although thyristor types are used for extremely high currents.

It was not the object of this work to investigate or evaluate any particular type of drive circuit, but it should be noted that rapid development in electronic technology is resulting in many improvements in this field. However, because the drive circuit must be regarded as an integral part of any stepper motor control system, an understanding of drive circuit techniques is required in order to evaluate control circuit performances.

The ideal drive circuit would supply a switchable or reversible constant direct current, with instantaneous switching. However the inductance of the windings makes this impractical, if not impossible to achieve. One method used to reduce the time constant of the circuit is to increase the applied voltage and insert a resistance in series with the field winding to limit the current to the required value. The power loss in this resistance makes this an inefficient method of improving motor performance.

Chopped high voltage supplies have been used as motor drives, the mark space ratio of the chopped waveform determines the average current supplied. Figure 1.1 shows the resulting waveforms of such a system. There is some danger that the oscillatory effect of the current would cause instability in the stepper motor, possibly at the systems natural frequency.

The type of drive circuit used for the work described in this thesis was of the bilevel voltage type. This system employs the higher voltage only during current switching; once the current has attained its required value it is maintained by a lower constant voltage. Waveforms of the current and voltage are shown in Figure 1.2. Although the machine used had 2 bifilar windings, enabling flux reversal to be achieved without current reversal, a system was preferred which employed a full bridge switching circuit, as shown in Figure 1.3. This enabled the current in the windings to be reversed using the transistors as switching elements.

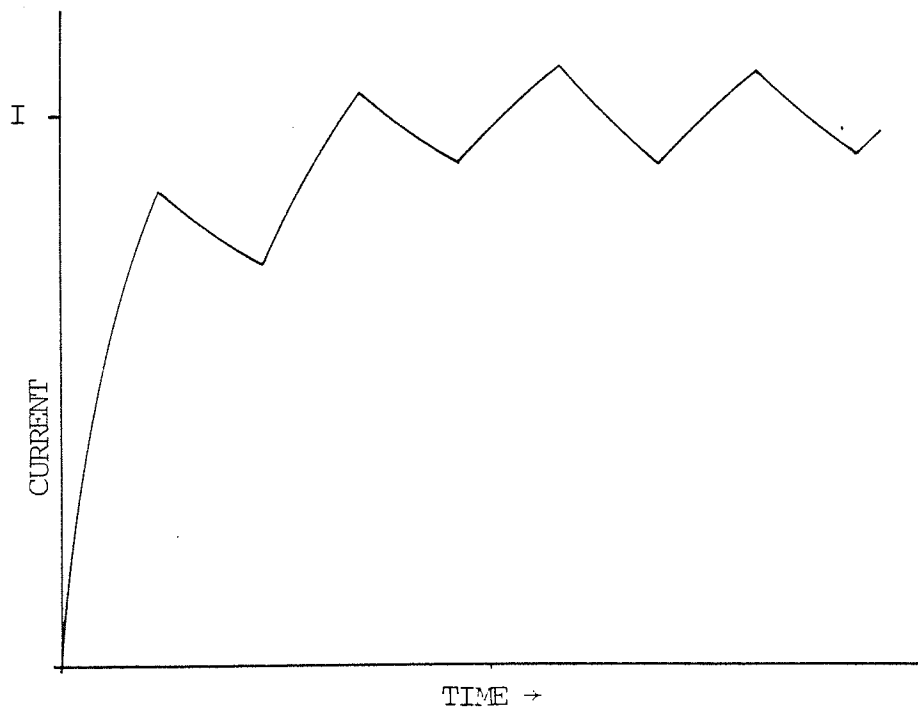
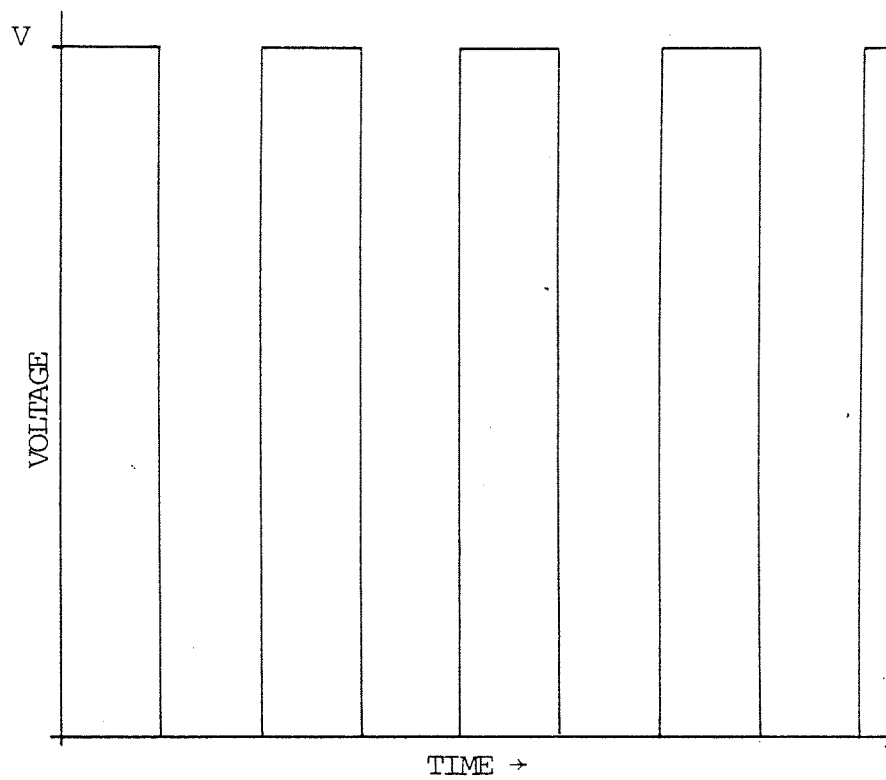


FIGURE 1.1 CHOPPED VOLTAGE WAVEFORMS

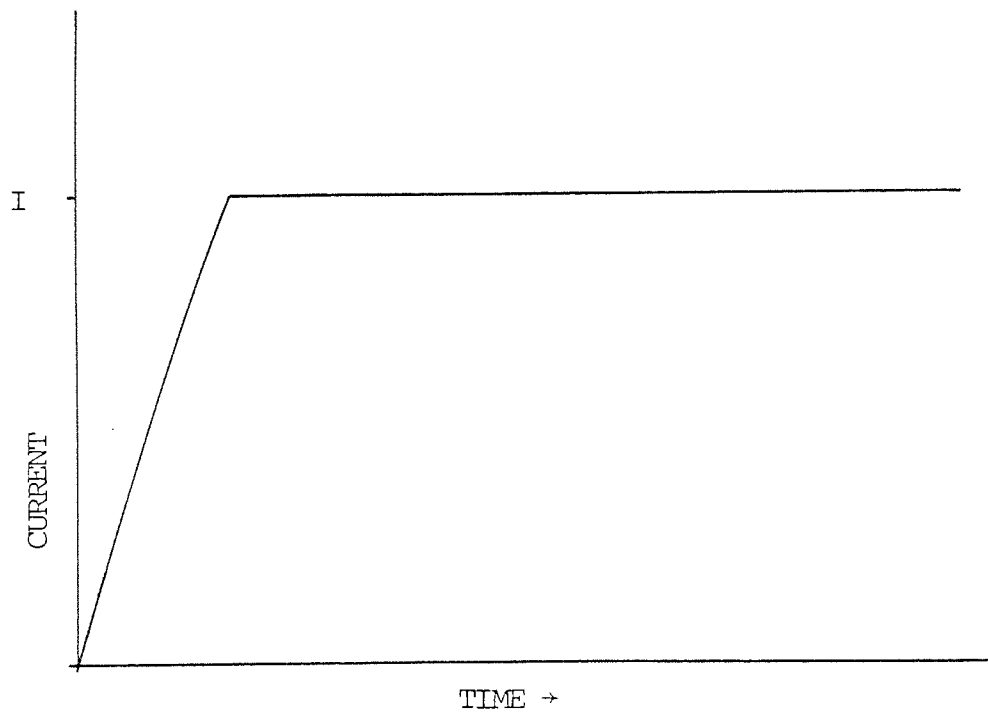
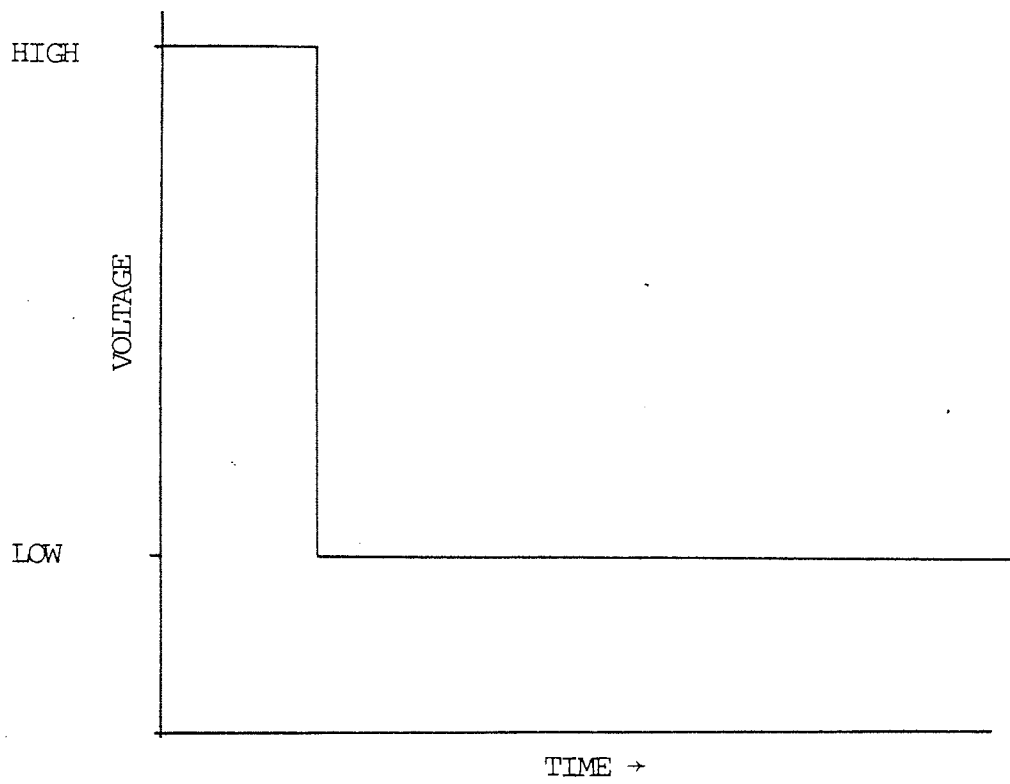


FIGURE 1.2 BILEVEL VOLTAGE WAVEFORMS

The manner in which the control is implemented is very much a function of the application for which the motor is intended, both open-loop and closed-loop control being possible. Chapter 2 of this thesis covers the study of methods and techniques which must be understood to enable a microprocessor control system to be designed. A study of both open-loop and closed-loop control is made in detail highlighting problems that were encountered during the development of the system. Position feedback with resolution of a fraction of a motor step is used in order to control step demands on the motor, which results in an improvement of dynamic response. Although the study was restricted to the use of only one type of microprocessor, most of the development techniques discussed could be applied to other types of system.

1.4 STATIC TORQUE CHARACTERISTIC

In 1974 Hughes et al.⁽⁷⁾ stated that the prediction of step motor performance does not present substantial difficulty! This statement is later qualified by adding that the assumption is made that "starting information for the calculation consists of measured data. This data might relate to torque/displacement curves....". In fact several authors have made accurate predictions of dynamic response for stepper motors, but each has taken some form of data measurement from a machine. In more recent years methods of true prediction (without the need to have a machine

available) have been explored. Most of these predictions have involved the assumption that the static torque characteristic may be simplified to a convenient curve. This approximation results in the accuracy of the dynamic prediction being reduced and the time period over which the prediction holds being limited. The accurate prediction of the static torque characteristic is also useful during the design of machines.

The work covered in Chapter 3 demonstrates the techniques used to accurately predict the static torque characteristic. The method used is based on the analysis of the magnetic circuit, thus providing a relatively simple approach in which the non-linearities of magnetic saturation may be included.

CHAPTER TWO

MICROPROCESSOR CONTROL

2.1 INTRODUCTION

The application of digital computers in the control of stepper motors is a field of research which has recently attracted much interest. It is the recent developments in digital techniques which has spurred along the development of such systems. However, the rapid development has tended to remain with motors which are comparatively smaller in size, such as paper tape readers, printer heads and electronic typewriters. It would appear that the medium and large size stepper motors have been seriously neglected and one can only postulate the following reasons for this:

Small stepper motors have drive circuits which require only one or two transistors and use power in the order of a few watts; whereas even medium sized steppers require in the order of 100 watts of power. The combination of digital electronics and medium power drives for stepper motors involves two quite different aspects of electrical engineering. In industrial applications the combination of expertise in those two different fields is not often found. Machine tools, traction engineering and heavy power control are industries using such combinations of technology.

One of the characteristics of medium and large stepper motors is the rapid change in current required to produce a good step response. Not only does this require high

voltages to be applied to the motor but may also result in large voltages being induced in circuitry involved with its control. Such voltage spikes can easily cause malfunction, or at the worst, breakdown of low voltage micro-electronic circuits.

Finally, it must be noted that many industrial applications where stepper motors should be applied are satisfied by digitally controlled d.c. servo motors. There are many d.c. servo systems available which do not require financial investment for further development . With such availability and adaptability, investment in new designs of stepper motor systems is uneconomic to the user.

The digital computer control of stepper motors can be split into three classifications.

- | | |
|-----------------------------|---------------------------------------|
| 1. OPEN-LOOP | No position feedback |
| 2. BOOK KEEPING CLOSED-LOOP | Position feedback of whole steps. |
| 3. STEP CONTROL CLOSED-LOOP | Position feedback during Single steps |

The object of building a microprocessor based stepper motor control system was to improve the response of the motor by the application of position feedback. Before this objective could be achieved many aspects of interaction between the microprocessor and the stepper motor had to be investigated.

2.2 POSSIBLE METHODS OF DRIVING THE STEPPER MOTOR

2.2.1 INTRODUCTION

The stepper motor used for the investigation had two field windings, each bifilar wound and for the correct stepping of the motor these windings had to be energised in a certain sequence. Table 2.1 shows the sequence for clockwise rotation with both phases excited and Table 2.2 shows the sequence for anti-clockwise rotation.

STEP	CURRENT DIRECTIONS	
	WINDING A	WINDING B
0	FORWARD	FORWARD
1	REVERSE	FORWARD
2	REVERSE	REVERSE
3	FORWARD	REVERSE
4	FORWARD	FORWARD

TABLE 2.1

WINDING EXCITATION FOR 2 PHASE CLOCKWISE ROTATION

Similar Tables to 2.1 and 2.2 may be drawn up showing the sequence of operation for single phase excitation.

STEP	CURRENT DIRECTION	
	WINDING A	WINDING B
0	FORWARD	FORWARD
1	FORWARD	REVERSE
2	REVERSE	REVERSE
3	REVERSE	FORWARD
4	FORWARD	FORWARD

TABLE 2.2

WINDING EXCITATION FOR 2 PHASE ANTICLOCKWISE ROTATION

2.2.2.1 MICROSTEPPING

In normal single stepping of the motor each winding current is either ON FORWARD; OFF; or ON REVERSED. The position which the rotor takes, when the windings are energised is different for each state. By using both the two phase and single phase excitation sequences, positions may be obtained which are half way between normal steps; this is the "Half Stepping Mode". When two phases are energised the torque produced is considerably more than when only one phase is energised, therefore to keep the torque for each half step constant, the currents used for two phase excitation must be reduced. Table 2.3 shows the sequence of excitation for half stepping.

The proportion of the current which is used during two phase excitation to produce an even torque at each half step

STEP	CURRENT DIRECTION	
	WINDING A	WINDING B
0	PART FORWARDS	PART FORWARDS
1	OFF	FULL FORWARDS
2	PART REVERSE	PART FORWARDS
3	FULL REVERSE	OFF
4	PART REVERSE	PART REVERSE
5	OFF	FULL REVERSE
6	PART FORWARDS	PART REVERSE
7	FULL FORWARDS	OFF
8	PART FORWARDS	PART FORWARDS

TABLE 2.3

WINDING EXCITATION FOR HALF STEP MODE CLOCKWISE ROTATION

may be found from the static torque characteristic of the machine.

The idea of half stepping may be carried further so that, say, between step 1 and step 2 another state could exist where winding A has a smaller reverse current and winding B has a greater forward current. This is known as MICROSTEPPING the motor. Taken to its limit the microstepping currents become sinusoidal and the motor runs as a synchronous induction machine.

For stepping in the microstepping mode a current which increases and decreases in discrete steps is required. Such arrangements can be made by using digital electronics combined

with a digital to analogue converter. Setting the two currents to appropriate values to keep the resulting torque even would require complex logic and to go from one micro-step position to another, omitting intermediate steps, would require intricate timing circuits. The complex logic required for microstepping can easily be achieved by the use of a microprocessor.

2.2.3 MICROPROCESSOR CONTROLLER

One of the main advantages of microprocessor control is that many of the variable functions may be programmed in the software of the system so that alterations to the functions may be made easily. It would therefore seem desirable to reduce the hardware of the system as much as possible. The minimum hardware system for controlling the stepper motor is shown in Figure 2.1. In this system complete control is given to the microprocessor. It must calculate the current which is required to flow in each field winding at any instant in time. Such a system would be capable of microstepping the motor and the only interfacing hardware required between the microprocessor and the stepper motor drive circuit is the digital to analogue circuitry to control the currents. A more simple, but less versatile adaptation of this system is obtained if the digital to analogue converters are replaced with current changeover devices so that the direction of a pre-set current could be controlled and the motor could be stepped on full steps only.

The main disadvantage of systems such as these, is the

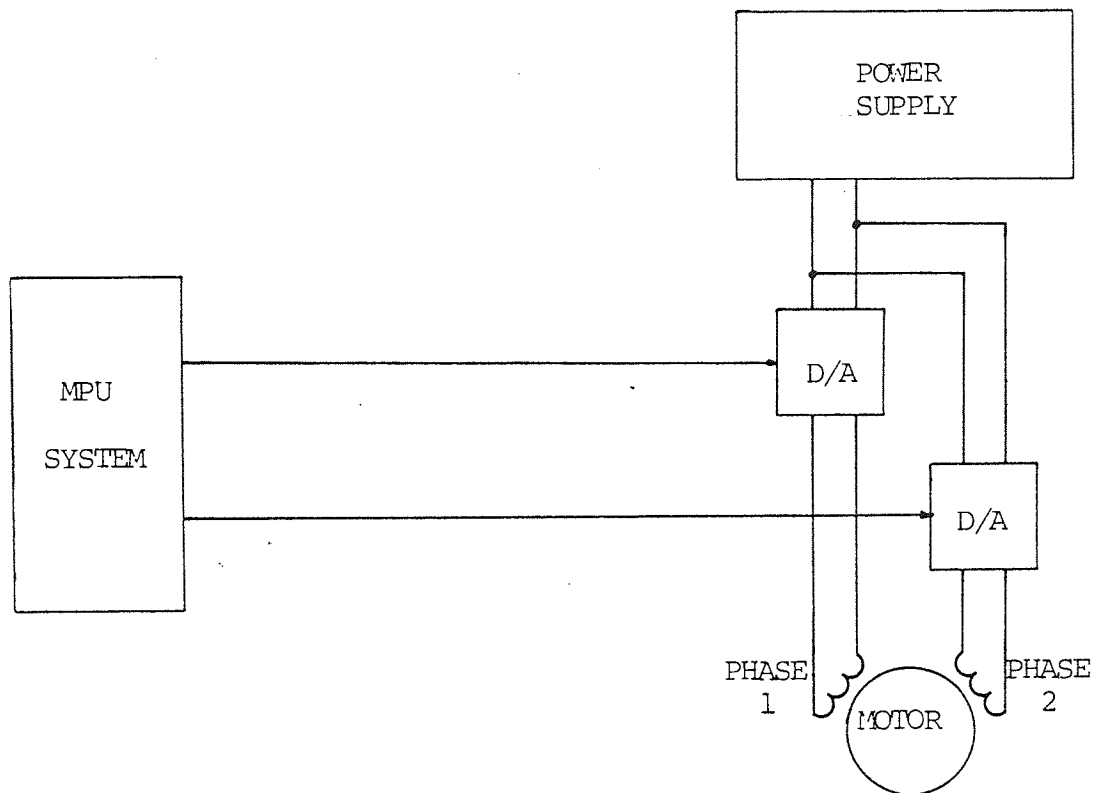


FIGURE 2.1 THE MINIMUM HARDWARE MPU SYSTEM OF STEP MOTOR CONTROL

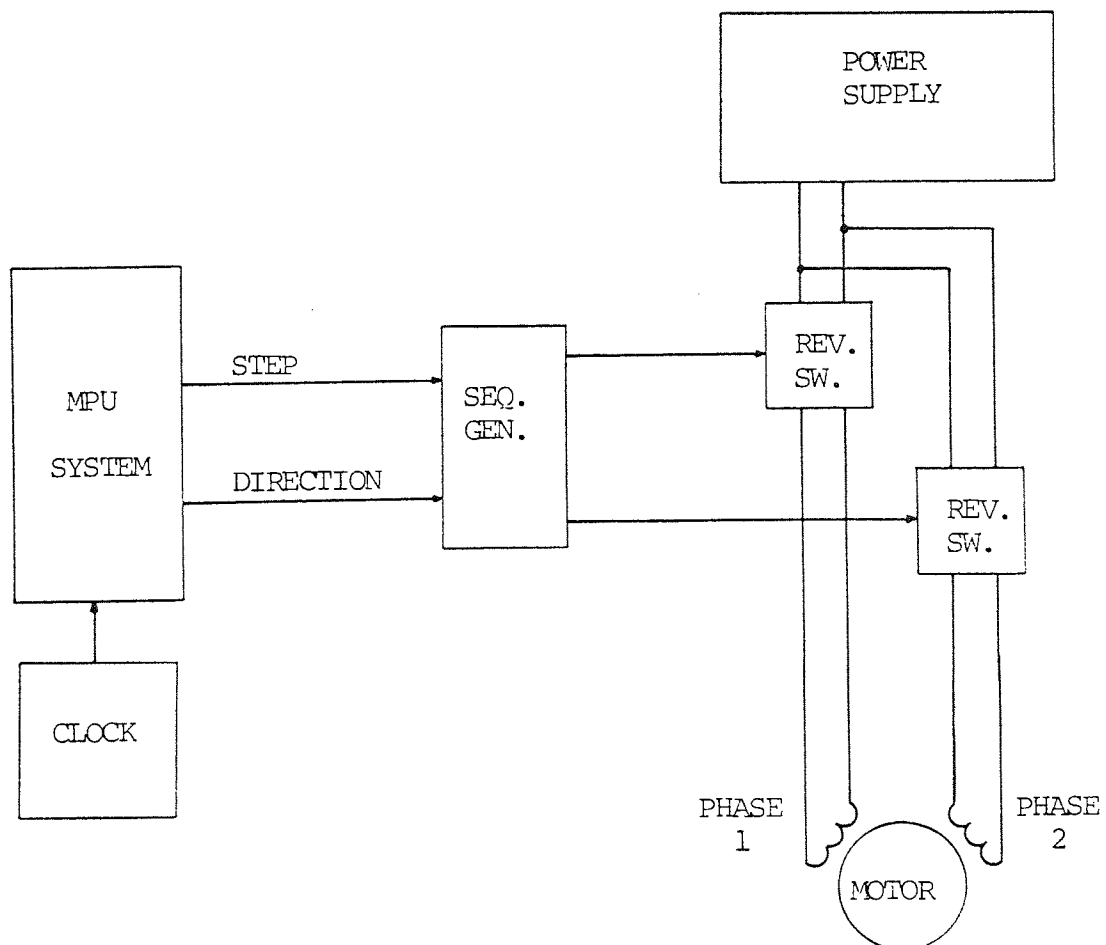


FIGURE 2.2 THE SYSTEM WITH THE SEQUENCE GENERATOR IMPLEMENTED IN HARDWARE

requirement for the microprocessor to output information at every step of the motor, hence the microprocessor must be working in real time. This means that it must have some form of clock so that it can calculate the correct moment in time to initiate the next step of the motor. The tasks which have to be performed by such a processor may be split into sections as follows:-

1. TIME KEEPING The microprocessor must have some form of register which keeps count of time. This register must be updated at small intervals in time so that the resolution of the clock is sufficiently accurate for the motor control.
2. POSITION TRACKING The microprocessor must keep count of each step the motor is requested to execute so that the position of the motor may be known.
3. ANTICIPATION The microprocessor must do all the necessary calculation to anticipate when the next step of the motor is required.
4. EXECUTION The microprocessor must combine the above three procedures and then initiate the next step at the required instant in time.

The minimum hardware system shown in Figure 2.1 may be changed by including a current sequencing device in the hardware. This modification to the circuit removes the task of sequencing from the microprocessor and so releases more time for tasks which are

more suited to software, whereas the sequencing is simple to implement in hardware and is a non-changing function. The resulting system is shown in Fig. 2.2. Although this system has to perform the same four tasks as the minimum hardware system, the task of execution is substantially reduced. To output a single pulse into the sequence generator, requesting a step is considerably faster than firstly determining which of the two currents has to be changed and secondly whether that current has to be set forwards or reverse.

Having realised a system of best compromise between hardware and software a consideration of timing factors can be made.

The time allowable for programme execution is the time between motor steps. During this time the microprocessor must calculate the instant at which the next step is to be executed. If the motor is to run at 100 steps per second then the time available is 10 ms, however, an increase in speed to 1000 steps per second limits the time to 1ms. The accuracy of the microprocessor clock must also be considered. If the motor is to step every 10 ms then a clock with a resolution of 100 μ s results in a step time accuracy of 1 per cent, however with 1 ms step intervals the clock time must be updated in the microprocessor every 10 μ s, to attain a similar accuracy. It can be seen that maintaining an accurate clock can take up quite a lot of programme time and so a system of operation has been devised which removes the task of time keeping from the software by implementing the real time clock in hardware.

This system shown in Figure 2.3 has two hardware registers which can be loaded from the microprocessor with numbers which represent the step rate of the motor and the number of steps to be executed at that rate. The hardware clock is used to count down the registers. When the first register reaches zero a step demand is output to the sequence generator, the second register is decremented by one count and the first register is reset to a value which is output from the microprocessor. When the second register counts down to zero it sends a signal back to the microprocessor to signify that the motor has executed the number of steps requested. This system configuration removes much of the work from the microprocessor, in fact the only two tasks which remain in software are:-

- (1) Position Tracking
- (2) Anticipation.

both as previously defined.

The first advantage of such a system is that the microprocessor is no longer required to work in real time, hence disposing of the need to regularly update its own clock register. The second advantage is that if the stepper motor is to be run at a constant speed, then the number of steps at that speed may be set in the external register and the microprocessor may use the time required for the total number of steps without interruption. However, if only one step is required at each speed this is no advantage.

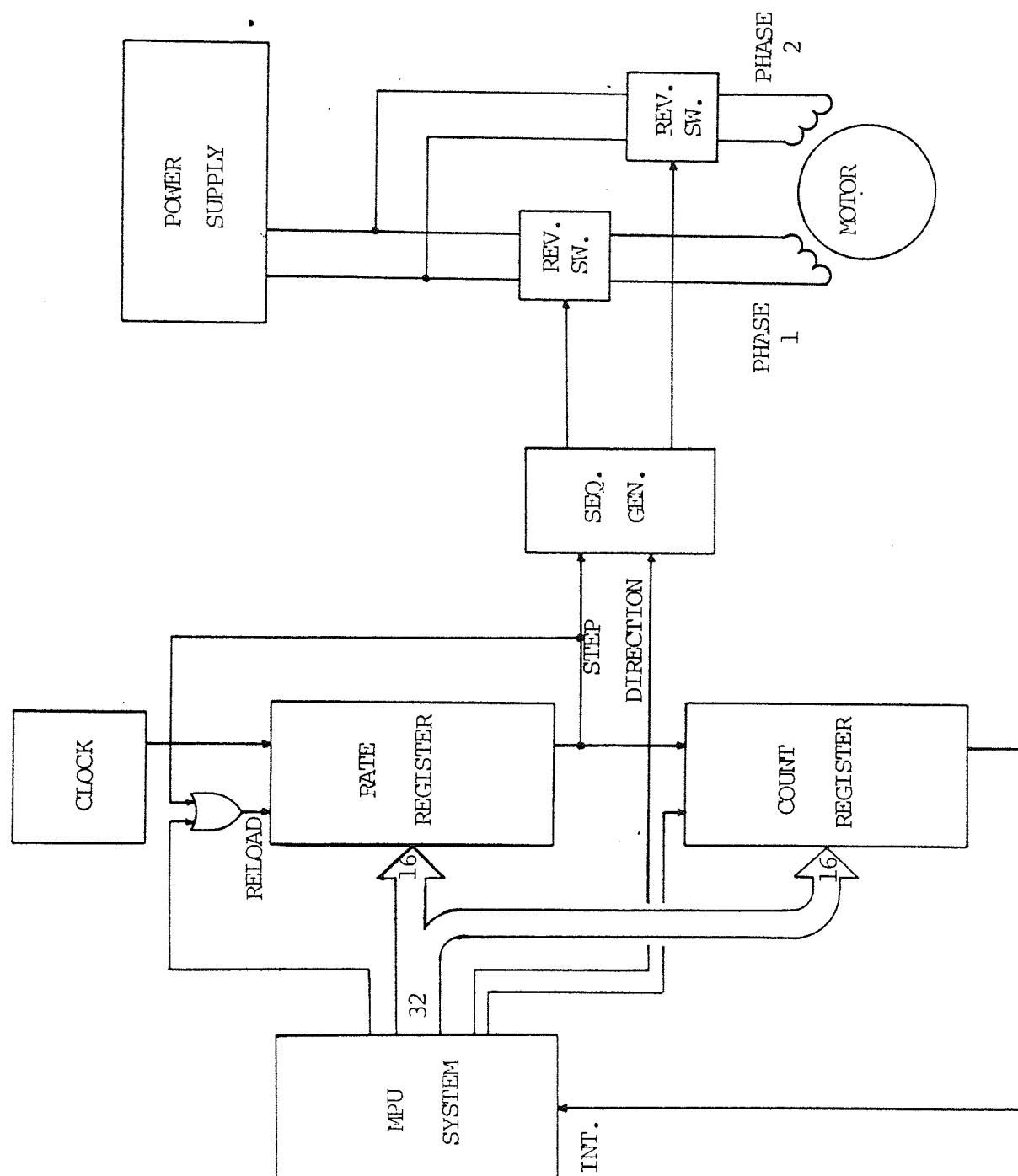


FIGURE 2.3 MOTOR CONTROL SYSTEM WITH EXTERNAL COUNT AND RATE REGISTERS

2.2.4 CONCLUSIONS

In an effort to provide the best microprocessor controlled drive circuit for a stepper motor a compromise has to be reached between hardware and software so that the timing requirements placed on the microprocessor are not too great. The capacity of a microprocessor to cope with the timing requirements depends not only upon its clock rate and speed of operation but also upon its instruction set. Some microprocessors may include instructions which fit well into a stepper motor control system whereas other microprocessor instruction sets would require such operations to be programmed using several single instructions. Examples of such operations are Multiply and Divide.

It is proposed that the two types of system shown in Figures 2.2 and 2.3 should be developed for stepper motor control.

2.3 RECORDING POSITION INFORMATION

It is necessary to include a position transducer in the control system for two reasons. Firstly, during open-loop tests some assessment of the operation of the machine may be made by observing the position of the output shaft of the motor. Secondly, any form of closed-loop control requires that position information be fed back to the microprocessor. Consequently, a brief review of shaft position encoders is given here.

There are two types of transducer which are suitable for recording the required position information. The first type of transducer to be considered generates electrical pulses at known increments of position. One cycle of these pulses indicates that the shaft has rotated through one increment of position. In order to detect the direction of motion it is necessary to have two separate lines giving pulses which are offset by one quarter of a cycle. Figure 2.4 shows the transducer output waveforms for both clockwise and anticlockwise rotation.

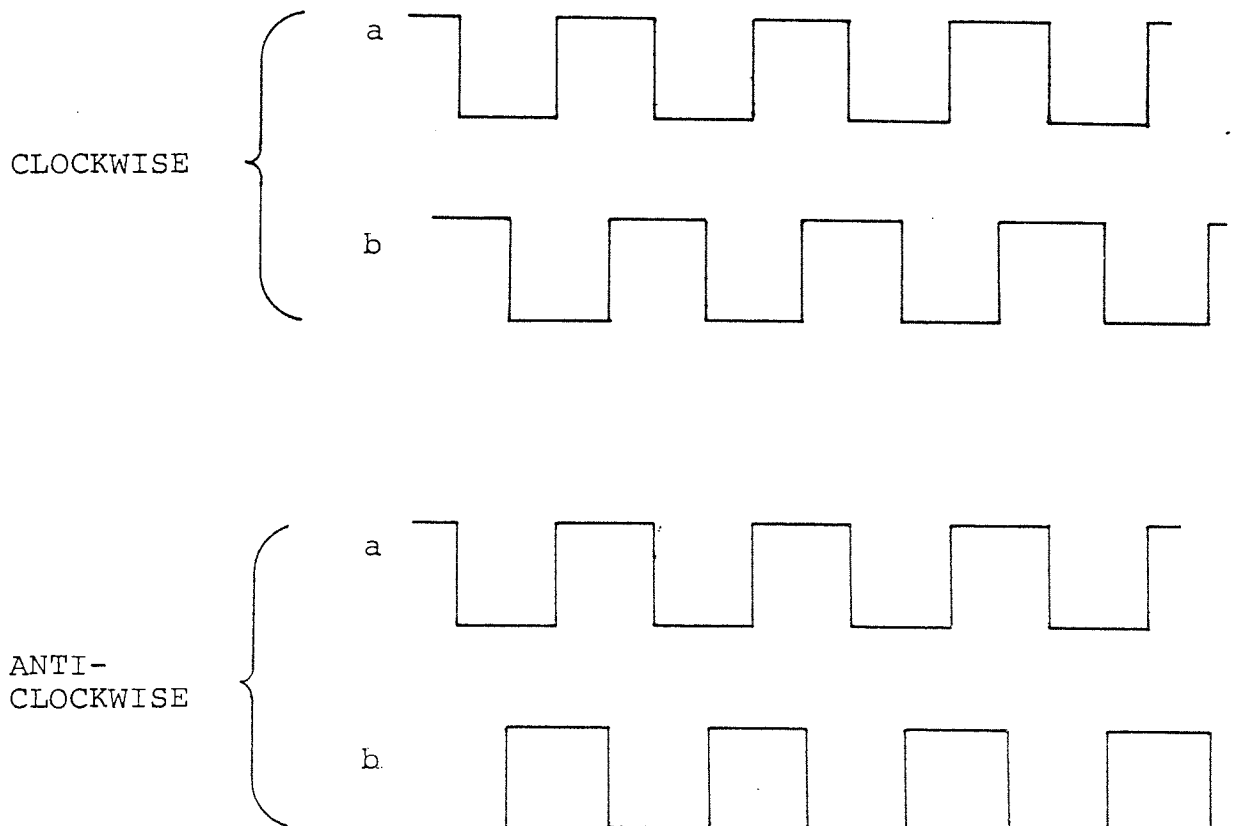


FIGURE 2.4 INCREMENTAL ENCODER OUTPUT

This type of device has the disadvantage that it only indicates increments in position. Therefore the pulses have to be counted within the microprocessor system. The device does not give an absolute reading of position.

A detailed description of the application of this type of transducer is given by M. D. Borman⁽⁸⁾.

The other type of position transducer is the digital encoder. The encoder operates using a disc with a pattern of windows which rotates on the spindle whose position is to be recorded. On one side of the disc is a lamp and a lens; on the other side is an array of photo transistors. The position of the shaft can be found by measuring output voltages from the array. The coding of the output is in Gray code which prevents any ambiguity arising when reading the photo transistors during a transition from one position to the next.

The reading of position information by the microprocessor may be achieved by either one of two different methods, as shown by Figures 2.5 and 2.6. The method shown in Figure 2.5 requires that the microprocessor takes a reading of position at predetermined regular intervals in time. The clock interrupts the microprocessor which then sends a signal to the encoder circuitry, which prevents the output from changing for a short period. During this period the microprocessor reads and stores the number representing the position. The advantage of such a system is that because the time interval is regular there is no need to

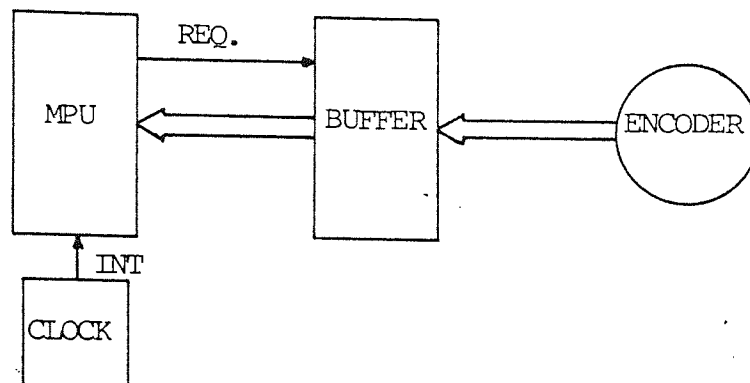


FIGURE 2.5 READING DIGITAL ENCODER BY TIME INCREMENTS

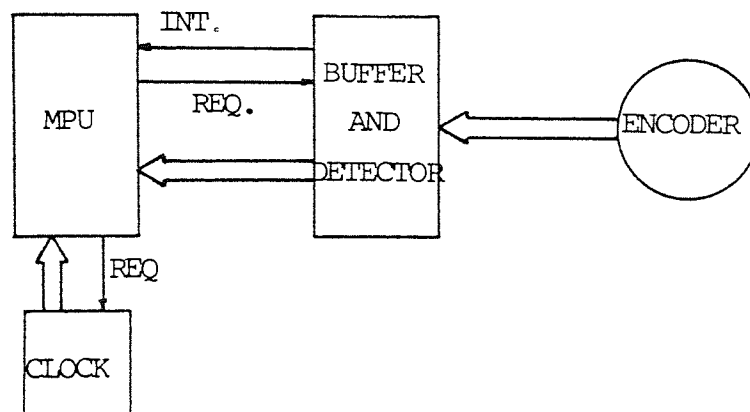


FIGURE 2.6 READING DIGITAL ENCODER BY POSITION INCREMENTS

store the time relating to each position reading. However, to obtain good resolution of results it is necessary to read the position at frequent intervals. At low step rates though, much of the information is redundant and this results in both programme run time and memory storage being used unnecessarily.

The system shown in Figure 2.6 records only the

information which is required. When the position changes through one increment, the encoder circuitry informs the microprocessor, which then reads the time, and the position of the shaft. This system has the advantage that if the shaft is not moving then no microprocessor time or memory is used, but the resolution of shaft movement is as accurate as the digital encoder will allow.

As an alternative to encoding transducers, an indication of motor movement may be obtained by the inclusion of a search coil placed within the motor to observe changes in magnetic flux. Although the unused position of the bifilar field windings may be put to this use, the output obtained would include voltages induced due to the change of current associated with each step. This type of system is of more use on slow step motors where the time required to change the current is small compared to stepping time.

2.4 ASPECTS OF MICROPROCESSOR TECHNOLOGY RELEVANT TO STEPPER MOTOR CONTROL

Many of the aspects influencing the choice of microprocessor in a stepper motor control system are common to all real time control systems. Some of the more important points are summarised here.

The speed of the microprocessor system is of great importance as this determines the number of programme steps which may be executed in a given time period. The speed

of the system is determined by the rate of the system clock and the number of clock cycles required during the execution of each programme instruction.

The availability of certain instructions is also a point which influences the choice of system. Many of the earlier microprocessors had a restricted instruction set. In some cases short subroutines could be written to be called when an instruction such as multiply or divide is required. However, instructions which operate directly on data in the memory can shorten execution time significantly compared with instructions which require data to be moved into an accumulator or a special register for operations to be carried out.

Input and output facilities are important since serial input or output of data can take a considerable amount of computing time. Also the number of bits of data which may be input or output with one instruction greatly influences the time required for peripheral communication.

The bus width, i.e. whether the system operates on 4, 8, 12 or 16 bits at one time, is important because if 16 bit accuracy is required during numerical operations, then an 8 bit device requires double precision arithmetic routines to be written to achieve the required accuracy.

The final point of relevance is the availability of system support in terms of both hardware and software.

The work chronicled in this chapter was commenced in

1977 and one of the first tasks was to assess the availability of microprocessors suitable for controlling the stepper motor. Due to the rapid advancement in microprocessor technology the same survey carried out 12 months later would have revealed a greater choice of systems and if carried out today would almost certainly result in a different choice of microprocessor system.

The majority of systems available were in fact 8 bit devices, however the TEXAS 9900 microprocessor was available within the department, as this was a recent development in 16 bit devices. Also available were the TEXAS TMS 990/4 and TMS 990/10 development systems for hardware and software respectively. The availability of these systems and the fact that the TEXAS 9900 was a 16 bit device proved to be a major factor in the choice of system for this work. Any other choice of microprocessor would have had to be programmed in machine code with all instruction assembly carried out manually, making development extremely difficult.

2.5 OPEN-LOOP CONTROL

2.5.1 INTRODUCTION

One main advantage of step motors over d.c. servo systems is that during correct operation of the stepper motor system it only moves one step for each electrical pulse applied to its input. Therefore, by counting the number of pulses over a period of time, both the position and average speed of the motor can be determined. There

is no need for feedback of this information as in d.c. servo systems.

It is therefore reasonable to allocate one microprocessor to control one stepper motor so that the microprocessor can count each output pulse sent to the motor. All the information required to enable the microprocessor to calculate the motor speed and acceleration can easily be obtained during dynamic control of the motor. This involves maintaining two registers within the system, one to keep track of motor position and the other to indicate time.

Alford⁽⁹⁾ has developed an open-loop control system using an INTEL 8008 microprocessor. The control system used the output from the microprocessor to control the direction of each phase current of the motor, but due to software restrictions the output signals had to be separated by at least 2.4 ms. This resulted in the maximum possible step rate being less than 500 steps per second.

The inclusion of predefined acceleration and deceleration ramps in this type of system is not difficult to achieve. However, such control systems could be manufactured from digital logic components using read only memories to store ramp data. The main advantage of using a microprocessor is that in industrial applications one hardware system may be produced in quantity and then the system's 'Personality' programmed to suit its particular application. Provided that only a low level of position

monitoring is required, then control at step rates in the order of two thousand steps per second would be possible.

As with all open loop controllers some form of precaution must be taken in case the torque or inertia of the load becomes too great and synchronism is lost.

2.5.2 HARDWARE DESIGN

The circuit diagram of the interface is given in Appendix 1, and only an outline of the hardware design is given here.

The circuit was designed using 74 series T.T.L. components. The Communication Register Unit (CRU) interfacing was taken from a standard design published by Texas Instruments as part of the hardware support for the 9900 series microprocessor⁽¹⁰⁾. This allows any one group of up to 16 bits of the CRU to be accessed using only one programme instruction. The interface circuit was designed so that either of the driving methods described previously could be used. In both cases one CRU bit was used to set the required direction of rotation of the motor. A logic high on the bit indicated that the motor was required to rotate clockwise, a logic low indicated an anticlockwise rotation.

For the direct drive mode another single bit of the CRU was fed into a monostable so that each time the bit went through a '1' to '0' transition the monostable was triggered. The period of the monostable was set to 250 μ s

which was the length of pulse required to reliably transmit the signal down the line to the step motor drive circuitry. To prevent interference from the drive circuit going back into the interface circuit an opto coupler was used. The monostable output was fed into the light emitting diode side of the coupler and the photo transistor side was connected to the input of the sequence generator.

The method of control using the external clock employed two 16 bit decrementing counters, each of which could be loaded directly from the CRU of the microprocessor. The clock period was set to 10 kHz and this was used to decrement the first counter, each time this counter reached zero its output pulse triggered the monostable and reloaded the counter from the CRU.

2.5.3 SOFTWARE DESIGN

The first method of control to be considered uses the direct microprocessor output to initiate each motor step. Some understanding of the system may be gained by inspection of the programme required to step the motor. Figure 2.7 shows the Assembly Language programme to step the motor using this method and Figure 2.8 shows the same programme in the form of a Flow Diagram.

The programme shown in Figures 2.7 and 2.8 will step the motor at any desired speed by inserting a variable delay for the parameter 'NUMBER' in line 10. The first 7 lines are for initialisation and are executed only once;

LINE No.	LABEL	INSTRUCTION	COMMENTS	EXECUTION TIME μs
1	CLCRU	EQU >1040	INITIALISATION	28 ² / ₃
2	WS	BSS 32		
3	START	LIMI 0	INSTRUCTION	
4		LWPI WS		
5		LI R12,CLCRU	EXECUTED	
6		LI R0,>0300		
7		LDCR R0,8	ONCE ONLY	
8	LOOP1	SBO 8		4
9		SBZ 8		4
10		LI R2,NUMBER	DELAY ROUTINE	4
11	LOOP2	DEC R2		3 ¹ / ₃
12		JNE LOOP2		3 ¹ / ₃
13		JMP LOOP1	RETURN FOR NEXT STEP	3 ¹ / ₃
14		END START		

Instruction mnemonics as defined in Reference 11

Instruction execution times defined in Reference 10

FIGURE 2.7 CONTINUOUS STEPPING

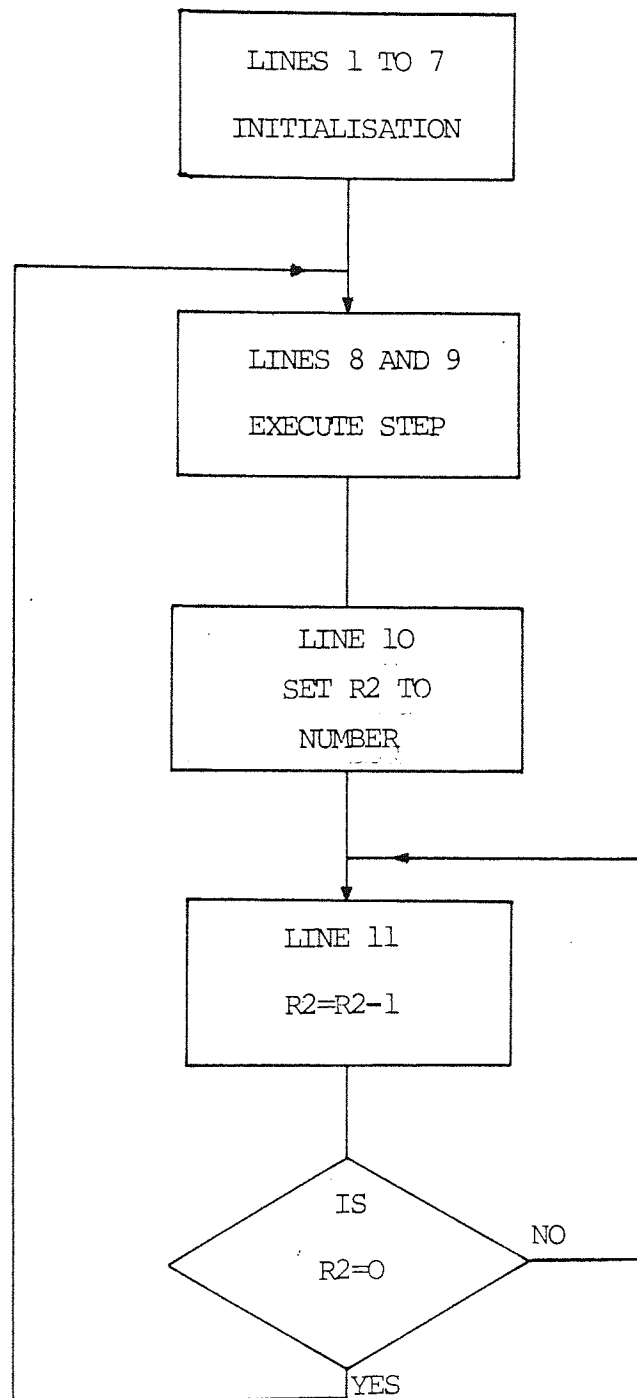


FIGURE 2.8 FLOW DIAGRAM OF CONTINUOUS STEPPING PROGRAMME

lines 8 and 9 execute the motor step; lines 10, 11 and 12 cause a delay proportional to the value 'NUMBER'; and line 13 implements a return to line 8 to output the next motor step. The execution time for each instruction is shown in the right hand column. From this programme it can be seen that a time of $22\mu\text{s}$ is required for each step of the motor, hence the computer time available for other functions at various step rates can be found.

At a rate of 500 steps per second the period between steps is 2ms, hence available time is $1978\mu\text{s}$. At a rate of 1000 steps per second the available time reduces to $978\mu\text{s}$. If the microprocessor is to execute other functions during this time then the computation time of each function must be known and subtracted from the delay. This simple method of controlling the motor is suitable only if the step rate can be predefined, in which case the variable 'NUMBER' may be stored in Read Only Memory (ROM) and a new value put into the programme for each step. This gives a range of time between steps from 1 execution of the loop i.e. $22\mu\text{s}$ to 2^{16} executions of the delay plus one execution of the loop = $436928\mu\text{s}$ (less than $\frac{1}{2}$ second).

A system of look-up tables for velocity profiles can greatly improve the performance of an open-loop step motor system if runs of many steps are to be made. When a motor is used to drive a load of high inertia, its maximum running speed will exceed the speeds at which it will reliably start or stop. Therefore precisely defined acceleration and

deceleration curves may be calculated to minimise the time required to move the inertial load over a known distance. It is the time intervals between steps during starting and stopping which may be stored in ROM.

A system based on this method of looking up step period values from a table has been implemented by B.C. Lafreniere⁽¹²⁾. His system is greatly enhanced by the addition of a development system, which creates optimum acceleration and deceleration tables in an interactive manner. However, during programme run time many instructions are used to produce the required time delay and have no other function. This results in the power of the microprocessor not being fully used. Such a system would be suited to a programmable clock, a number of which are available in large scale integrated circuits.

A method of control which operates in real time intervals rather than a decrementing register between steps can be achieved by including a clock within the microprocessor system. The main advantage of this being that procedures may be of variable length and their execution time need not be calculated. The resolution of the clock must be sufficiently accurate so that the period between steps when the motor is running at its maximum speed can be accurately timed. For the motor to run at 1000 steps per second with a resolution of 10% the clock must be updated every 100µs. A routine which services the clock is shown in Figure 2.9.

The time required to execute this simple clock updating routine is 66µs and for a resolution of 100µs the time

LINE No.	LABEL	INSTRUCTION	COMMENTS	EXECUTION TIME μ s
1	CKINT	LI R12,CKCRU		4
2		SBO -1		4
3		LDCR @CKVAL,14	RESET CLOCK	$18\frac{2}{3}$
4		SBZ -1		4
5		INC @CKCOUNT		6
6		C @CKCOUNT,@VALUE	TEST IF STEP REQ'D	10
7		JL RET		$3\frac{1}{3}$
8		BL @STEP	STEP MOTOR	4
9	RET	LI R12,IFCRU		4
10		SBO CKINTL		4
11		RIWP		$4\frac{2}{3}$
				<hr/> $66\frac{2}{3}$ <hr/>

LABELS TO BE INCLUDED ELSEWHERE IN MAIN PROGRAMME

CKINT Label of this CLOCK INTERRUPT routine

CKCOUNT Running total of clock interrupts and hence time

CKCRU Number of first CRU bit allocated to the clock

CKINTL Clock interrupt level

CKVAL Clock code for required interrupt timing

IFCRU Number of first CRU bit allocated to interface circuit

STEP Label of routine to execute one motor step

VALUE Value of step at next desired step.

FIGURE 2.9. REAL TIME CLOCK SERVICE ROUTINE

keeping would take 66% of the available computing time. At a step rate of 1000 steps per second another 2% of the time is taken by outputting the step demand, hence only 32% of the time is left for calculating the value of the clock when the next step is required. At 1000 steps per second the time available is 320 μ s. A motor running at 500 steps per second, however, would leave 1.3 ms of available time and still achieve similar resolution.

This type of real time operating is only possible if either speed restrictions are placed on the motor to be controlled or if any high speed control is executed with the aid of a predefined look up table of step times.

The method of microprocessor control using an external clock, as shown in Figure 2.3 is of greater advantage for machines which are required to run at step rates in the order of 1000 steps per second. The resolution of the step period is dependent upon the rate of the hardware clock. For comparison a clock rate of 10 kHz gives a resolution of 100 μ s, with a maximum time between steps of $2^{16} \times 100\mu\text{s}$ (6 $\frac{1}{2}$ seconds).

A programme suitable to run the motor via this type of interface is given in Figure 2.10. The total time required for the execution of this procedure is 85 μ s and this represents less than 10% of available time for a step rate of 1000 steps per second. Although this interrupt procedure takes more time to execute than the routine for stepping the motor, shown in Figure 2.7, it does not need any form

of software timing, and only requires executing once for each step of the motor. This method of control has the added advantage that if more than one step is required at a particular rate, then this can be achieved without the need to interrupt the microprocessor after each step. Of the two systems investigated the one using the external clock and registers was used for subsequent testing and system evaluation.

LINE No.	LABEL	INSTRUCTION	COMMENTS	EXECUTION TIME μ s
1	START	LI R12,CLCRU		4
2		SBZ 4		4
3		LI R12,RACRU	} LOAD RATE REGISTER	4
4		SBZ >21		4
5		LDCR @RATE,0		20
6		SBO >21		4
7		LI R12,CTCRU	} LOAD COUNT REGISTER	4
8		SBZ >10		4
9		LDCR @COUNT,0		20
10		SBO >10		4
11		LI R12,CLCRU	} RESET INTERRUPT	4
12		SBO 4		4
13		RTWP		4 $\frac{2}{3}$
				<hr/> 84 $\frac{2}{3}$ <hr/>

LABELS TO BE INCLUDED ELSEWHERE IN MAIN PROGRAMME

CLCRU	Number of first CRU bit allocated to control lines
COUNT	Number to be loaded into Count Register
CTCRU	Number of first CRU bit allocated to Count Register
RACRU	Number of first CRU bit allocated to Rate Register
RATE	Number to be loaded into Rate Register

FIGURE 2.10 EXTERNAL REGISTER SERVICE ROUTINE

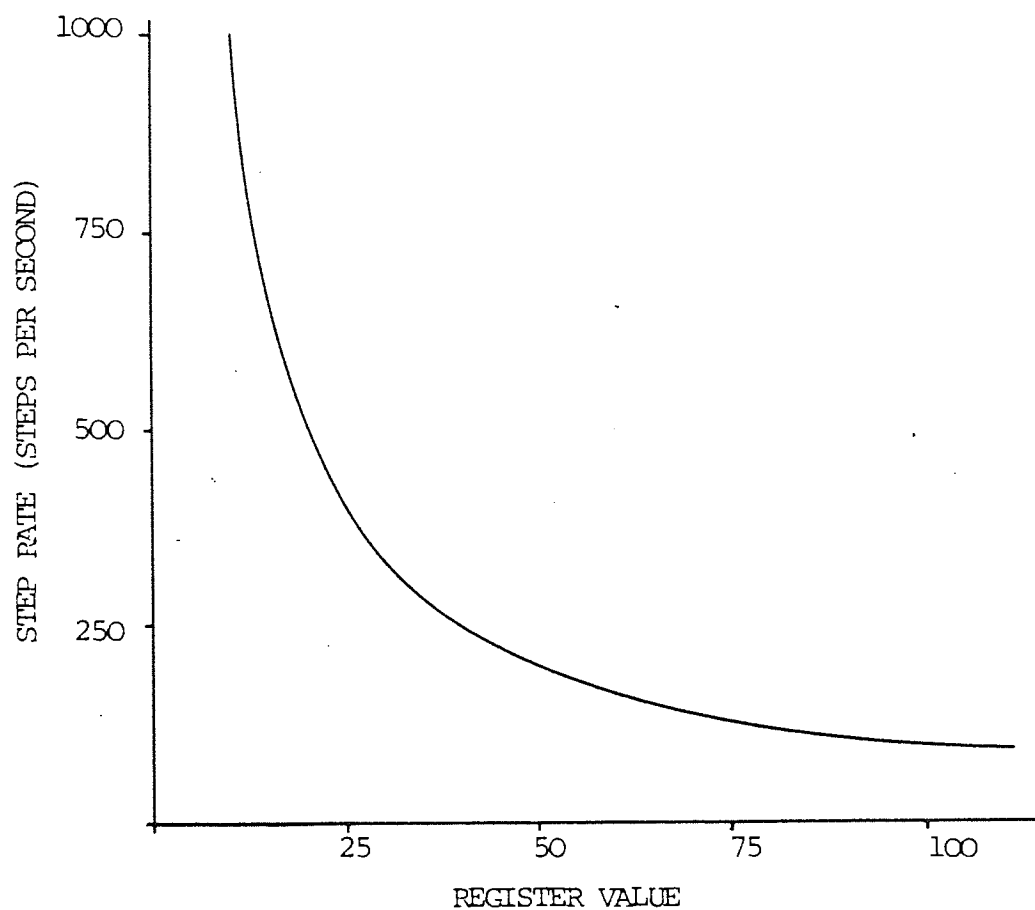


FIGURE 2.11 CURVE OF STEP RATE AGAINST REGISTER VALUE

REGISTER VALUE	PERIOD ms	STEP RATE Hz
10	1	1000
11	1.1	909
20	2	500
21	2.1	476
100	10	100
101	10.1	99
110	11	91

TABLE 2.4 STEP RATE FROM REGISTER VALUE

2.5.4 RESULTS

The first tests carried out assessed the timing capabilities of the system. Table 2.4 shows how step rate varies with the number placed into the register. Figure 2.11 expresses this data in a graphical form.

These results show the non linear relationship between the number entered into the rate register and the resulting step rate. At the high step rate of 1000 steps per second an increment of 1 causes a 10% change in the period, which represents a 91 step per second reduction in rate. At a step rate of 100 steps per second, however, 1 increment results in only a 1 step per second change in rate. The linearisation of this relationship can be carried out as part of the microprocessor programme.

The results of step rate and position presented in this section were obtained by the use of a digital encoder. The encoder did not take an active part in the control of the machine but acted purely as a means of observing the position. An explanation of the operation of the encoder is left until the section on closed loop control as it is in this context that the techniques of the encoder have more relevance. It is sufficient to say at this stage that the position information was read in and stored in its prime form during motor operation. Due to the time requirements for processing the data, conversions and plotting were left until after the motor run was completed.

The single step response of the motor for various currents is shown in Figure 2.12. The significance of these results is that they show how the natural frequency of the machine depends upon the phase current. Results are shown for the single step response at 1A, 3A and 5A . with both field windings excited, the resulting data is summarised in Table 2.5.

CURRENT A	TIME TO 1ST OVERSHOOT ms	TIME TO 1ST UNDERSHOOT ms	DIFF ms	NATURAL FREQUENCY Hz
1	16.8	35.2	18.2	27
3	7.5	18.8	11.3	44
5	7.0	16.5	9.5	52

TABLE 2.5 SINGLE STEP RESPONSE NATURAL FREQUENCIES

The two continuous step rates which are examined are such that the time at which each step occurs coincides with; (1) The first overshoot, (2) The first undershoot, of the previous step. To calculate these step rates the results of the single step at 3A was used. Figure 2.13 shows the multistep response at 44 steps per second. At 3 amps the position of the rotor progresses in an oscillatory manner as each step is demanded at the first undershoot of the next. At 1A, however, the natural frequency changes and this unstable effect no longer exists. Figure 2.14 shows that at 94 steps per second the step response of the machine

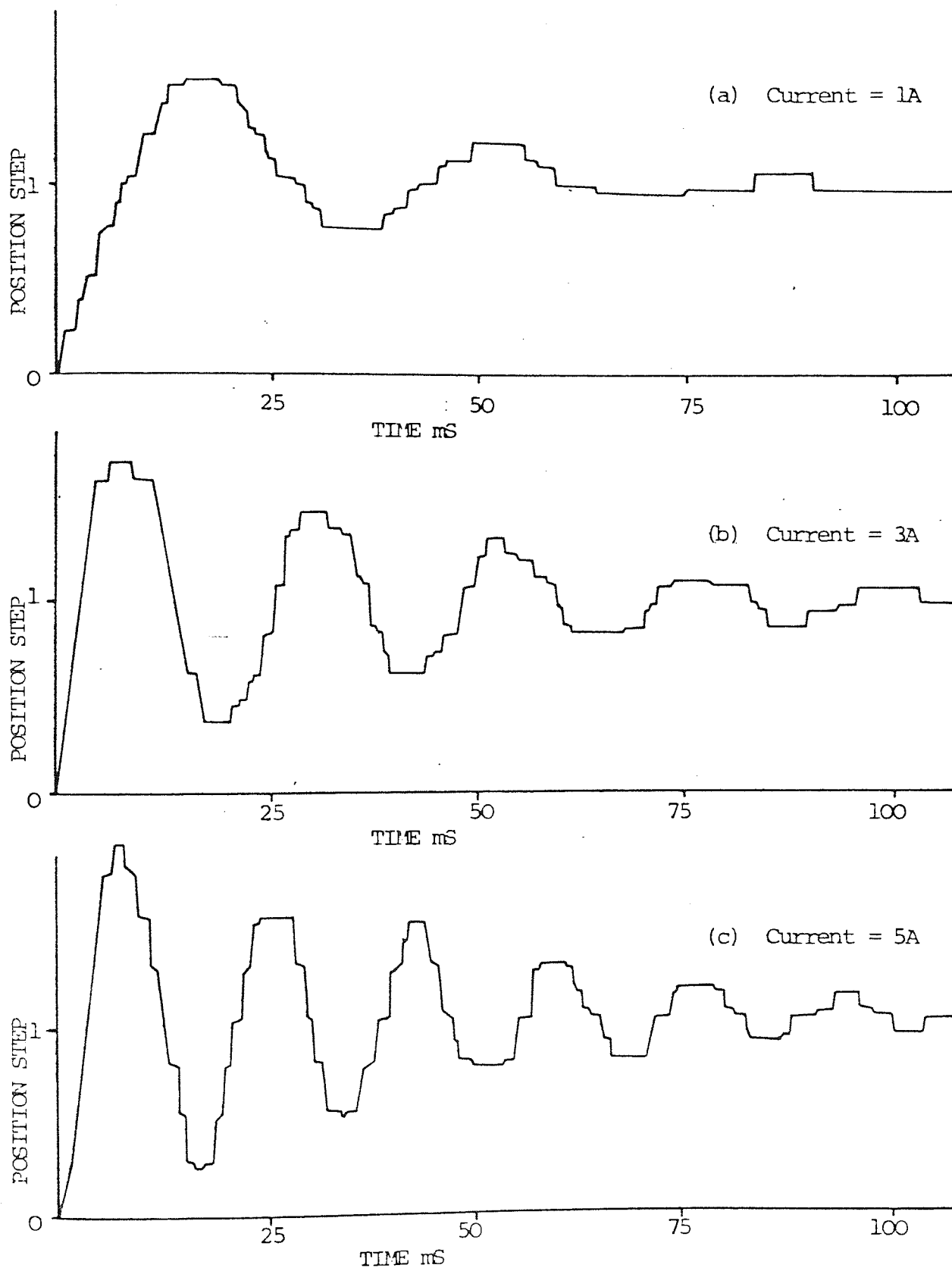


FIGURE 2.12 SINGLE STEP RESPONSE OF VARIOUS CURRENTS

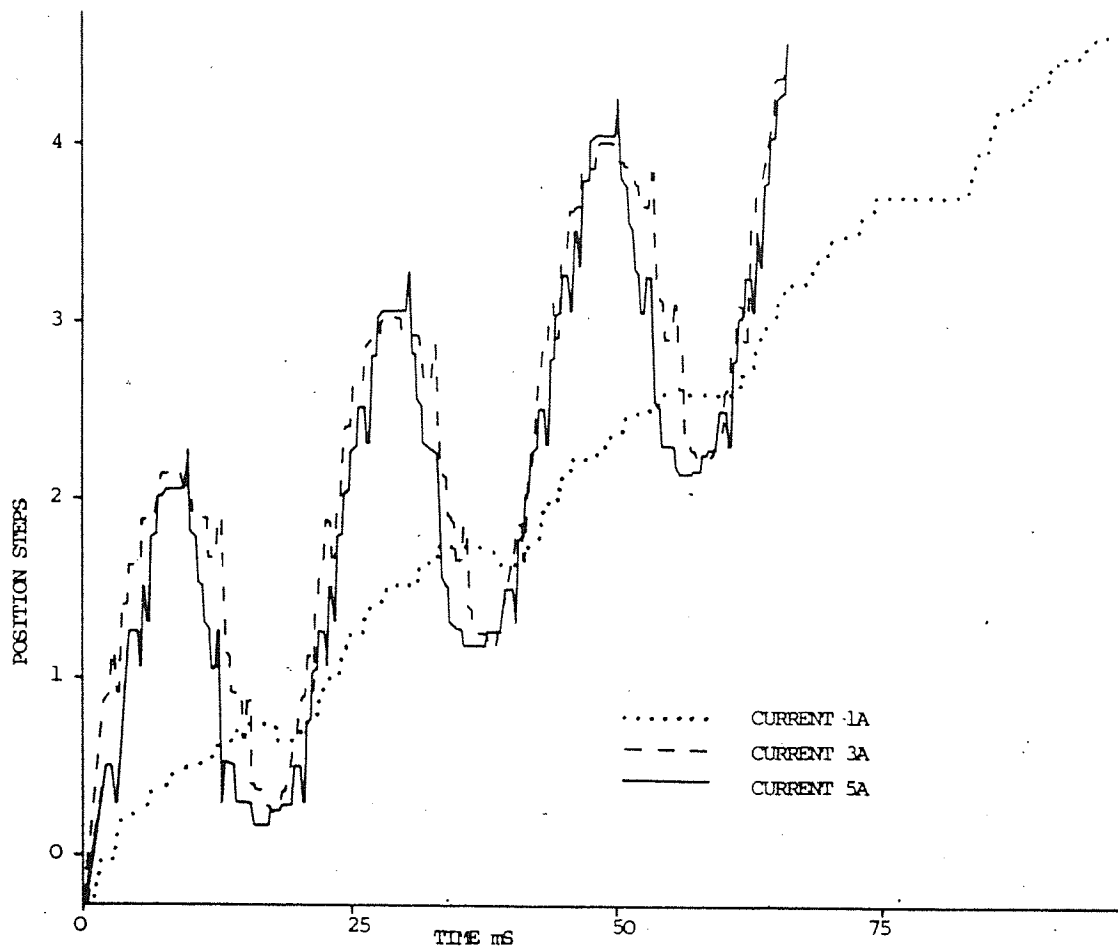


FIGURE 2.13 MULTISTEP RESPONSE OPEN LOOP 44 s.p.s.

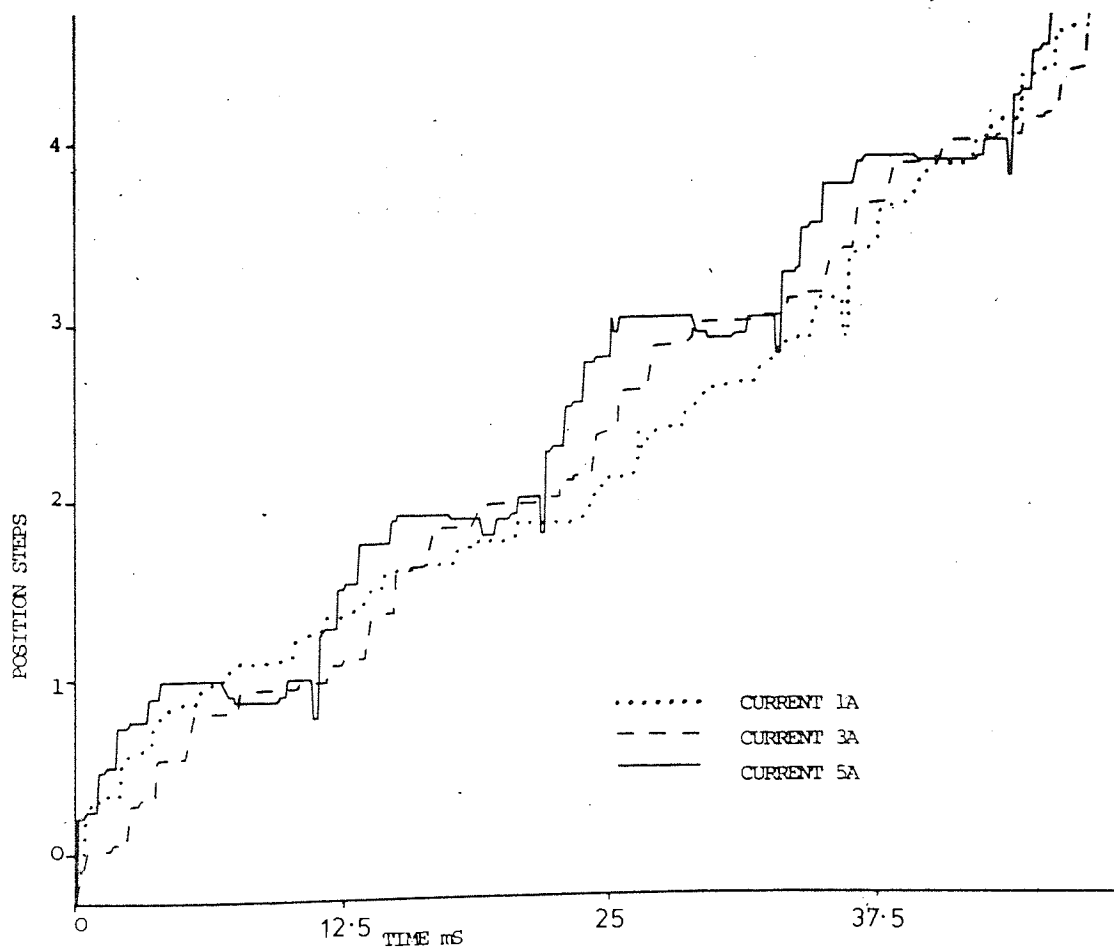


FIGURE 2.14 MULTISTEP RESPONSE OPEN LOOP 94 s.p.s.

is greatly improved when each step is demanded as the overshoot reaches a peak from the previous step.

Although only one response is shown for each case, these are typical for each current, and the data shown in Table 2.5 was taken from the mean values of several recorded step responses.

2.5.5 CONCLUSION

Two methods of microprocessor control have been investigated and the motor has been run using both methods. During simple ramp tests the motor was observed to behave in a similar manner as when operated from a conventional control circuit using a pulse generator as a source. For simple tests where the step rate was not calculated by the microprocessor, both of the methods were able to run the motor at its maximum step rate. By observation of the waveforms generated within the interface circuits the timing of the control procedures discussed was confirmed.

It can be concluded that of the two methods of control investigated the method using an external clock and registers is superior. It is capable of the same standard of control even when only one step is required at a very high rate but required far less computing time at slower rates. The system is sufficiently versatile because the resolution of time may be varied easily by adjusting the hardware clock rate.

The direct driving method is suitable for adaptation to enable phase current control to be achieved and hence

microstepping made possible, however the maximum rate at which microstepping could take place would be quite slow.

2.6 CLOSED-LOOP CONTROL

2.6.1 INTRODUCTION

It is often stated that one of the most important advantages of the stepper motor is that open loop operation can be used with ease. Each step is of a known size and by counting the number of steps demanded and the rate demand, the position and speed of the motor may be assumed. Open-loop control however, does have certain disadvantages in terms of control of the motor. Malfunctions of the motor or its control system can manifest themselves in many ways, some of which could be detected and corrected if feedback information was available.

When a microprocessor is used as part of the control system the possibilities of feedback take two distinct forms:

1. The feedback may be used to check that each step has been correctly executed, or that the motor is in the correct position at the end of a sequence of steps. Such procedures may be referred to as "Book keeping" closed-loop control.
2. The feedback may be used to improve the performance of the machine, either by controlling phase currents to compensate for varying loads

or to ensure that steps are not demanded when the motor is not in a position to respond correctly.

i.e. during excessive undershoot or at an excessive rate for the load conditions of the motor.

A demonstration of this latter type of feedback is given by Kuo and Singh⁽¹³⁾ and although the system does not involve the use of a microprocessor, it demonstrates the type of control that can be achieved by using feedback applied to stepper motors. Feedback for the system is generated by an incremental encoder which produces one feedback pulse for each step of the motor. The encoder sensors are arranged so that each feedback pulse occurs before the motor reaches its detent position. By deriving the next step demand from the feedback pulse the machine may be run continuously. The addition of electronic time delay circuit in the feedback path enables the lead angle of the step demand to be varied.

2.6.2 INPUT OF POSITION DATA

Information relating to the position of the motor at any instant in time was fed back to the microprocessor system from an eleven bit digital encoder. The relationship between motor steps and encoder increments was unsuitable resulting in the following relationships:-

No. of steps per revolution	= 168
angle of each step	= 2.1428°

$$\begin{aligned}
 \text{No. of increments per revolution} &= 2^{11} = 2048 \\
 \text{angle of each increment} &= 0.17578 \\
 \text{No. of increments per step} &= \frac{2048}{168} = 12.2
 \end{aligned}$$

Although such a system would be feasible for the recording of angular position to within 0.2 degree, the problems caused by one in five of the motor steps giving 13 instead of 12 encoder increments made dynamic closed-loop control very difficult. To overcome this problem, the encoder shaft was geared up by a factor of 84 to 32 (using non-backlash type gears). The resulting relationship was:-

$$\begin{aligned}
 1 \text{ revolution of the motor gives } & \frac{2048 \times 84}{32} = 5376 \text{ encoder} \\
 & \text{increments}
 \end{aligned}$$

1 step of the motor gives 32 encoder increments exactly.

The advantages in using these gears are, firstly, an integer number of increments per step makes dynamic closed-loop control easier. Secondly, the integer 32 can easily be divided by 2, 4, 8, 16 in the binary format of the microprocessor. Also 32 increments per step gives a very good resolution of position measurement.

The fact that the encoder uses a 'Gray Code' format is a problem which is not so easily overcome. The Gray code is used for the encoder because of its significant feature that whenever an increment transition occurs only one bit of the

code has to change to indicate the new position. This is unlike the binary code which will change from 011_2 to 100_2 . It is quite likely that during such a transition one bit would actually change marginally before the other, and this would necessitate inhibiting the change of code while it was being read into the microprocessor. The use of the Gray code avoids this inconvenience, but presents the problem of converting from Gray code to binary so that arithmetic operations can be performed on the position information within the microprocessor. Figure 2.15 shows the general algorithm for converting a Gray coded number into a binary code, a full explanation of this procedure may be found in Reference 14.

The most convenient method of converting from Gray to binary code would be some form of hardware parallel conversion having eleven input lines and eleven output lines. Although 8 bit devices were available, 11 bit devices were not, so such a circuit would have to be hard wired logic. This type of system would require all the output bits to change simultaneously otherwise any advantage of using a Gray coded encoder would be lost. The most practical design of the 11 bit parallel decoder involved the use of programmed read only memory of size 2^{11} by 11 bits (22k bits). The expense and availability of such devices necessitated the design of an alternative system.

The Gray to binary conversion was tried in software using the programme shown in Figure 2.16. The time required

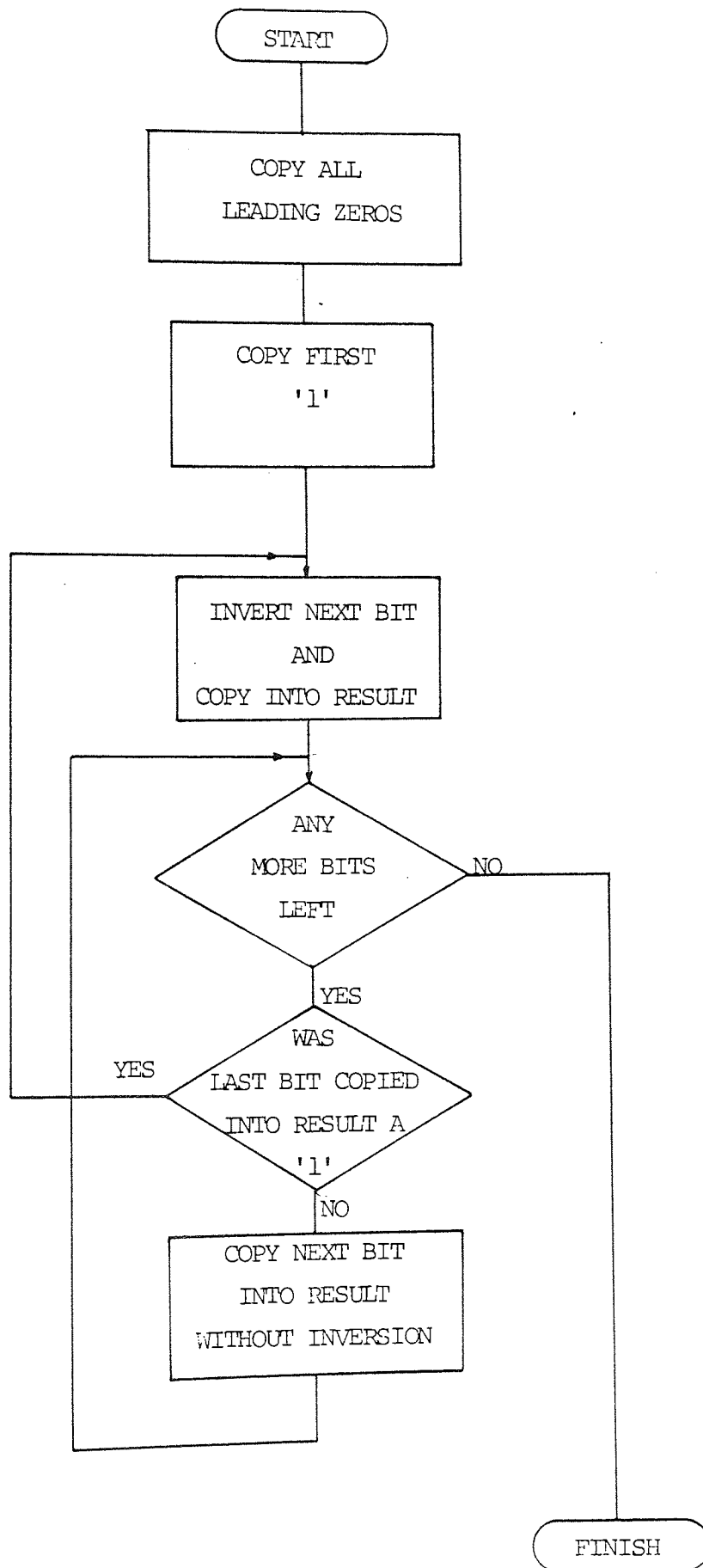


FIGURE 2.15 ALGORITHM FOR GRAY TO BINARY CONVERSION

LINE No.	LABEL	INSTRUCTION	COMMENTS	EXECUTION TIME μ s
1	RDPOS1	LI R12, ENCRU		4
2		SBZ >1F		4
3		STCR R2, 11	READ GRAY CODE	$19\frac{1}{3}$
4		LI R1, 0400		4
5		CLR R3		$3\frac{1}{3}$
6		JMP MSB		$3\frac{1}{3}$
				<u>38</u>
7	ONF	A R1, R3	ONE IN ANS	$4\frac{2}{3}$
8		SRL R1, 1		$4\frac{2}{3}$
9		JEQ ANS	TEST FOR FINISH	$3\frac{1}{3}$
10		COC R1, R2		$4\frac{2}{3}$
11		JNE ONF	TEST NEXT BIT	$3\frac{1}{3}$
				<u>20$\frac{2}{3}$</u>
12	ZEF	SRL R1, 1	ZERO IN ANS	$4\frac{2}{3}$
13		JEQ ANS	TEST FOR FINISH	$3\frac{1}{3}$
14	MSB	COC R1, R2		$4\frac{2}{3}$
15		JEQ ONF	TEST NEXT BIT	$3\frac{1}{3}$
16		JMP ZEF		$3\frac{1}{3}$
				<u>19$\frac{1}{3}$</u>
17	ANS	SBO >1F	CONVERSION COMPLETE	4
18		RIWP		$4\frac{2}{3}$
				<u>8$\frac{2}{3}$</u>

$$\begin{aligned} \text{Average Time} &= 46\frac{2}{3} + 11 \left(\frac{20\frac{2}{3} + 19\frac{1}{3}}{2} \right) \mu\text{s} \\ &= 266\frac{2}{3} \mu\text{s}. \end{aligned}$$

RDPOS1 LABEL OF THIS READ POSITION PROCEDURE
 ENCRU NUMBER OF FIRST CRU BIT ALLOCATED TO THE ENCODER

FIGURE 2.16 GRAY TO BINARY CONVERSION

to execute this routine varied depending on the number being converted, but on average took approximately 266 μ s. With a step rate of 1000 steps per second and the time required to output control information of 85 μ s, there would be time for only 3 readings of position to be made during each motor step. This would be sufficient for a book keeping system where feedback information is required only to check on whether the motor has lost synchronism. However, three position readings per step is not sufficient for any form of control within each step of either phase currents or step demand.

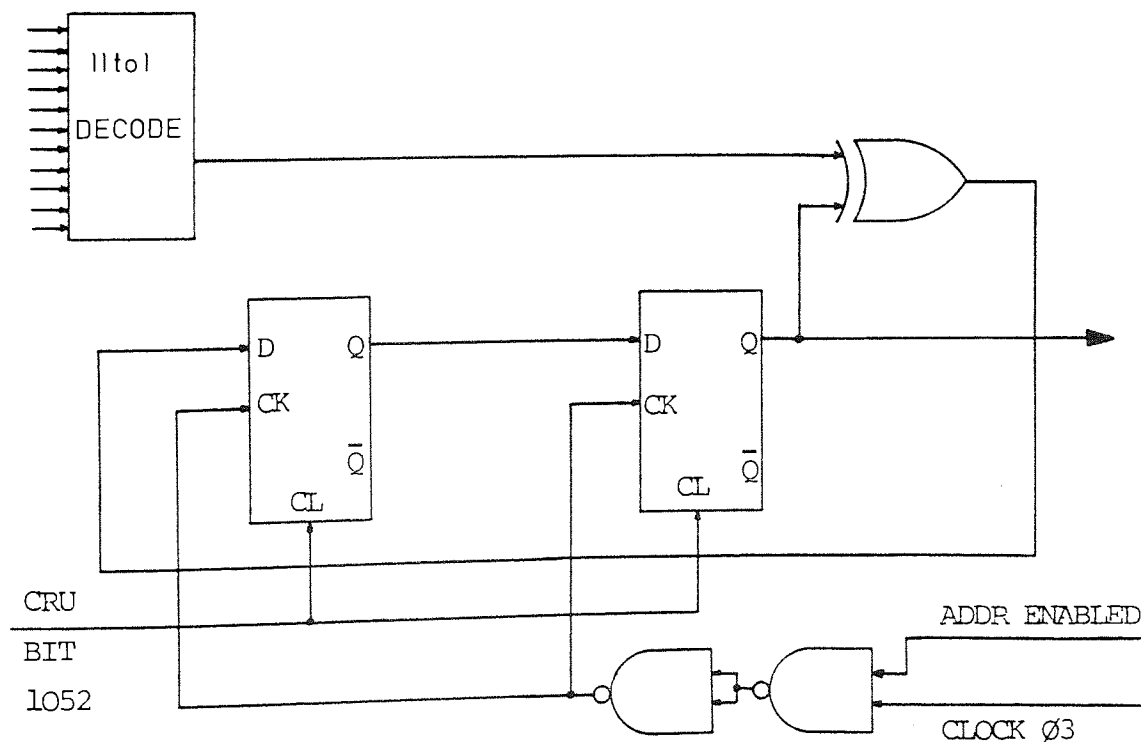


FIGURE 2.17 HARDWARE GRAY TO BINARY CONVERSION

The final attempt at a faster input of position information to the microprocessor was to use a serial hardware Gray to binary converter as shown in Figure 2.17. The device was simple to construct consisting of only 3 T.T.L. integrated circuits and was included in the CRU input circuit as shown. This method however has one shortcoming, in that the serial decoder requires that the Gray code be transmitted with the most significant bit first. This is simple to arrange. The Texas 9900 microprocessor, however requires that inputs through the CRU system be presented with the least significant bit first. The result is that when the position information is loaded into the microprocessor register it is back to front and has to be reversed. The reversal is achieved by outputting the data onto other CRU output lines which are directly wired to CRU input lines in the required order. Figure 2.18 shows the programming required to execute this task.

This method results in a time saving of over 70% when compared with the software decoding method shown in Figure 2.16. It was the serial hardware decoding method which was adopted for use during tests because this method takes less time and less memory space. Although extra hardware was required this did not have to be built specially as standard input-output boards were available. With this type of input and conversion there was time for 12 position reading to be taken, with the motor running at a rate of 1000 steps per second.

LINE No.	LABEL	INSTRUCTION		COMMENT	EXECUTION TIME μ s
1	RDPOS2	LI	R12, ENCRU	} RESET HARDWARE DECODER	4
2		SBZ	33		4
3		SBO	33		4
4		STCR	R1, 11	} STORE REVERSED CODE CORRECT CODE	$19\frac{1}{3}$
5		INV	R1		$3\frac{1}{3}$
6		LI	R12, IOCRU		4
7		LDCR	R1, 11		14
8		STCR	R1, 11		$19\frac{1}{3}$
					<hr/> 72 <hr/>

RDPOS2 Label of this READ POSITION procedure

ENCRU Number of first CRU bit allocated to the ENCODER

IOCRU Number of first CRU bit allocated to the INPUT/OUTPUT DEVICE

FIGURE 2.18 READ POSITION VIA HARDWARE DECODER

2.6.3 BOOK KEEPING CLOSED-LOOP CONTROL

The section on open-loop control has shown how the stepper motor may be controlled using a microprocessor, and provided step rates of 1000 steps per second are not exceeded, control may be achieved using about 10% of the computing time available. It is quite acceptable that the spare computing time may be used to check the true position of the motor against the anticipated position.

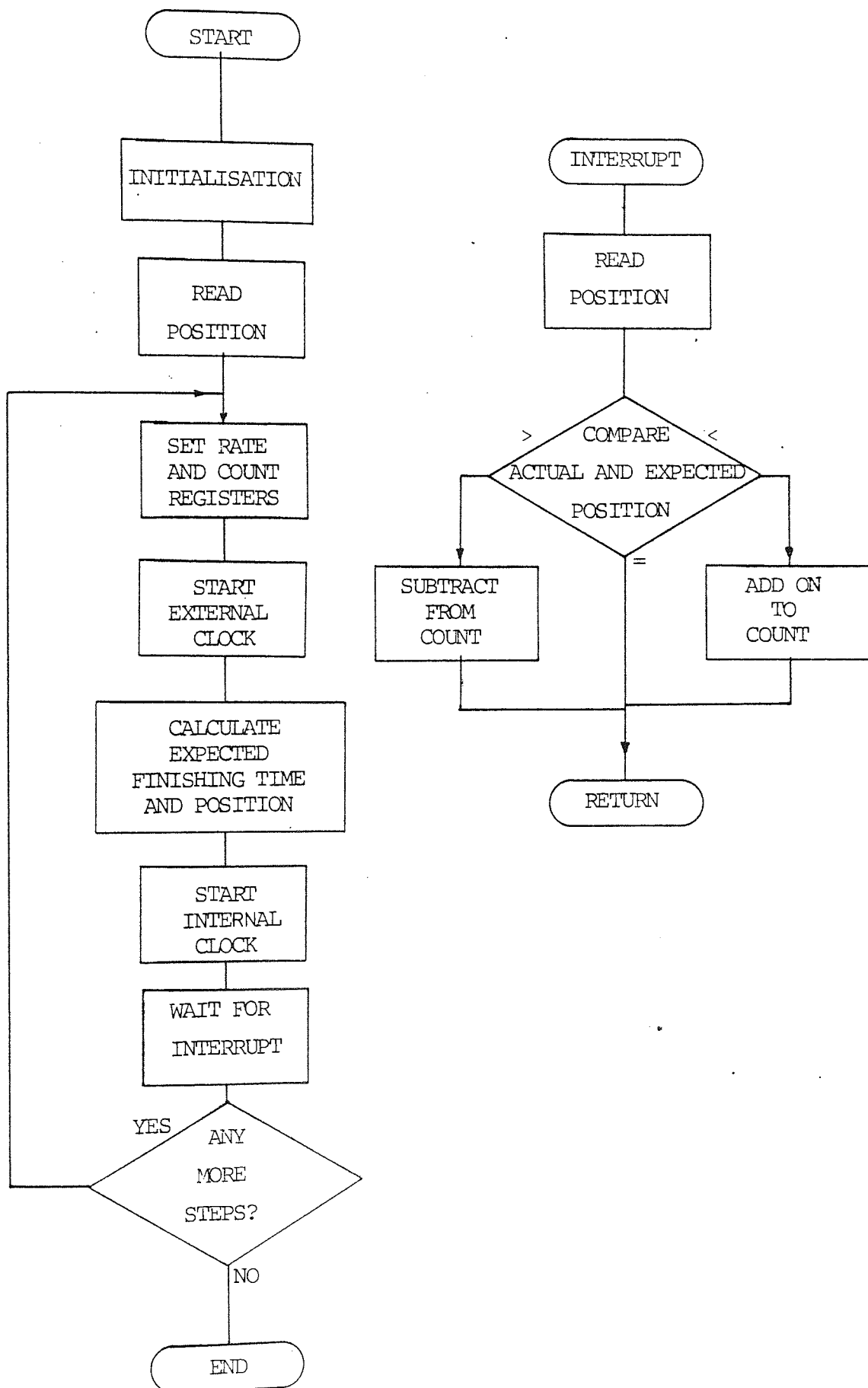


FIGURE 2.19 FLOW DIAGRAM FOR BOOK KEEPING
CLOSED LOOP CONTROL

Ideally this should be done for each step executed, however to reduce the computing time required one check after a block of steps would be quite sufficient. This is a simple procedure provided that only the position is to be checked, without regard to the rate of change of position. However a real time clock of low resolution can be used to implement a maximum time limit to execute each block of steps. If the motor is found to be in an incorrect position after the time limit has expired then extra step demands may be output to correct the position. Figure 2.19 shows a flow diagram for this type of control system.

2.6.4 CLOSED-LOOP STEP CONTROL

The method of motor control which makes most use of the microprocessor facilities is a system which is able to observe the acceleration of the stepper motor and control the step demands to match the load conditions of the motor. It has been shown by the open loop results, how the instant at which the next step is initiated considerably influences the response of the motor. This type of system controls the instant at which each step is demanded and hence can avoid problems associated with the resonant frequencies of step motor systems.

One method of closed-loop step control using an Intel 8080 microprocessor system is described by M. M. Radulescu and D. Stoia⁽¹⁵⁾. The method described used an incremental encoder to count the number of whole

steps executed by the motor and did not measure the absolute position of the motor. The timing of each step demand was derived directly from the encoder. The transducer was arranged in such a way that the pulse was sent to the microprocessor in advance of the equilibrium step position, thus the actual advance of the step demand was expressed in terms of a time delay after the feedback pulse was detected. This time delay was calculated from the average speed of the motor which had been observed over the previous few steps. The system was in fact a microprocessor implementation of the control strategy described by Kuo and Singh⁽¹³⁾. This type of system gives good acceleration torque and improved running conditions. However, it lacks the ability to relate demanded position with actual position after a number of steps have been executed. Therefore it is most important that spurious pulses are not created by the position transducer either by overshoot to the next step position, or by undershoot during settling.

A closed-loop step control system has been developed using an absolute position encoder so that step demand may be derived directly from the motor position. Any advancement of step demand can be achieved within the system software by indicating how many encoder increments before the equilibrium position, the step is required. The resolution of the encoder is $1/32$ of a step, therefore this is the accuracy to which the step demand may be executed. The use of an absolute position encoder also gives the advantage that the actual position can be checked

to ensure correct execution.

The major problem with the system was the time required to determine the position. The method described in section 2.6.2 using the serial Gray to binary conversion required a time of 72 μ s. During this time the position of the rotor changed considerably. At 1000 steps per second the rotor moves 6% of a step (2 encoder increments). A good parallel decoding method would substantially reduce this time.

2.6.5 RESULTS

The results described in this section are typical responses taken from a series of several results for each case.

The first set of results shown in Figures 2.20 and 2.21 refer to closed-loop step control and show how the motor responds from standstill as the step lead angle is increased. An advance of 1 represents each step being initiated when the encoder indicated that the motor had rotated through 31/32 of the previous step. The results show that in the lower current case an advance of 2 or 3 gives a good response, whereas any further advance results in an erratic performance of the motor. At the higher current however, advances of 4, 5 and 6 improve the response of the motor. The reason for these different results is the time delay incurred by the reading and converting of the encoder information, at the higher current the motor will accelerate faster and

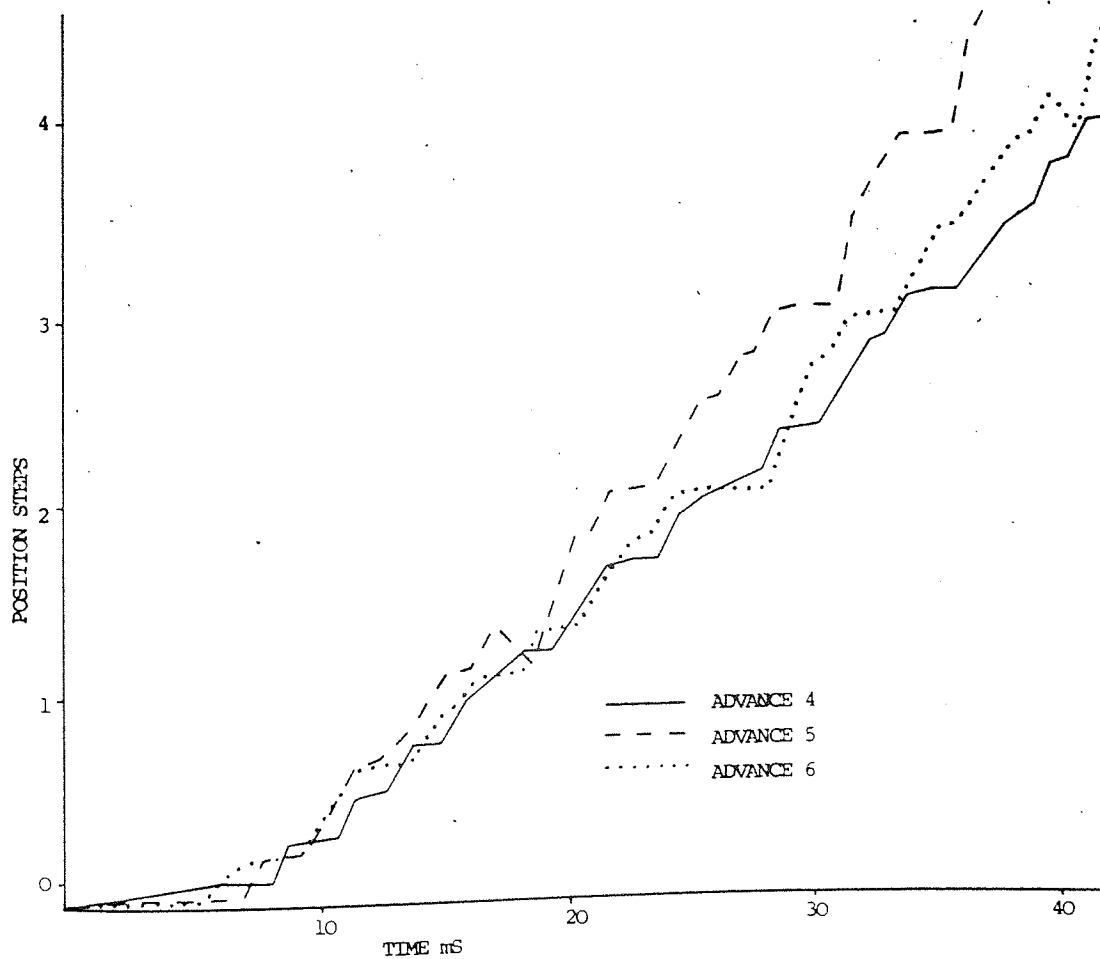
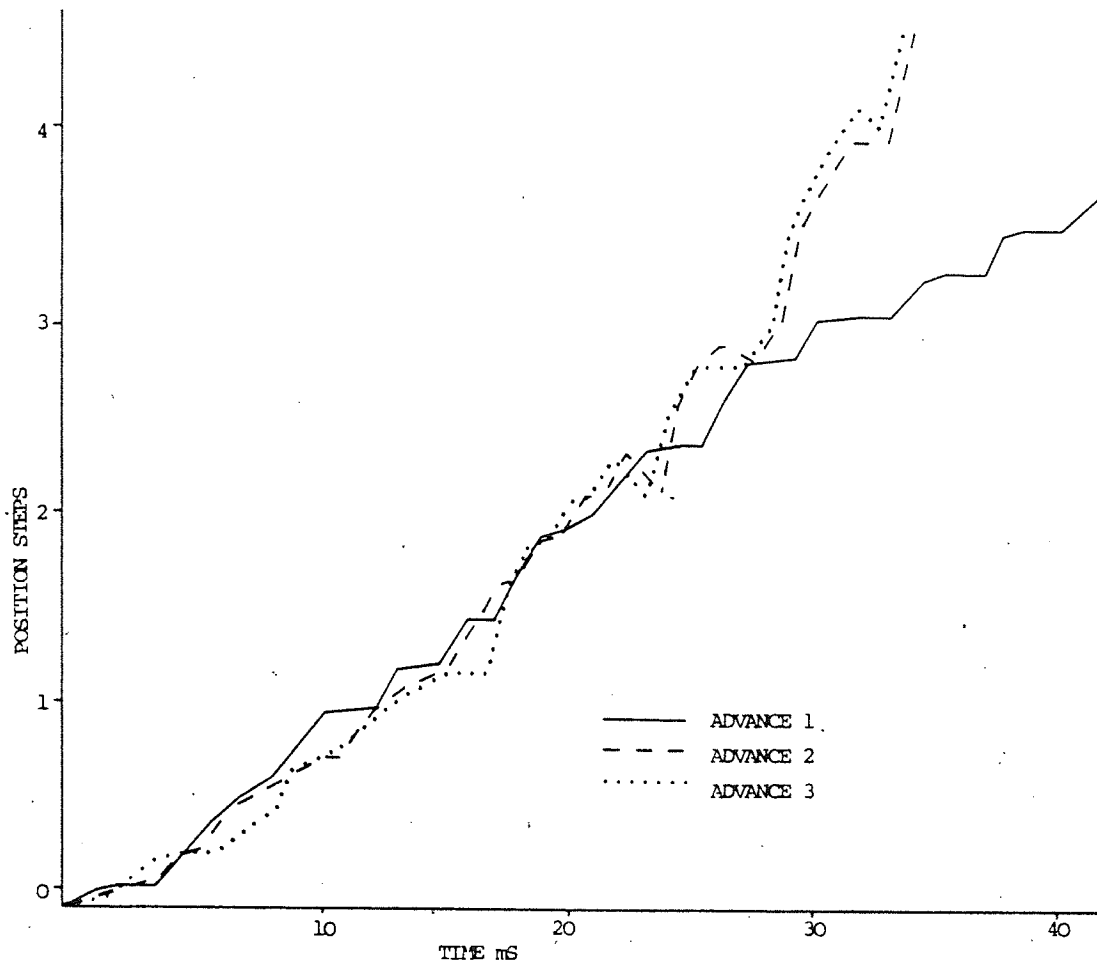


FIGURE 2.20 DYNAMIC RESPONSE 1 AMPERE

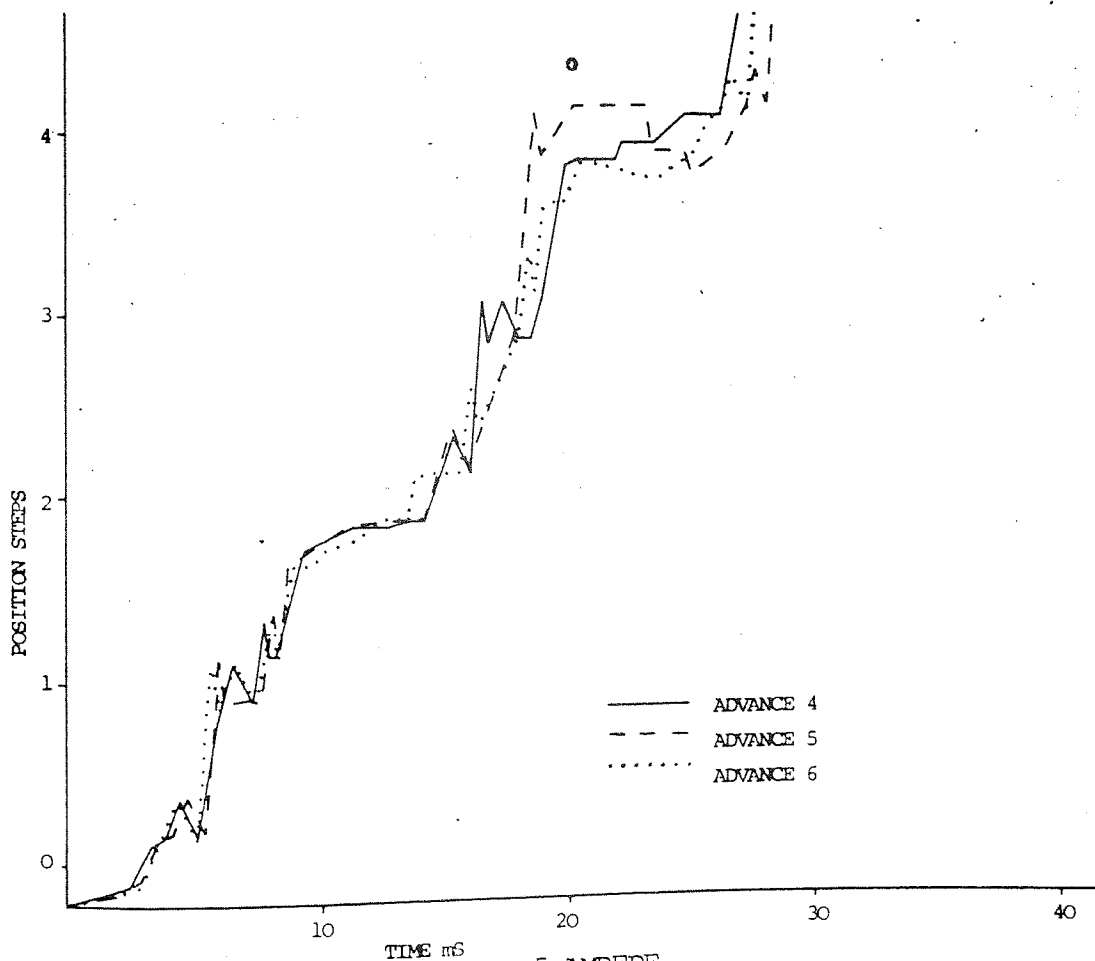
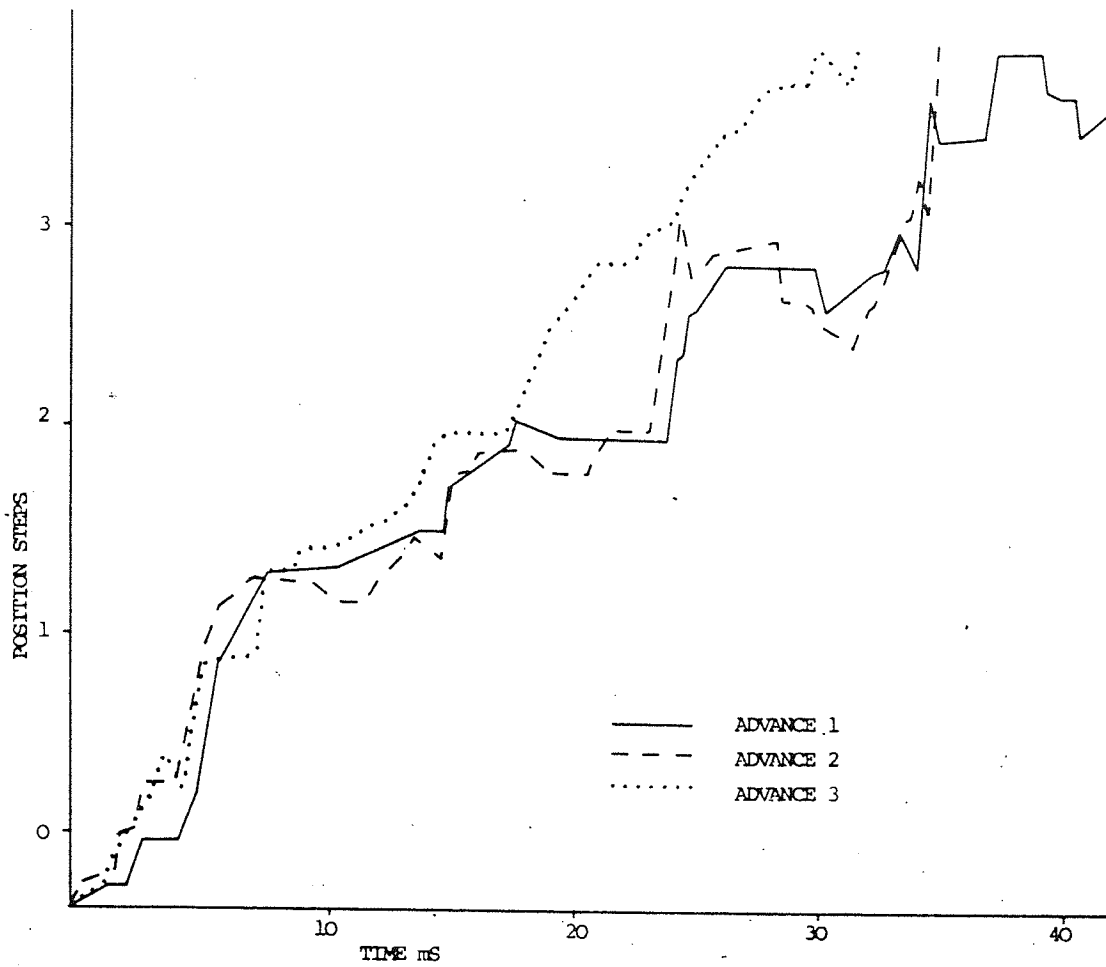


FIGURE 2.21 DYNAMIC RESPONSE 5 AMPERE

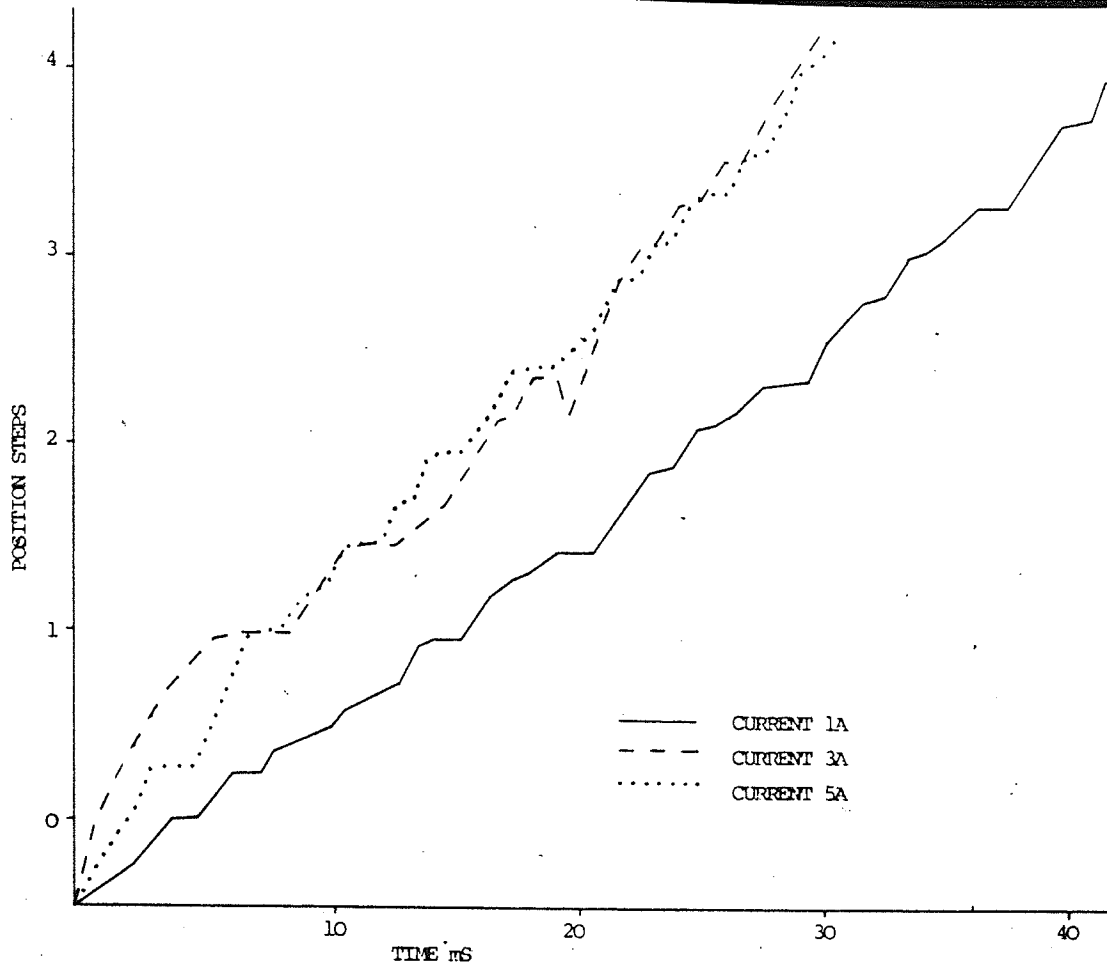


FIGURE 2.22 DYNAMIC RESPONSE VARIOUS CURRENTS

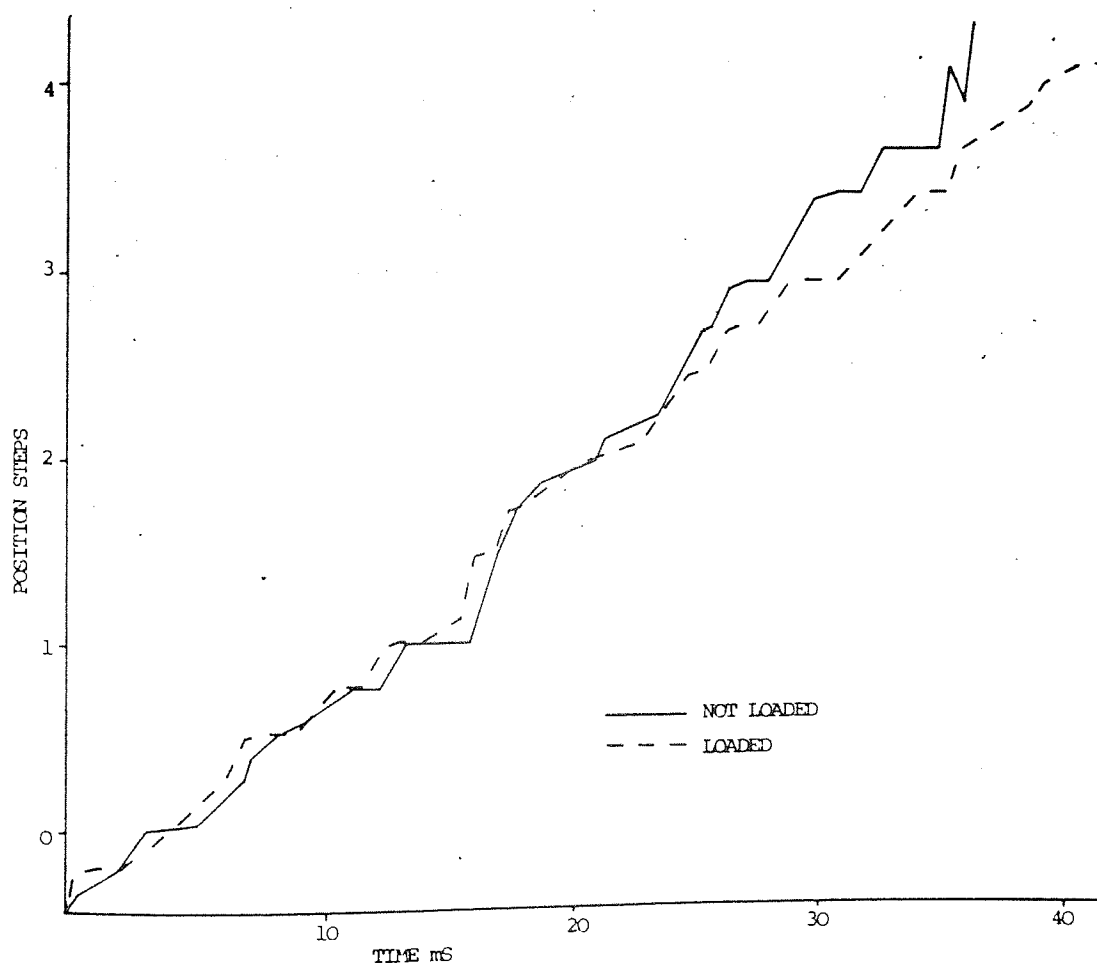


FIGURE 2.23 LOADED AND UNLOADED RESPONSE 1.5 AMPERE

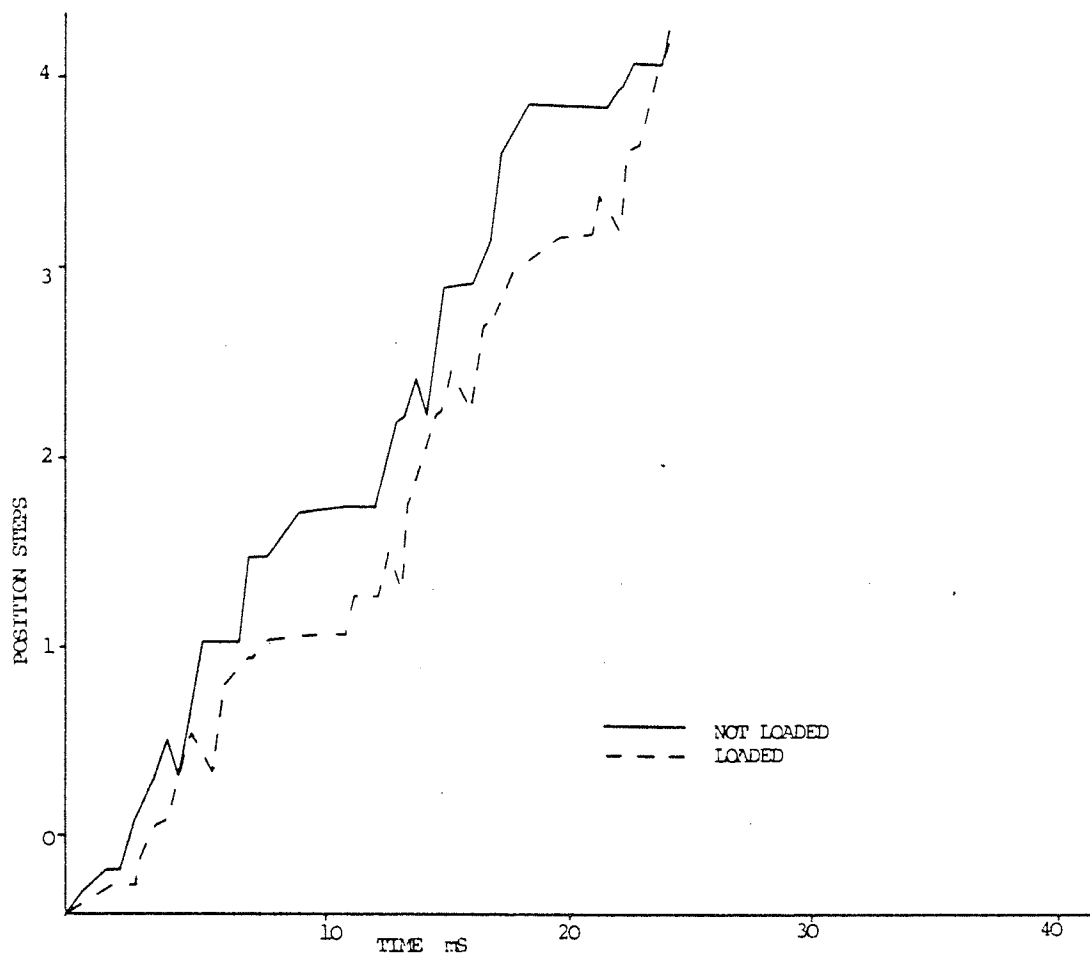


FIGURE 2.24 LOADED AND UNLOADED RESPONSE 5 AMPERE

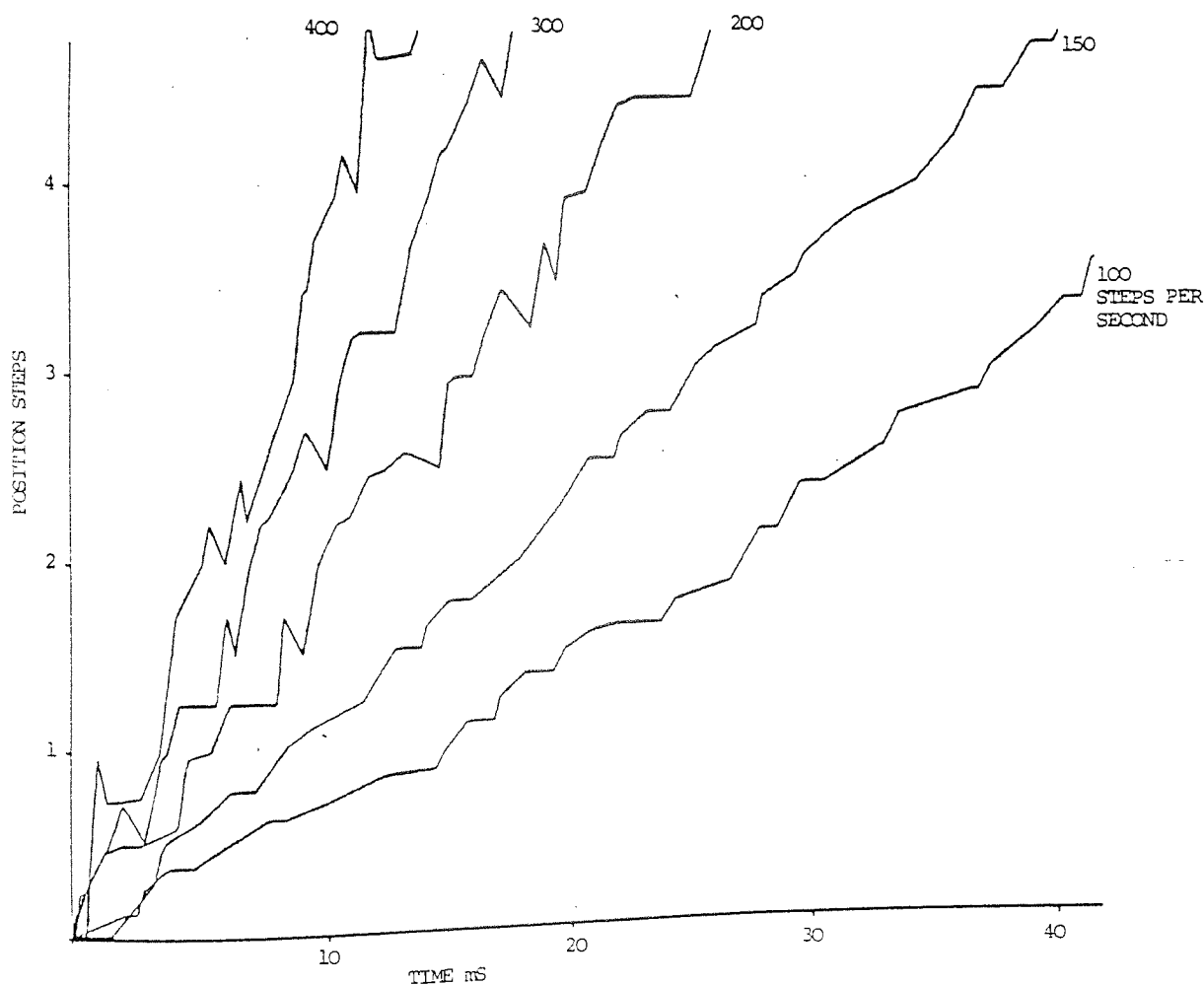


FIGURE 2.25 COMPARISON OF STEP RATES

hence require a further advance of step demand. This is shown more clearly by Figure 2.22. Due to the low torque and poor acceleration during each step, the 1A dynamic response is much slower than the higher current responses. The difference in acceleration during each step at different currents is shown clearly by the single step responses in Figure 2.12.

Figures 2.23 and 2.24 show how the system is able to cope with a load applied to the machine without loss of synchronism. The load slows the response of the motor and in turn the control system reduces the step rate demanded.

The results shown in Figures 2.20 to 2.24 are all presented to the same scale and to give some indication of motor speed Figure 2.25 is included. The results for this figure have been obtained from open-loop tests and are presented to the same scale as the closed-loop tests.

2.6.6 CONCLUSION

It has been shown how a system of closed-loop control is possible which checks the position of the motor after each block of steps has been executed. The system will safeguard against loss of synchronism and correct any position error incurred, it will not, however improve the actual performance of the motor.

Position feedback has been used to initiate step demands on the motor and it has been shown how the dynamic

response of the machine may be controlled by varying the instant of step demand. The ability of the system to cope with frictional load is demonstrated and the results show that although the motor runs at a slower rate, synchronism is maintained.

2.7 CONCLUSIONS

A variety of possible methods of microprocessor based stepper motor control have been investigated. It has been concluded that the microprocessor system used was not fast enough to maintain a real time clock of sufficient resolution to control the motor accurately. Open-loop control was achieved by using an external clock and the system is shown to function with adequate control for high step rates to be achieved. The most serious problem was encountered when closed-loop control was attempted, caused by the time required to obtain the position information in a usable form.

It is certain that in the near future faster and better microprocessor systems will be developed, but the manner in which they will be applied to stepper motors is not so certain. Open-loop control lends itself readily to the microprocessor control system, but no increase in motor performance is to be gained by their use. Closed-loop control however could result in a much improved motor performance by the use of microprocessors. If this is to be achieved then an integral design approach should be used so that a motor and encoder may be matched to produce a

suitable number of encoder increments per step.

Large Scale Integrated circuits (LSI) are now manufactured for many specialised applications and step motor controllers must surely develop along these lines. The possible result may be a dedicated motor control system based on a purpose built microprocessor system, rather than a general use system.

CHAPTER THREE

STATIC TORQUE DISPLACEMENT CHARACTERISTIC

3.1 INTRODUCTION

When the field windings of a stepper motor are energised the rotor settles to a precisely defined position which is determined by the method and direction of excitation, and the type and construction of the motor. The rotor is held in this position by forces set up due to the magnetic fluxes of the field windings. Any attempt to change the position of the rotor by applying an external torque will produce a motor torque equal in magnitude but opposite in direction. If the applied torque is removed the rotor will return to its original position. The torque which must be applied to just overcome the motor torque, and hence produce rotation is known as the HOLDING TORQUE.

The Static Torque Characteristic defines how the torque varies as a function of rotor position. A typical Static Torque Characteristic is shown in Figure 3.1.

The characteristic is symmetrical and cyclic. Figure 3.2 shows the progression of the rotor through four successive steps, the electrical excitation required for each step is shown in Table 2.1 and it can be seen from this table that after four steps have been executed the excitation currents have progressed through one cycle. It can be seen from Figure 3.2 that after four steps the rotor has rotated

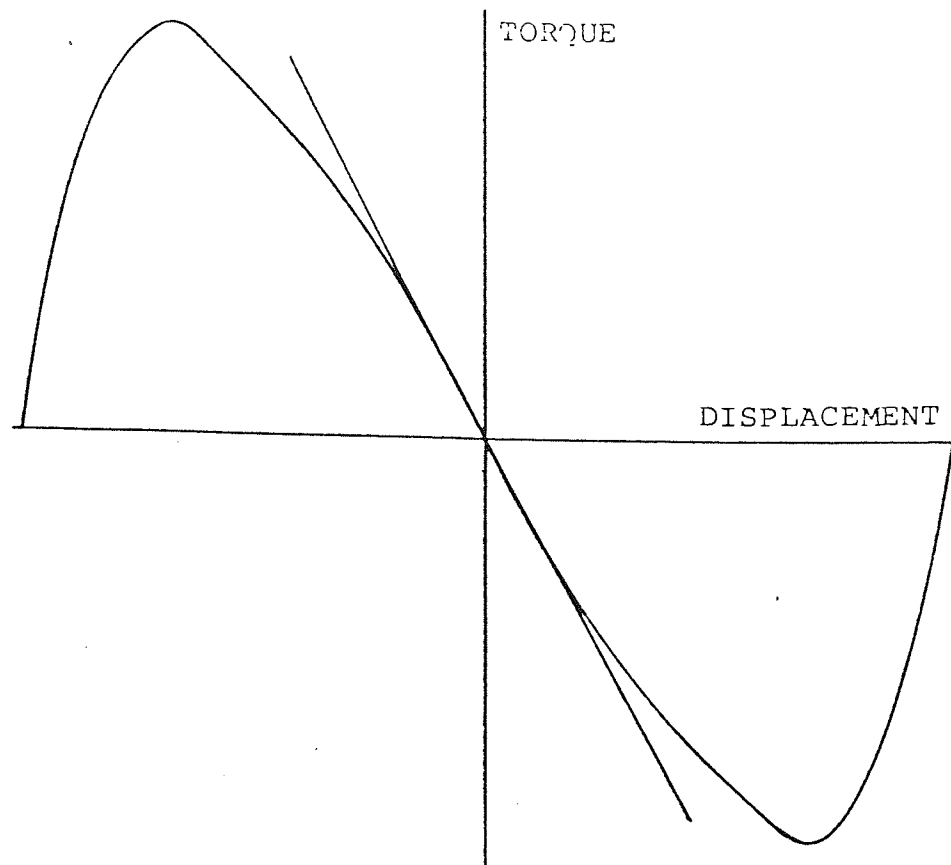


FIGURE 3.1a LINEAR APPROXIMATION

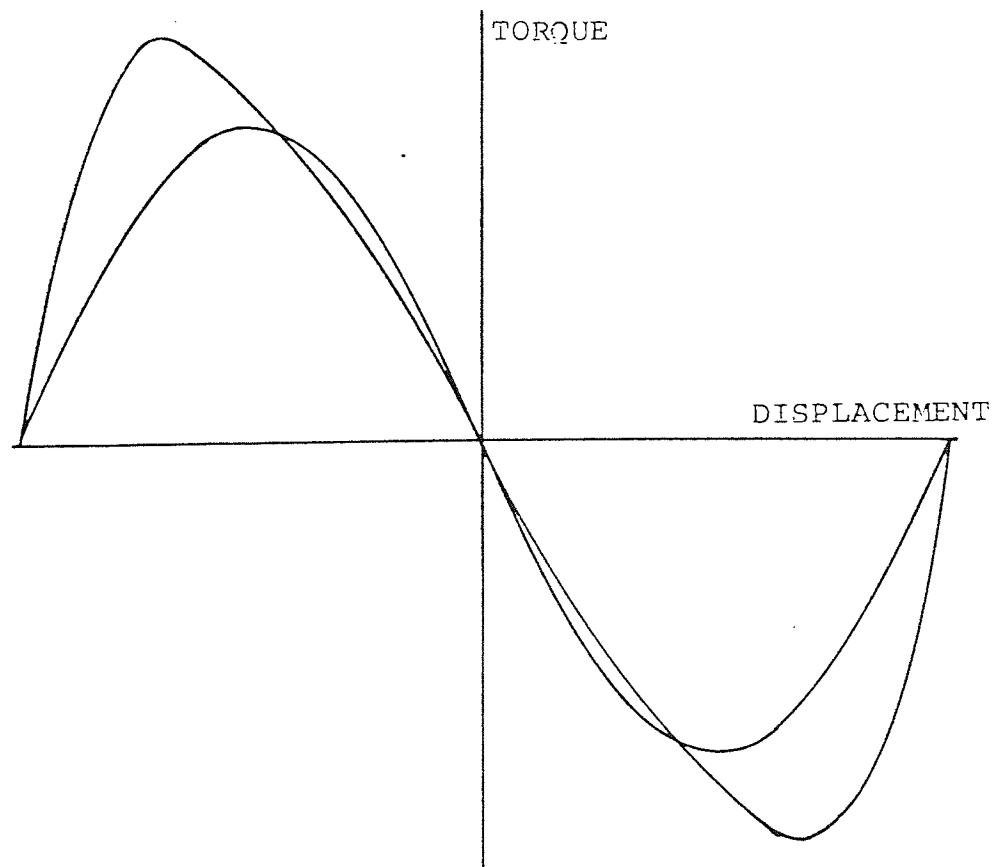


FIGURE 3.1b SINUSOIDAL APPROXIMATION

FIGURE 3.1 TYPICAL STATIC TORQUE CHARACTERISTIC AND ITS APPROXIMATIONS

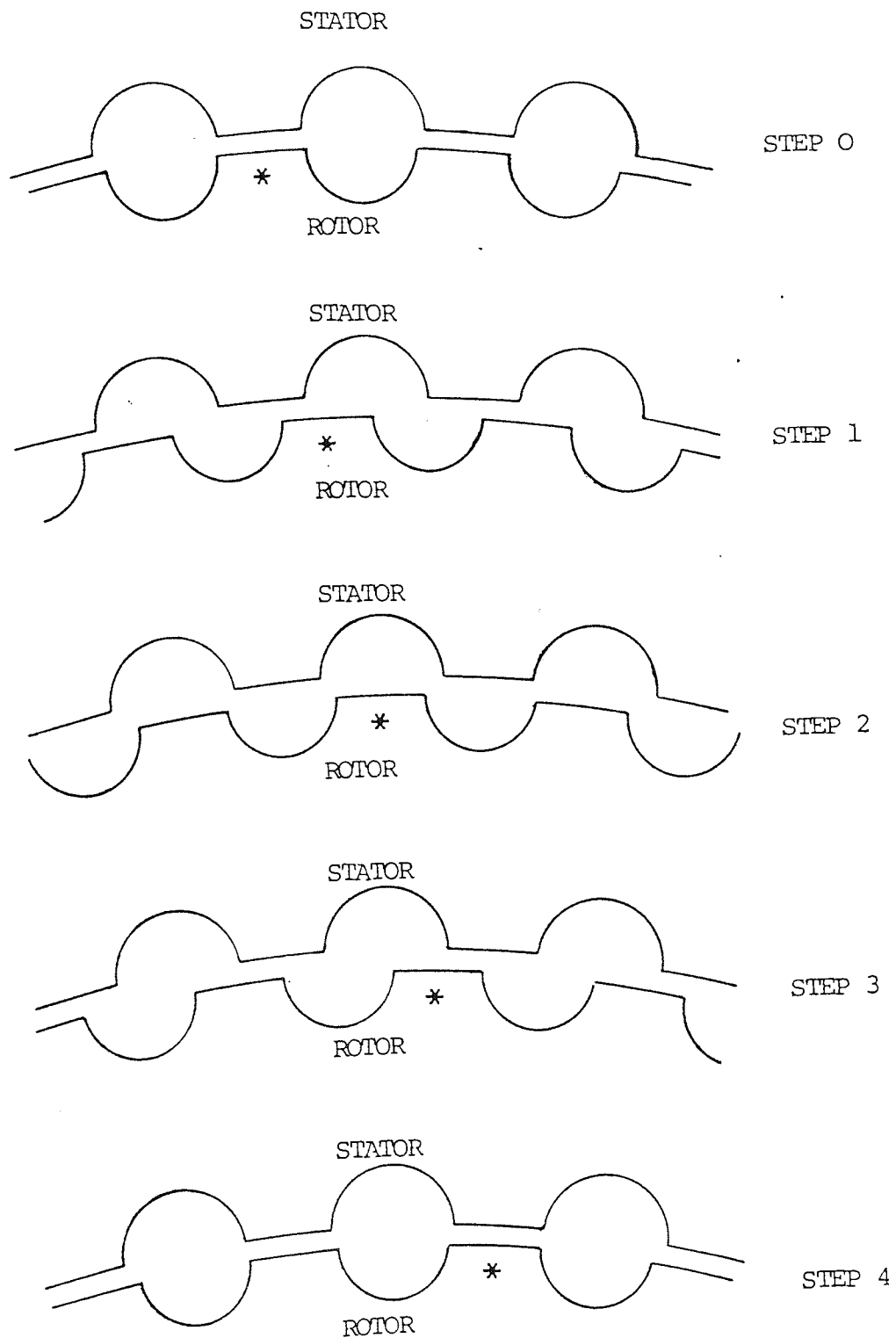


FIGURE 3.2 ONE STEPPING CYCLE

through an angle equal to one tooth pitch, and is in a mechanically similar position to the start of the first step. Thus it can be seen that one electrical cycle is equal to one cycle of the torque characteristic. For convenience the displacement of the torque characteristic is referred to in electrical degrees. The full characteristic as shown in Figure 3.1 duplicates information because of its symmetry, therefore results shown in this thesis are reduced to show only one half cycle.

Once the Static Torque Characteristic has been established for a particular motor under specific operating conditions, predictions of dynamic response to one or more distinct steps are possible. If an instantaneous change in the excitation condition occurs, then at that instant the equilibrium position changes but the inertia of the rotor prevents instantaneous stepping. Provided the excitation change produces a suitable step change in the equilibrium position the torque will increase to a near peak value. This results in the rotor moving to its new position. If the mechanical load and the inertia are known, then using the value of torque obtained from the characteristic, the single step response of the motor can be predicted and by complex equations the dynamic response over several steps may also be estimated.

One method of measuring the static torque is to clamp a lever to the rotor shaft, apply weights at a known radius and measure the angle of rotation. However, this method

requires that a machine be designed and constructed before the static torque can be determined. A method of predicting the torque accurately at the design stage would be a desirable advance in the development of stepping motors.

3.2 METHODS OF PREDICTING THE STATIC TORQUE CHARACTERISTIC

3.2.1 INTRODUCTION

The torque produced by a stepper motor is dependent upon its design and the intensity of its field currents which produce magnetic flux. Therefore the static torque characteristic can only be defined by a family of curves, one curve for each value of current.

The basic torque equation for reluctance type machines, states that the torque produced is proportional to the square of the flux across the air gap and from such data it would appear that a simple relationship between field current and torque could be deduced. However, the complex geometry and construction of the motor from different types of iron makes the torque-current relationship far more complex than ordinary saturation effects. Within the magnetic circuit there are 'Bottle Necks' and the flux density in these parts is considerably higher than the average, also the shape of the teeth on both the stator and the rotor causes an increase in the flux density to occur at the tooth corners. The result of this is that magnetic saturation occurs in certain parts of the motor while other points still have a relatively low flux density.

The idea of developing a model to determine the static torque characteristic of stepper motors has attracted considerable interest over recent years, the aim of most authors being to devise easier and more accurate methods of prediction. Any attempt to predict the dynamic response of a stepper motor with reasonable accuracy requires that the static torque characteristic be known over the normal operating range including, where appropriate, the effects of saturation which may occur. In this context many authors have taken the static torque, and applied different approximations to obtain linear models which have provided a physical insight into the operation of the step motor. Such models, however, have proved to be inadequate in accurately predicting the behaviour of practical stepper motors due to the neglect of magnetic saturation.

3.2.2 METHODS NEGLECTING MAGNETIC SATURATION

Methods of calculating the static torque in conjunction with the dynamic response came initially from Bailly⁽¹⁶⁾ O'Donohue⁽¹⁷⁾ and Kiebertz⁽¹⁸⁾ in 1960, 61 and 64 respectively. These authors approximated torque to a simplified linear characteristic as shown in Figure 3.1a. This approximation is quite reasonable for most applications, providing that the extent of angular displacement over which the approximation is valid is not exceeded. In all three cases the constant of proportionality was calculated from torque data obtained by direct measurement of the machine torque.

Robinson and Taft⁽¹⁹⁾ improved this approximation by

using a sinusoidal relationship between displacement and torque as shown in Figure 3.1b. This required only the maximum value of torque to be measured from the machine. In common with the linear approximation, no account was taken of the magnetic effects within the air gap of the motor, which generally produce a significant proportion of harmonic distortion.

One of the first attempts to predict the static torque characteristic was made by Snowdon and Madsen⁽²⁰⁾ who looked closely at the "Characteristics of a Synchronous Inductor Motor". They considered operation in the step mode and produced an equation to calculate torque from displacement and current. They considered the magnetic effects within the air gap of the machine and started with the premise that the permeance of the gap, associated with each pole, was not constant, but was a cosinusoid superimposed on a constant value. This resulted in an expression for torque, with one phase excited, which was periodic and included the fundamental and the second harmonic. Snowdon and Madsen then continued by calculating the torque for both phases excited, by adding the torque produced in one phase to the torque produced in the other phase but shifted by ninety electrical degrees. This resulted in the characteristic returning to a sinusoid. These equations give a result of zero torque for an unexcited motor, which in practice is not true.

Methods of predicting the static torque characteristic

which require flux linkage information of the machine come from Pickup and Russell⁽²¹⁾ and Stephenson and Corda⁽²²⁾. Such methods obviously take account of the magnetic nonlinearities of the machine, but require that a machine be available for the flux linkage tests to be carried out. Methods of estimating flux linkage information from the machine geometry would overcome the main disadvantage of this type of torque prediction. However, the complexity of the magnetic circuit of the stepper motor makes accurate estimation very difficult, even if the magnetic fluxes are restricted to their linear regions. Any attempt to estimate flux linkage information for saturated magnetic circuits would not produce reliable results.

Determining the flux linkage characteristics of a machine by experiment, rather than directly obtaining the static torque characteristics, can only be justified if the flux linkage data is required for other reasons as well. Hence such methods of determining the static torque are most useful as part of a dynamic response prediction.

The approach to the derivation of an equation for the static torque characteristic which is to be used in this research was originated by H. D. Chai⁽²³⁾ and later extended by M. Justice⁽²⁴⁾.

Chai developed an equivalent magnetic circuit and analysed it in terms of its major components, that is the M.M.F.'s generated in each winding and the permeances of

all the air gaps which are active in producing torque. The effects of machine iron was neglected with the exception of the permanent magnet circuit.

Chai considered the equivalent magnetic circuit of a permanent magnet type stepper motor, and because the reluctance of the pole pieces was regarded as negligible, the magnetic circuit reduced to 4 identical, simplified circuits. One of these circuits was then used for the formulation of static torque.

Chai defined the permeance of the air gaps by placing the following restrictions on them:-

- (1) Permeance must be periodic with respect to displacement.
- (2) Permeances of the poles relative to each other vary only in angular displacement.
- (3) The permeance is such that it results in a torque due to the permanent magnet in the absence of the excitation m.m.f.

As a result of these conditions, he showed the permeance to be represented by a constant value with a fundamental and fourth harmonic superimposed. This resulted in a cogging torque which was proportional to the fourth harmonic of the normally excited torque. The torque equation developed included terms for the excited m.m.f.s of the windings and can be easily modified for single phase

excitation by substituting a zero value for one of the values of m.m.f.. The permanent magnet motor model may also be modified to represent the variable reluctance motor by equating the m.m.f. of the permanent magnet to zero.

Justice extended this development by assuming that the permeance function contains Fourier coefficients up to, and including the fourth harmonic. This extension removes the restriction which states that for two phase simulation the phase currents should be equal. The advantages of removing this restriction are demonstrated by investigating the single step dynamic response. Because of the inductance involved it is impossible to produce a step change in the field current; in fact the current increases to the required value in a manner which depends upon the dynamic characteristics of the machine at that instant. To predict the dynamic response it is necessary to calculate the torque at small increments in time, during which one of the field currents is changing. Justice used a digital computer programme to find the static torque at each instant from the known phase currents and the instantaneous angular displacement.

The equivalent magnetic circuit used by Chai and Justice takes no account of the magnetic fluxes going into the non-linear region, caused by magnetic saturation of the iron components of the motor. However, Justice showed how modifying the values of magnetic permeance for the air gap results in an improvement of the predicted torque for higher values of field current.

3.2.3 METHODS WHICH CONSIDER MAGNETIC SATURATION

The importance of including the effects of magnetic saturation in any model used to predict the static torque, is clearly shown by Figures 3.3 and 3.4. These figures show that at a low current of 3 Ampere there is little saturation and a model neglecting saturation, such as that proposed by Justice⁽²⁴⁾, returns acceptable results up to this current. However if the current is increased to a value of 7 Amperes then the non-linearities of the motor restrict the torque production, and so the model returns values of torque in excess of the experimental results.

In 1975 Harris et.al.⁽²⁵⁾ devised a method of calculating the average torque from the machine geometry which takes account of the effects of magnetic saturation. This method analysed the conditions at both the stable and unstable positions of zero torque and found the average torque by using the differences in total flux and position. This method gives a very useful measure of the overall torque capabilities of the machine, as the complete characteristic can often be predicted from experience, once the average and peak values of torque are known. However, prediction of the value of torque at a particular angle for a machine, using this method, becomes a matter of estimation.

H. D. Chai⁽²⁶⁾ approached the problems of saturation by approximating the saturation effects to one parameter in the form of a hyperbolic tangent as shown in Figure 3.5 such that, at low m.m.f.'s the characteristic is linear, but

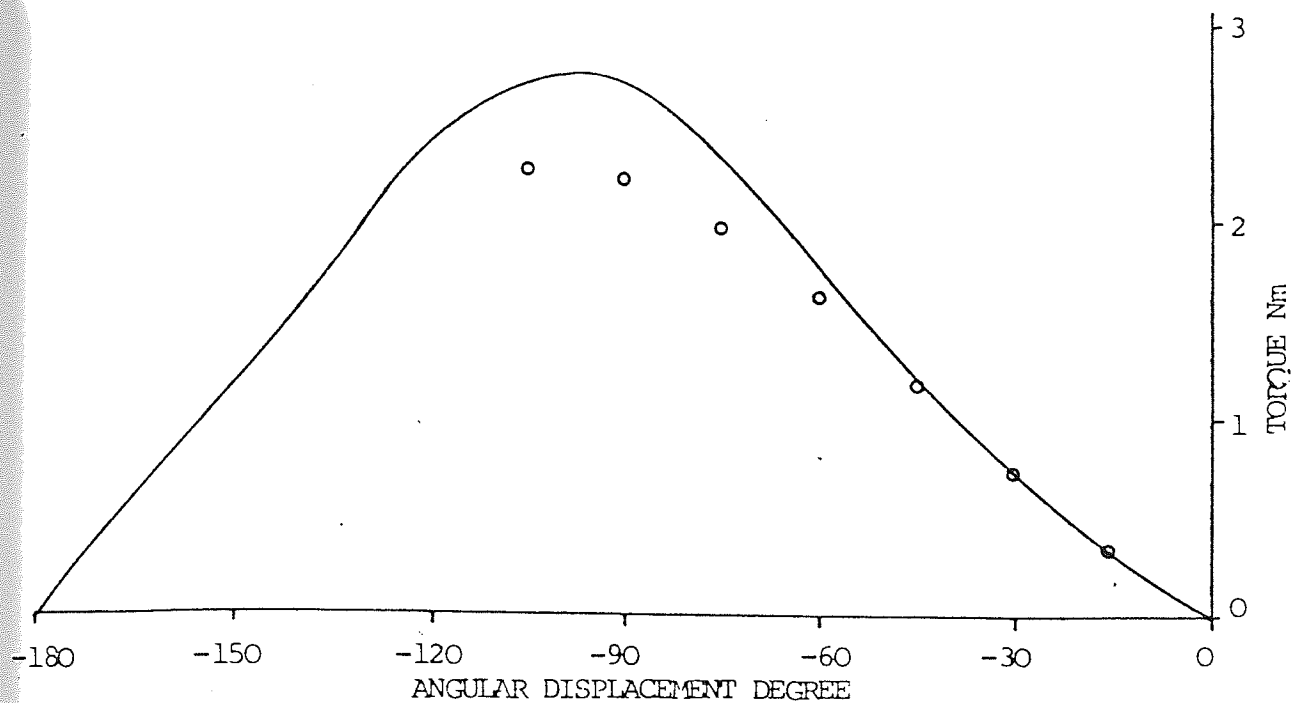


FIGURE 3.3 TORQUE ANGLE CHARACTERISTIC FOR 3A. TWO PHASE USING JUSTICE'S MODEL

NOTE THE SYMBOL O IS USED THROUGHOUT TO DENOTE VALUES OF TORQUE MEASURED FROM THE MACHINE.

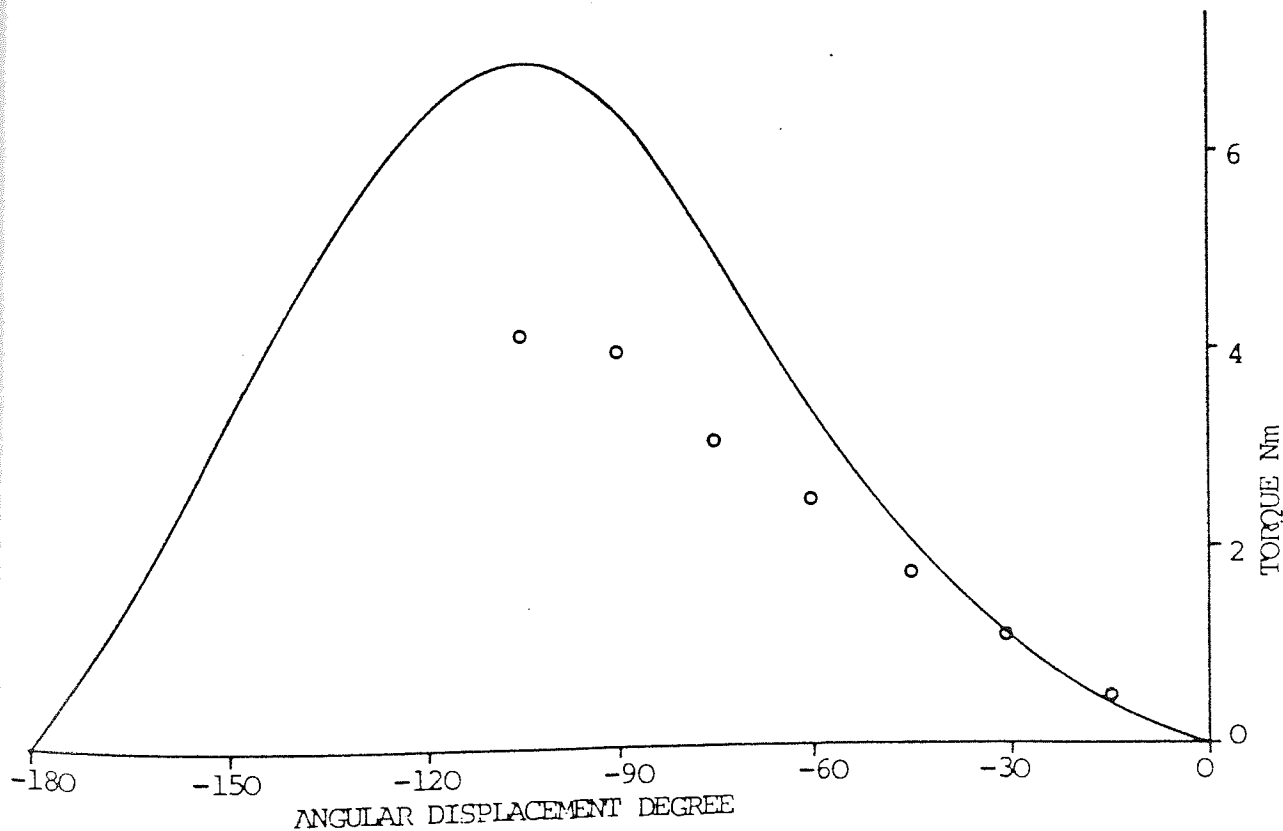


FIGURE 3.4 TORQUE ANGLE CHARACTERISTIC FOR 7A. TWO PHASE USING JUSTICE'S MODEL

at high m.m.f.s the flux is asymptotic to a saturation value. Suitable characteristics can be selected so that the saturation value and the linear portion are correct, however the points between are fixed by the tangential expression.

The 'Lumping' of all the saturation effects, for all the different iron components into just one variable, is an over simplification. Results produced are obtainable in practice once the function has been correctly scaled for the machine under investigation. This type of approximation is most useful to aid dynamic response prediction, perhaps as part of a digital computer programme but is of limited use to the machine design engineer.

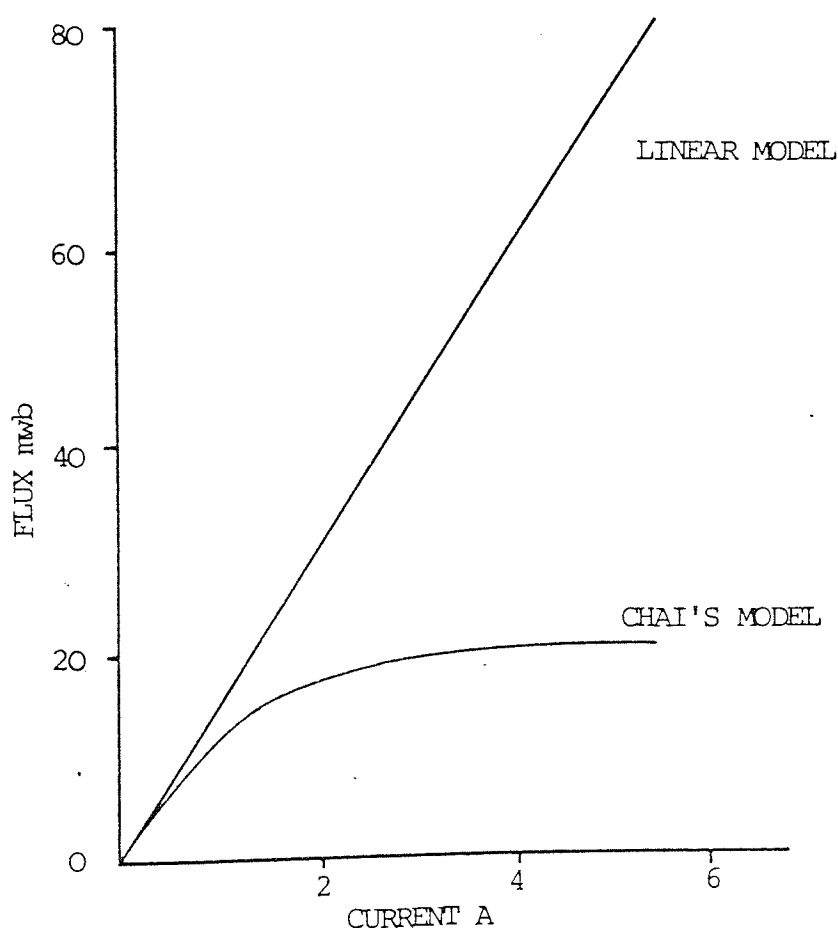


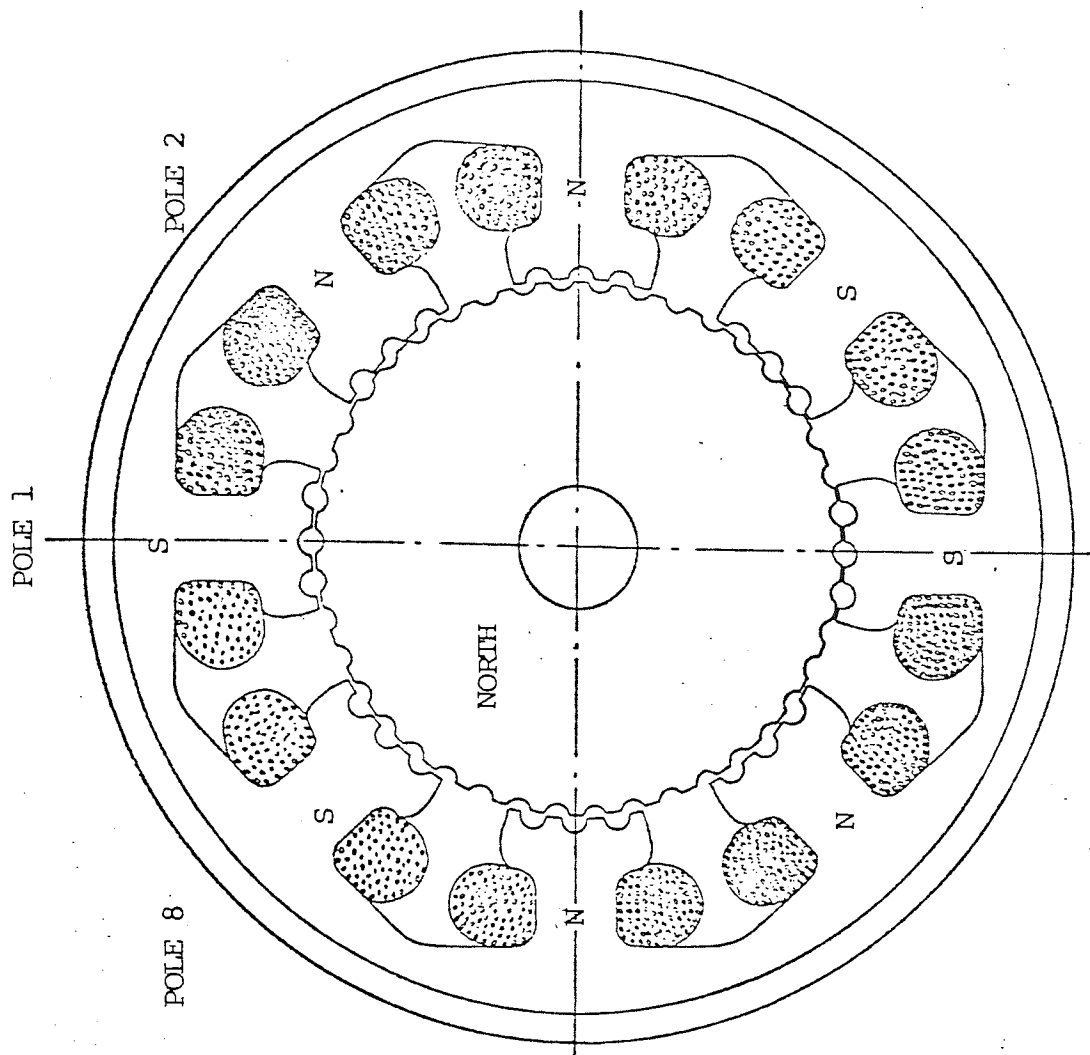
FIGURE 3.5 H. D. CHAI'S APPROXIMATION TO THE HYPERBOLIC TANGENT

Kenjo and Ichikawa (27) propose a method of torque analysis in terms of Stieltjes Integral. The theory begins with a previously established expression for magnetisation torque which is valid for non-linear magnetic properties, including hysteresis. By introducing the idea of the 'Periodic Stieltjes Integral' the theory is developed into a systematic method of torque production analysis. The theory may be applied to reluctance motors, hysteresis motors, permanent magnet motors and step motors. The use of this method to calculate torque requires the magnetising force or flux density to be known at certain points around the rotor tooth structure and the paper illustrates a graphical method of estimating these values. In the paper no effort is made to show the accuracy of the graphical techniques used.

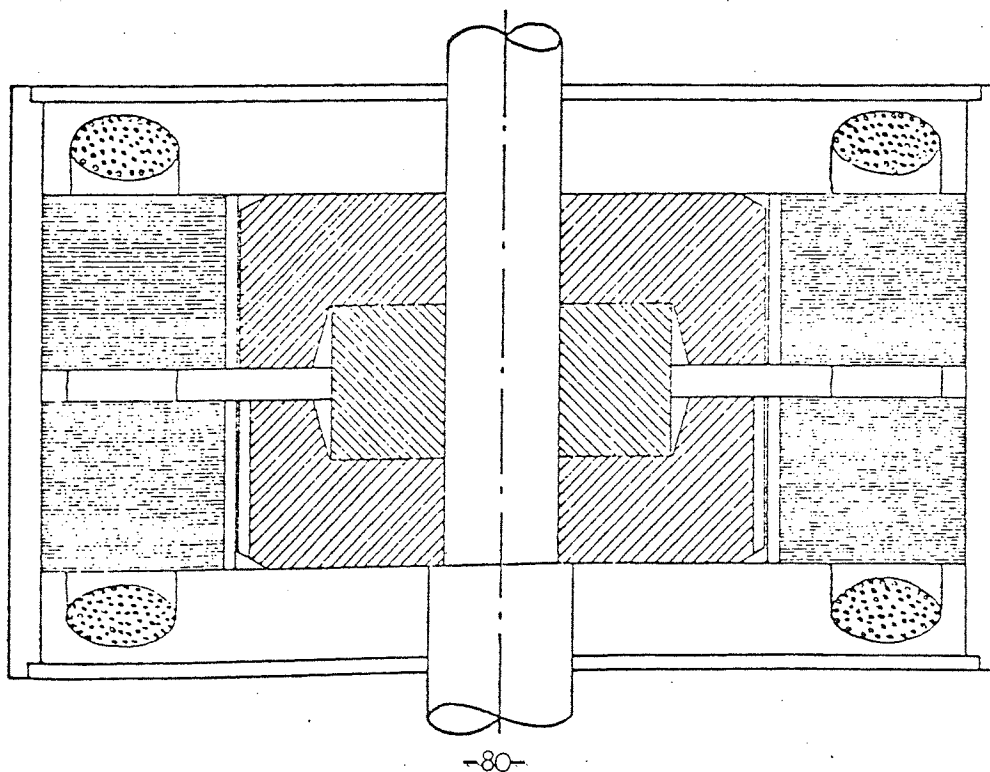
3.3 EQUIVALENT MAGNETIC CIRCUIT OF THE MOTOR

3.3.1 INTRODUCTION

The method of torque calculation used by both Chai and Justice may be extended further by including in the model, terms to represent the reluctance of the iron components in the magnetic circuit. However, this requires the re-examination of the basic magnetic circuit and further evaluations of previously accepted assumptions. The equivalent magnetic circuit was derived from the geometry of the machine, the construction of which is shown in Figure 3.6.



CROSS SECTION PERPENDICULAR TO SHAFT



CROSS SECTION PARALLEL TO SHAFT

FIGURE 3.6 THE CONSTRUCTION OF THE HYBRID VERNIER STEPPER MOTOR

The rotor consists of a cylindrical permanent magnet with a soft iron cap on each pole, the whole assembly being mounted on the rotor shaft. Each pole cap has forty-two teeth protruding radially, with semi-circular slots between each tooth. The teeth on each pole cap are offset by half a tooth pitch, so that the teeth of the north pole align with the slots of the south pole and vice versa.

The stator consists of eight salient poles constructed of laminations and positioned axially to coincide with the rotor pole caps. The stator is then placed in a sleeve type of casing. The pole pieces of the stator have teeth and slots similar to the rotor, but the pitch of the stator teeth is $2\pi/40$. The two phase windings are wound in such a manner as to produce the magnetic polarities shown in Figure 3.6, phase No. 1 exciting poles 1,3,5 and 7 and phase No. 2 exciting the other poles.

It can be seen from Figure 3.6 that there are sixteen distinct and separate flux paths in the stator, two in each pole piece. These flux paths are kept separate in the development of the model because the flux, due to the permanent magnet, flows in opposite directions at the front and rear of the motor.

For the purposes of identification of components and flux paths within the motor the terms 'Front' and 'Rear' have been adopted. The FRONT refers to the end of the machine which houses the NORTH pole of the rotor permanent

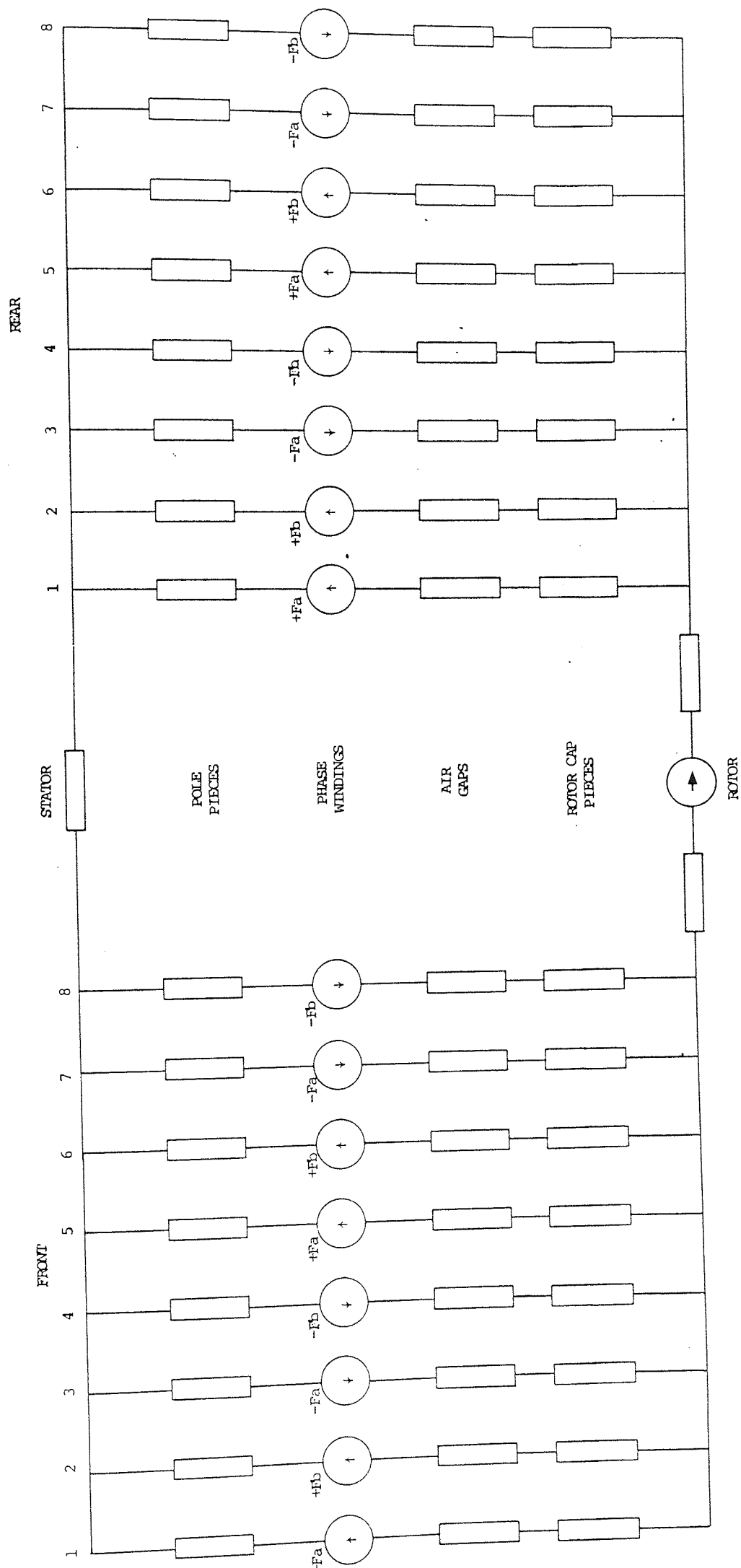


FIGURE 3.7 THE 16 LIMB EQUIVALENT MAGNETIC CIRCUIT

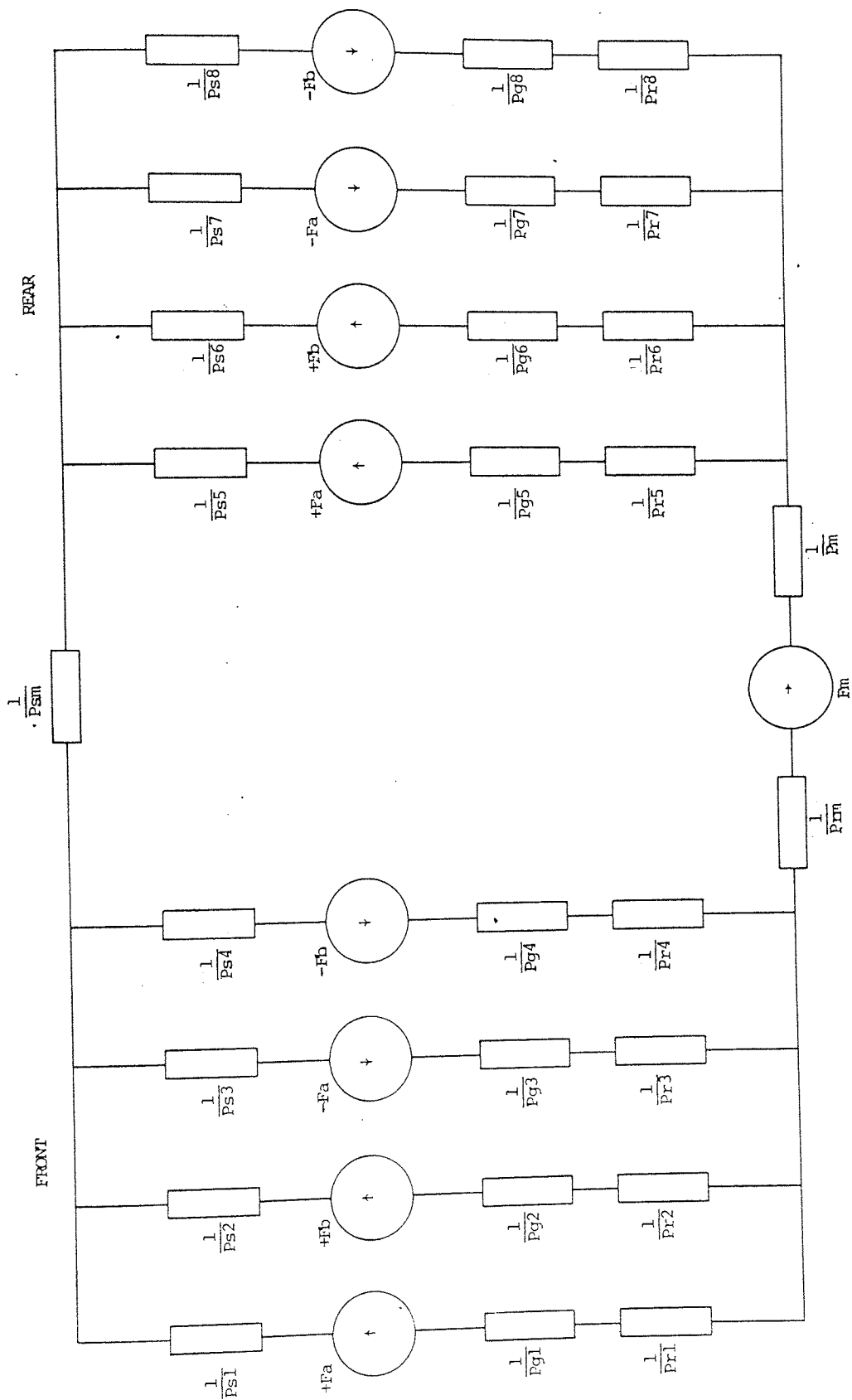


FIGURE 3.8 THE 8 LIMB EQUIVALENT MAGNETIC CIRCUIT

magnet. The terms 'North' and 'South' ends of the machine have been avoided to prevent confusion with the varying magnetic polarities of the stator poles.

The full sixteen limb magnetic representation of the motor is shown in Figure 3.7. From this figure it can be seen that certain limbs of the model are identical under all conditions and these limbs can therefore be taken in parallel and the model reduced to eight limbs. The eight limb equivalent model is shown in Figure 3.8. It must be noted that each permeance in the eight limb model actually represents a double permeance in the machine. It may also be seen that certain other limbs are similar but not identical and although it may be mathematically acceptable, no further reduction is made in the model at this stage because it would involve combining limbs in parallel at opposite ends of the machine.

THE ELEMENTS OF THE EIGHT LIMB MODEL

- i 1 to 8 limb number, limb 1 combines poles 1 and 5 of Figure 3.6 at the Front of the machine.
- Psi Permeance of the flux path in the stator pole pieces. All eight are identical but vary depending on the flux in each limb.
- Pri Permeance of the flux path in the pole cap on the rotor associated with one limb. All eight are identical but vary depending on

the flux in each limb.

F_i m.m.f. generated by the winding on each pole in limb 1 $F^1 = I^1 N$

limb 3 $F^3 = -I^1 N = -F^1$ etc.

The positive direction of flux is from stator to rotor, therefore F_i is positive for north poles.

P_{gi} Permeance of the air gap associated with one limb. $P_{g1} = P_{g7}$ at all times.

P_{sm} Permeance of the stator associated with the permeant magnet flux i.e. the flux path from the front laminations via the sleeve casing to the rear laminations.

P_{rm} Permeance of the rotor associated with the permeant magnet flux i.e. the sum of both paths from the rotor teeth of the pole caps to the permanent magnet.

P_m Permeance of the permanent magnet.

F_m m.m.f. of the permanent magnet.

3.3.2 PERMEANCE OF THE AIR GAP

Much work has been published concerning the permeance of toothed structures and air gaps, which can be applied to stepper motors. Due to the complex form of the teeth on the

rotor and stator, the air gap changes shape with angular position and hence the value of permeance is periodic. Figure 3.9 shows the variation of permeance as the rotor teeth move relative to the stator. The most convenient method of expressing the permeance of the air gap is to use the Fourier Cosine Series of the periodic function:-

$$P_t = \mu_o t \left[C_o + \sum_{n=1}^{\infty} C_n \cos n \theta_e \right] \quad (3.1)$$

where P_t is the permeance of each stator-rotor tooth air gap

C_n is the nth Fourier Cosine Series Coefficient

t is the stack thickness

$t = 0.04$ m for the machine under investigation.

Calculation of the permeance of such air gaps is complex, however three different methods are considered, all of which involve digital computer techniques to solve the resulting equations.

H. D. Chai⁽²⁸⁾ showed how the permeance of toothed structures could be estimated by using a 'Straight Line Arc' method. This involved a permeance formula which is developed by using field patterns where the lines of flux consist of only straight lines and circular arcs. For this method of calculation of permeance, the shape of the teeth has to be approximated to the rectangular form shown in Figure 3.10. Two other limitations are that the tooth depth must be large compared with the air gap, and that the tooth width is less than the valley width, but not less

than half the valley width. This may be expressed as a ratio of tooth width t_w , to tooth pitch, t_p , so that the limitation becomes:-

$$0.33 < \frac{t_w}{t_p} < 0.5$$

It is widely acknowledged that to obtain the greatest static torque from a given motor this ratio should be about 0.4, and it is generally found that the designed value of t_w/t_p lies between 0.35 and 0.42. Therefore for stepper motors this limitation on gap geometry causes no problems. For example, the machine used for the tests reported in this chapter has a ratio t_w/t_p of 0.42. As the air gap in the machine is generally made as small as possible, within mechanical constraints, typically 0.13 to 0.15 mm, the requirement that tooth depth is large compared with the gap is also satisfied.

Permeance is calculated for one pair of teeth as their relative positions vary from maximum permeance to minimum permeance, and this is taken to be one half cycle of the function to be expressed as the Fourier series. The results of such a procedure carried out on the tooth structure shown in Figure 3.10 are given in Table 3.1.

Jones⁽²⁹⁾ proposed a different method for the prediction of the permeance of the air gap from the machine geometry, which is known as the 'Conformal Transformation' method. The same restrictions as the Straight Line Arc method apply to this method, and so the same approximation to the tooth

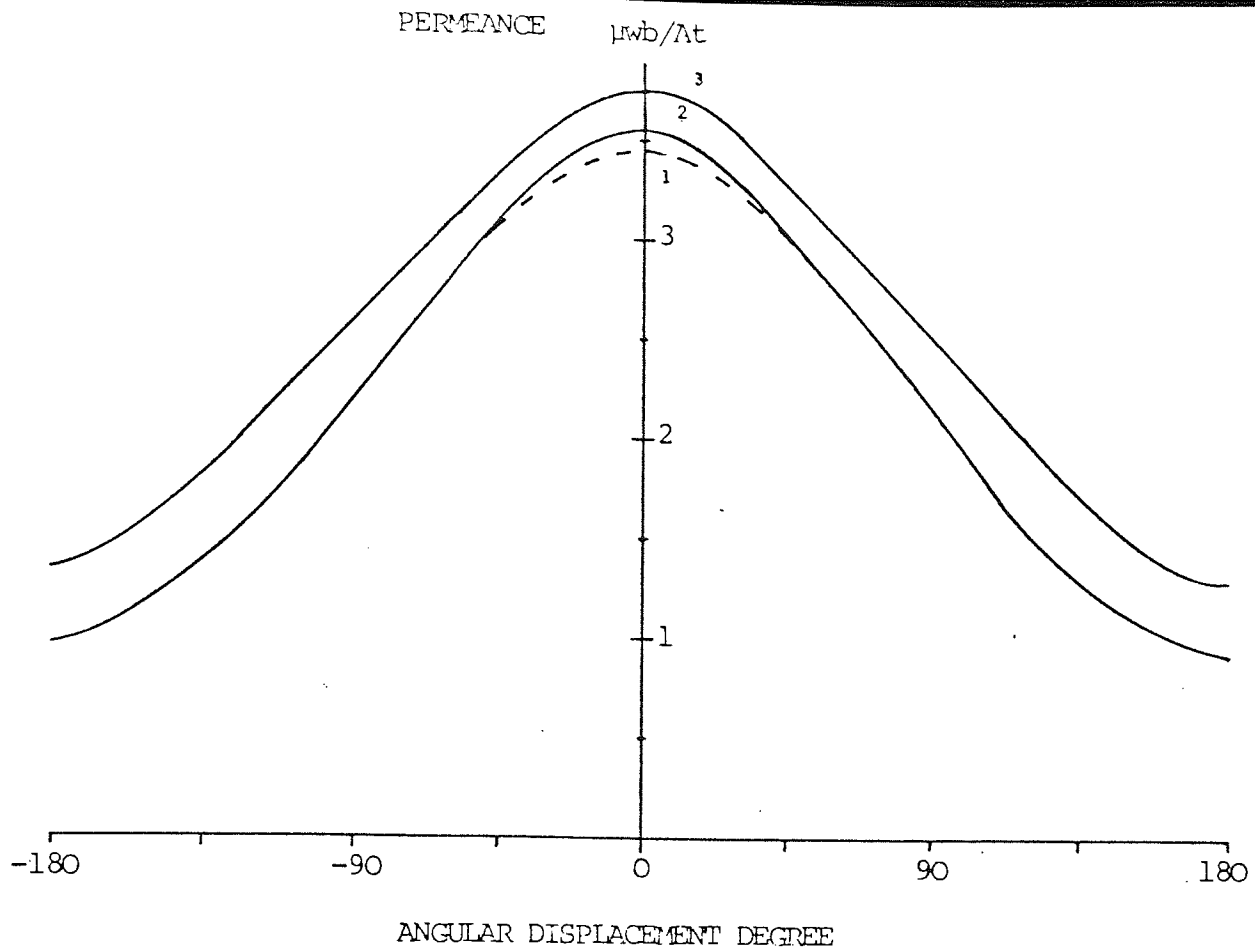


FIGURE 3.9 PERMEANCE AGAINST ANGLE CHARACTERISTIC

structure of the machine has to be made. The 'Conformal Transformation' method considers two conditions. The first condition is when the teeth are almost aligned and the reluctance force is due mainly to the flux between the faces and sides. The second condition is when the teeth are misaligned and the reluctance force is mainly due to the flux between the corners of opposing teeth. The author then develops force equations for the two configurations using conformal transformation techniques. The simpler fields problem is solved in the mapped plane, and the force involved found by integrating the normal derivative of field strength along the boundary for each condition. The

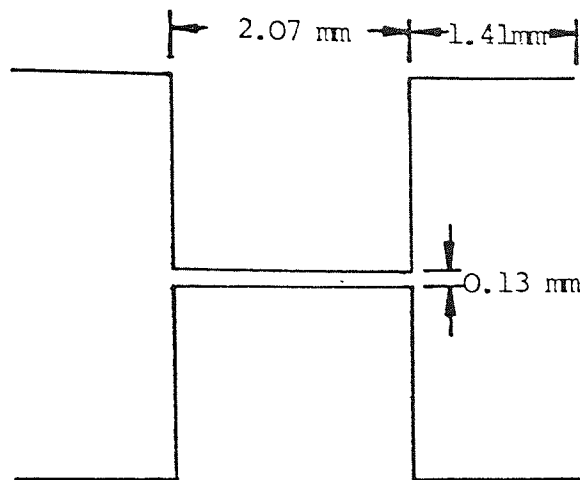


FIGURE 3.10 RECTANGULAR APPROXIMATION TO TOOTH PROFILE

total force being found by superposition of the two conditions. The permeance is then evaluated from the integral of the total force. The resulting permeance function is then converted to its Fourier series. The results obtained using this method are shown in Table 3.1.

Finally Chai⁽³⁰⁾ has proposed a method of calculating the permeance between toothed structures of arbitrary shape. This method does not require the geometry of the teeth to be approximated to rectangles but instead used the shape of the teeth as shown in Figure 3.11. The technique which Chai used is based on the 'Moment Method' of field computation and involves the solving of two-dimensional integral equations for potential. For the moment method of calculation the tooth boundary is split into N segments and it is assumed that the magnetic charge is uniform within each segment. The integral equation can then be solved for each segment by applying the appropriate boundary conditions to obtain permeance. Calculations are by matrix numerical methods using a digital computer. The accuracy depends upon the number and size of the segments. As the number of segments increase, the size of the resulting matrix to be solved increases, and hence the required computer space becomes considerable. The results for permeance using the moment method are shown in Table 3.1.

Air gap permeance was calculated by the three methods described, and the results are shown in Table 3.1. These results were provided by Dr. H. D. Chai.

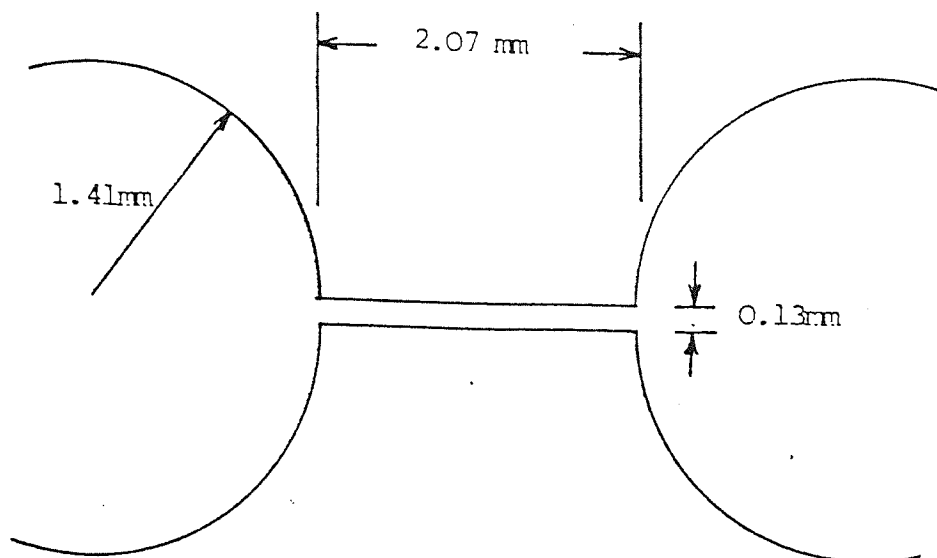
	STRAIGHT LINE ARC	CONFORMAL TRANSFORMATION	MOMENT METHOD
C_0	10.9	10.9	12.7
C_1	6.62	6.36	6.04
C_2	0.137	0.183	0.111
C_3	0.487	0.432	0.409
C_4	0.0914	0.121	0.227

TABLE 3.1 NORMALISED TOOTH PERMEANCE COEFFICIENTS

Table 3.1 compares the results of the three different methods of obtaining the permeance coefficients of the air gap between two teeth. Both the Straight Line Arc method and the Conformal Transformation method require that the tooth geometry be approximated to the rectangular form shown in Figure 3.10. The moment method, however, uses the tooth geometry as shown in Figure 3.11.

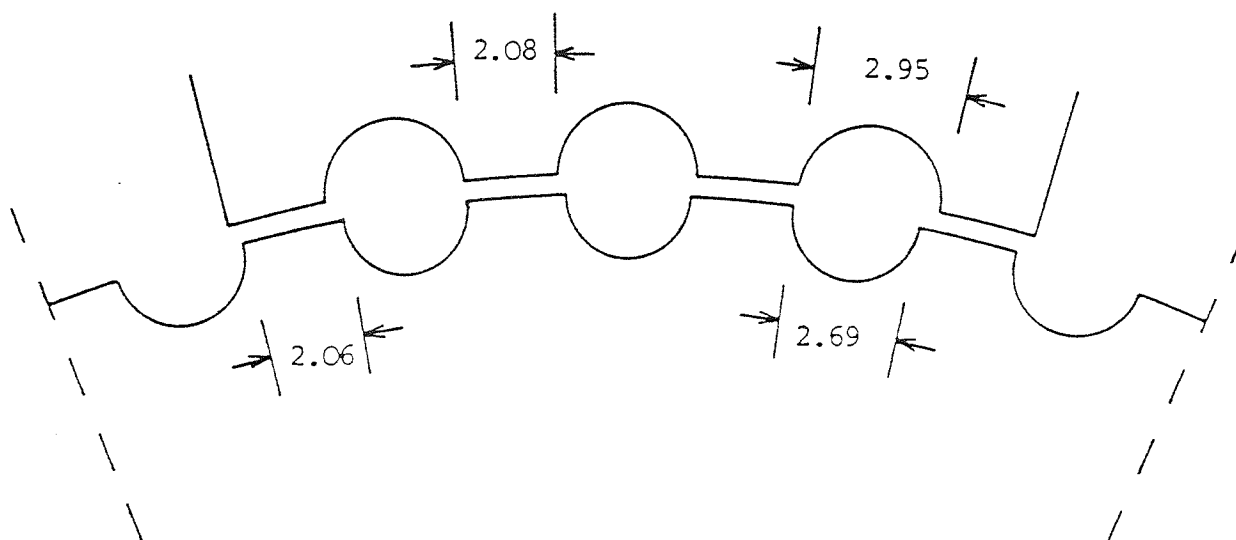
The geometry of one pole piece of the motor under investigation is shown in Figure 3.12 and it can be seen from this diagram that the pole consists of four identical teeth. With the pole in a position of maximum permeance, as shown, two tooth pairs are approaching maximum permeance and the other two pairs are just past the point of maximum permeance. The permeance characteristics for each tooth pair are in fact offset by eighteen electrical degrees.

The permeance of each tooth pair may be expressed:-



DIMENSIONS IN MILLIMETRE

FIGURE 3.11 SEMICIRCULAR APPROXIMATION TO TOOTH PROFILE



AIR GAP = 0.13 mm

DIMENSIONS IN MILLIMETRE

FIGURE 3.12 AIR GAP PROFILE FOR ONE POLE

$$\text{First Pair } P = \mu_o t \{ C_o + C_1 \cos(\theta e - 27^\circ) + C_2 \cos 2(\theta e - 27^\circ) \\ + C_3 \cos 3(\theta e - 27^\circ) + C_4 \cos 4(\theta e - 27^\circ) + \dots \}$$

$$\text{Second Pair } P = \mu_o t \{ C_o + C_1 \cos(\theta e - 9^\circ) + C_2 \cos 2(\theta e - 9^\circ) \\ + C_3 \cos 3(\theta e - 9^\circ) + C_4 \cos 4(\theta e - 9^\circ) + \dots \}$$

$$\text{Third Pair } P = \mu_o t \{ C_o + C_1 \cos(\theta e + 9^\circ) + C_2 \cos 2(\theta e + 9^\circ) \\ + C_3 \cos 3(\theta e + 9^\circ) + C_4 \cos 4(\theta e + 9^\circ) + \dots \}$$

$$\text{Fourth Pair } P = \mu_o t \{ C_o + C_1 \cos(\theta e + 27^\circ) + C_2 \cos 2(\theta e + 27^\circ) \\ + C_3 \cos 3(\theta e + 27^\circ) + C_4 \cos 4(\theta e + 27^\circ) + \dots \}$$

The permeance of the air gap for the pole piece is the summation of these four equations

$$P_g = \mu_o t \{ 4C_o + \sum_{n=1}^{\infty} C_n [\cos n(\theta - 27^\circ) + \cos n(\theta - 9^\circ) \\ + \cos n(\theta + 9^\circ) + \cos n(\theta + 27^\circ)] \}$$

simplifying

$$P_g = \mu_o t \{ 4C_o + \sum 2C_n (\cos 27^\circ n + \cos 9^\circ n) \cos n\theta e \} \quad (3.2)$$

Comparison of equations (3.1) and (3.2) will show that the relationship between the tooth and pole Fourier

coefficients is:-

$$C_n(\text{pole}) = 2C_n(\text{tooth}) (\cos 27^\circ n + \cos 9^\circ n)$$

or in terms of permeance of the pole:-

$$P_n = 2\mu_o t C_n(\text{tooth}) (\cos 27^\circ n + \cos 9^\circ n) \quad (3.3)$$

where P_n is the nth Fourier Coefficient of the permeance of the pole.

It is convenient to calculate the numerical relationship between C_n for a tooth and P_n for a pole of the machine under investigation.

$$P_0 = 2.01 \times 10^{-7} C_0 \quad \text{wb/At}$$

$$P_1 = 1.89 \times 10^{-7} C_1 \quad \text{wb/At}$$

$$P_2 = 1.55 \times 10^{-7} C_2 \quad \text{wb/At}$$

$$P_3 = 1.05 \times 10^{-7} C_3 \quad \text{wb/At}$$

$$P_4 = 5.03 \times 10^{-3} C_4 \quad \text{wb/At}$$

Applying these figures to the permeance coefficients given in Table 3.1 we have:-

	STRAIGHT LINE ARC	CONFORMAL TRANSFORMATION	MOMENT METHOD
	$\mu\text{wb/At}$	$\mu\text{wb/At}$	$\mu\text{wb/At}$
P_0	2.20	2.20	2.55
P_1	1.25	1.20	1.14
P_2	0.0212	0.0283	0.0172
P_3	0.0513	0.0455	0.0430
P_4	0.00459	0.00608	0.00114

TABLE 3.2 POLE PERMEANCE COEFFICIENTS

Table 3.2 compares the three methods of obtaining permeance data in terms of permeance coefficients for the air gap of one pole piece.

3.3.3 PERMEANCE OF THE IRON COMPONENTS

In the equivalent magnetic circuit diagram, Figure 3.8 all the motor components are represented. A number of these components represent permeances of the iron parts of the motor. These iron components have been considered negligible by previous authors, because under low excitation conditions the value of permeance which they represent is large compared to the permeance of the air gaps. However, as magnetic excitation increases to a point where magnetic saturation begins to occur in these components their permeance values greatly reduce and become comparable to the values of the air gaps. For this reason it is essential that any analysis of the equivalent magnetic circuit should include all the iron components.

Some method had to be devised to represent the non-linear characteristic of the iron components and as numerical evaluations of the magnetic circuit were to be carried out on a digital computer, the most direct method of representation was chosen. This involves converting flux-magnetisation information of the iron into flux-permeance data for each component. The 'B-H' curves for the types of iron used in the motor are available to motor designers and manufacturers, however as it is the permeance of the

iron components which are the parameters of interest in the magnetic circuit, the data of the B-H curves has to be converted to permeance against the flux curves for the particular components of iron represented in the magnetic circuit.

Figure 3.13 shows the B-H curves for the two types of iron used in the stator and rotor. These curves may be converted to flux-m.m.f. curves by applying the dimensions of the machine to the axes of the curves, thus:-

$$\text{FLUX } \phi = \text{FLUX DENSITY} \times \text{SECTIONAL AREA } [B \times a]$$

$$\text{m.m.f.} = \text{MAGNETISING FORCE} \times \text{ACTIVE LENGTH } [H \times l]$$

The final stage to obtain a curve representing permeance is

$$\text{PERMEANCE } P = \frac{\text{FLUX } \phi}{\text{m.m.f.}}$$

The results obtained for both the stator and rotor iron are shown in Figures 3.14 and 3.15 respectively.

In obtaining the permeance-flux characteristics the values of active area and active length have to be deduced, which were measured from scale drawings of the machine. In the stator, the flux path is well defined, therefore accurate data is easily obtained. In the rotor however, the flux path undoubtedly varies as the flux changes, therefore the values used in the calculations were an estimate obtained by taking a mean value from a maximum

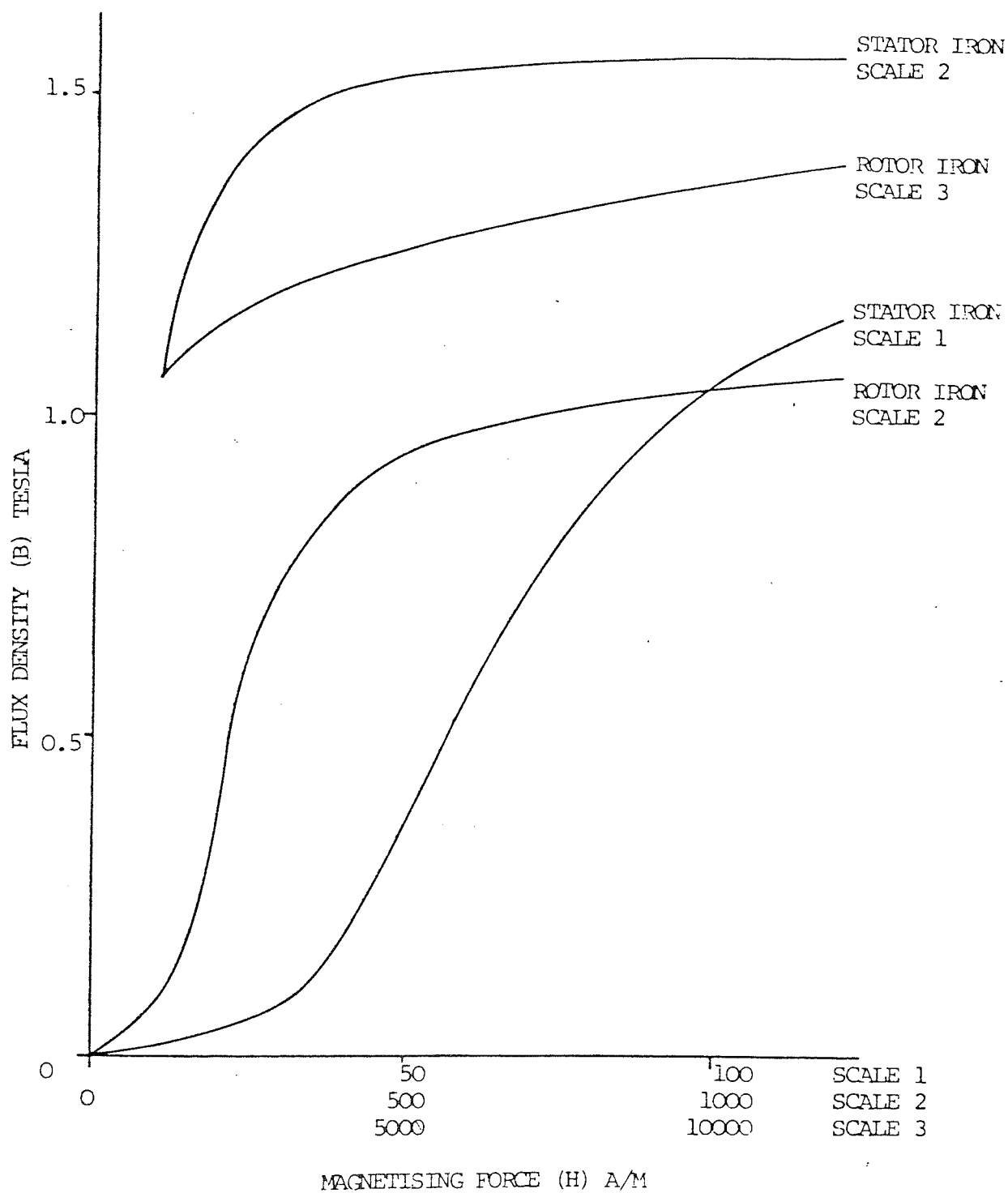


FIGURE 3.13 B-H CURVES FOR BOTH STATOR AND ROTOR IRON TYPES

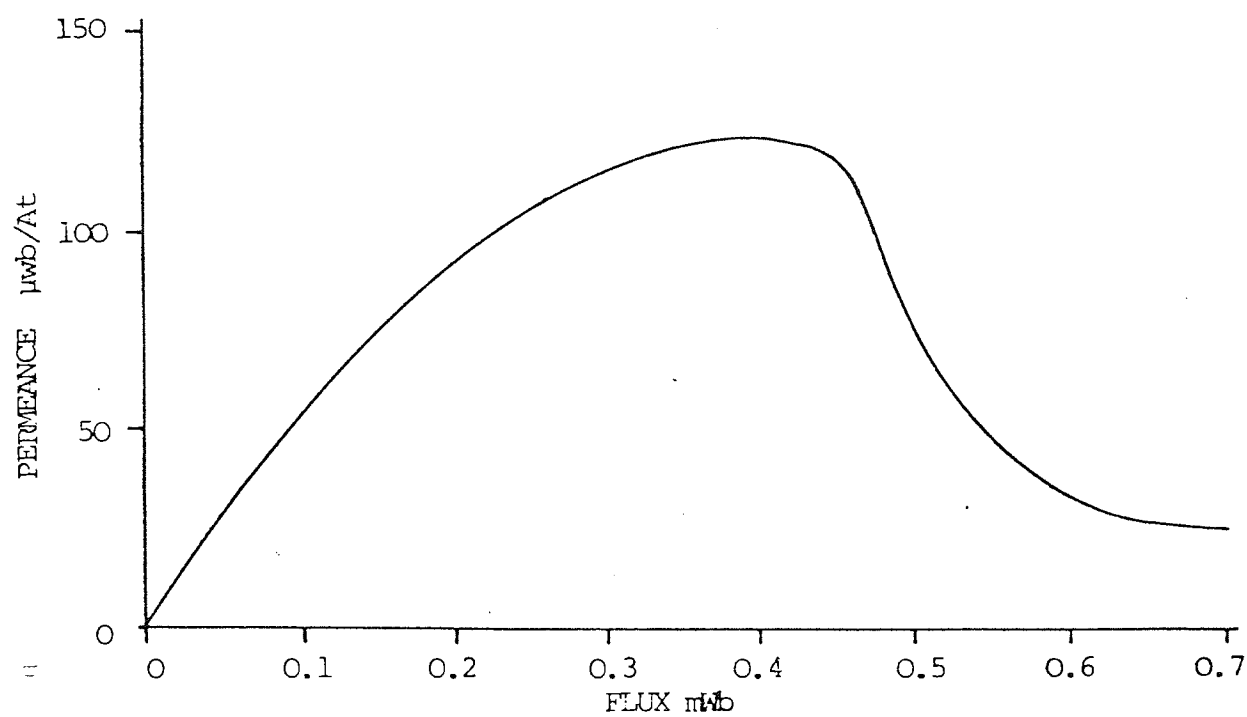


FIGURE 3.14 PERMEANCE-FLUX CHARACTERISTIC FOR THE STATOR COMPONENTS

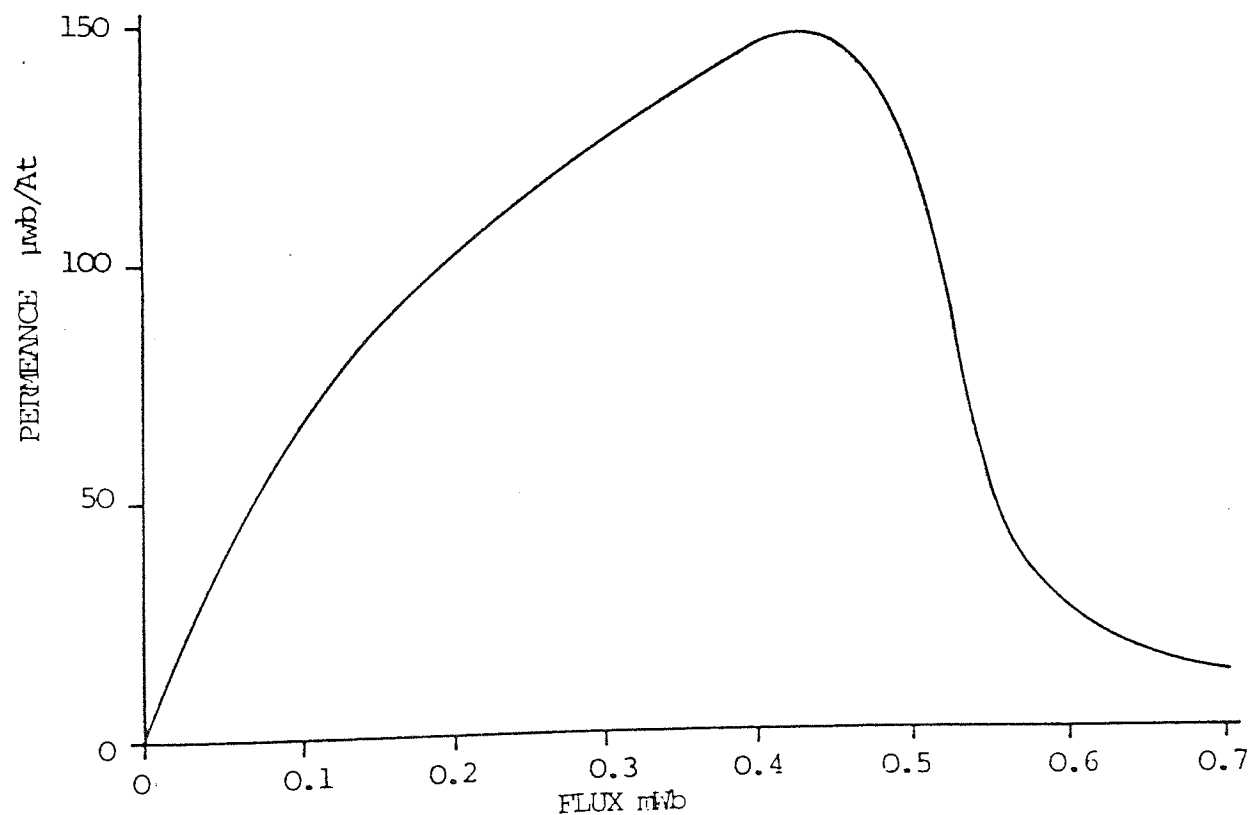


FIGURE 3.15 PERMEANCE-FLUX CHARACTERISTIC FOR THE ROTOR COMPONENTS

possible path and a minimum possible path. The way in which the resulting permeance-flux curve varies due to errors in this estimation can be seen in Figure 3.16. and the effects in the resulting torque characteristic are shown in Figures 3.36 and 3.37 for the non-saturated and saturated cases respectively.

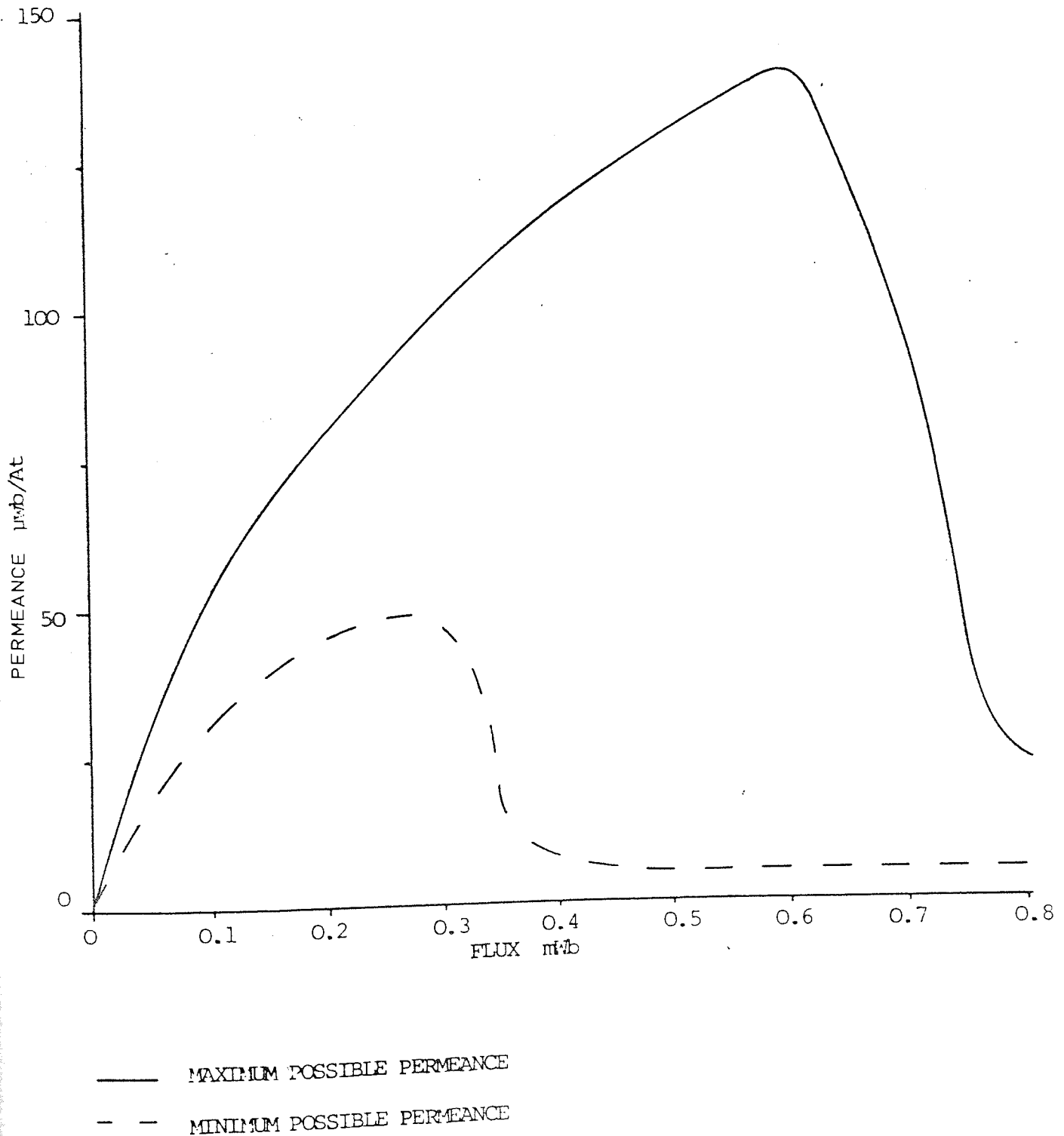


FIGURE 3.16 EXTREME PERMEANCE-FLUX CHARACTERISTIC FOR ROTOR COMPONENTS

The inclusion of flux-permeance curves in a computer programme requires that it be split into sections and a series of pairs of co-ordinates included in the data for the programme. When a value of permeance is required during a programme run, linear interpolation is used to obtain the correct value. Linear interpolation is sufficiently accurate in this application because of the smooth continuity of the curves and the choice of data points used for the co-ordinates.

PERMEANCE OF THE PERMANENT MAGNET COMPONENTS

The permanent magnetic circuit contains four components F_m ; P_{rm} ; P_{sm} and P_m .

F_m is the effective m.m.f. of the permanent magnet; its value was found from the demagnetisation curve by extrapolating the curve from the approximate operating point to the intersect with the axis. This occurs at 360,000 A/m. The length of the magnet is known to be 0.0195 metre. Hence F_m may be calculated

$$F_m = H \times l = 360,000 \times 0.0195 = 7020$$

The values of P_{rm} and P_{sm} remain relatively constant as the flux flowing from one end of the machine to the other is affected very little by the excitation in the field windings, these values were therefore estimated from their

geometry and remained constant throughout the execution of the programme. The values used were

$$P_{rm} = 140 \mu\text{wb/AT}$$

$$P_{sm} = 37 \mu\text{wb/AT}$$

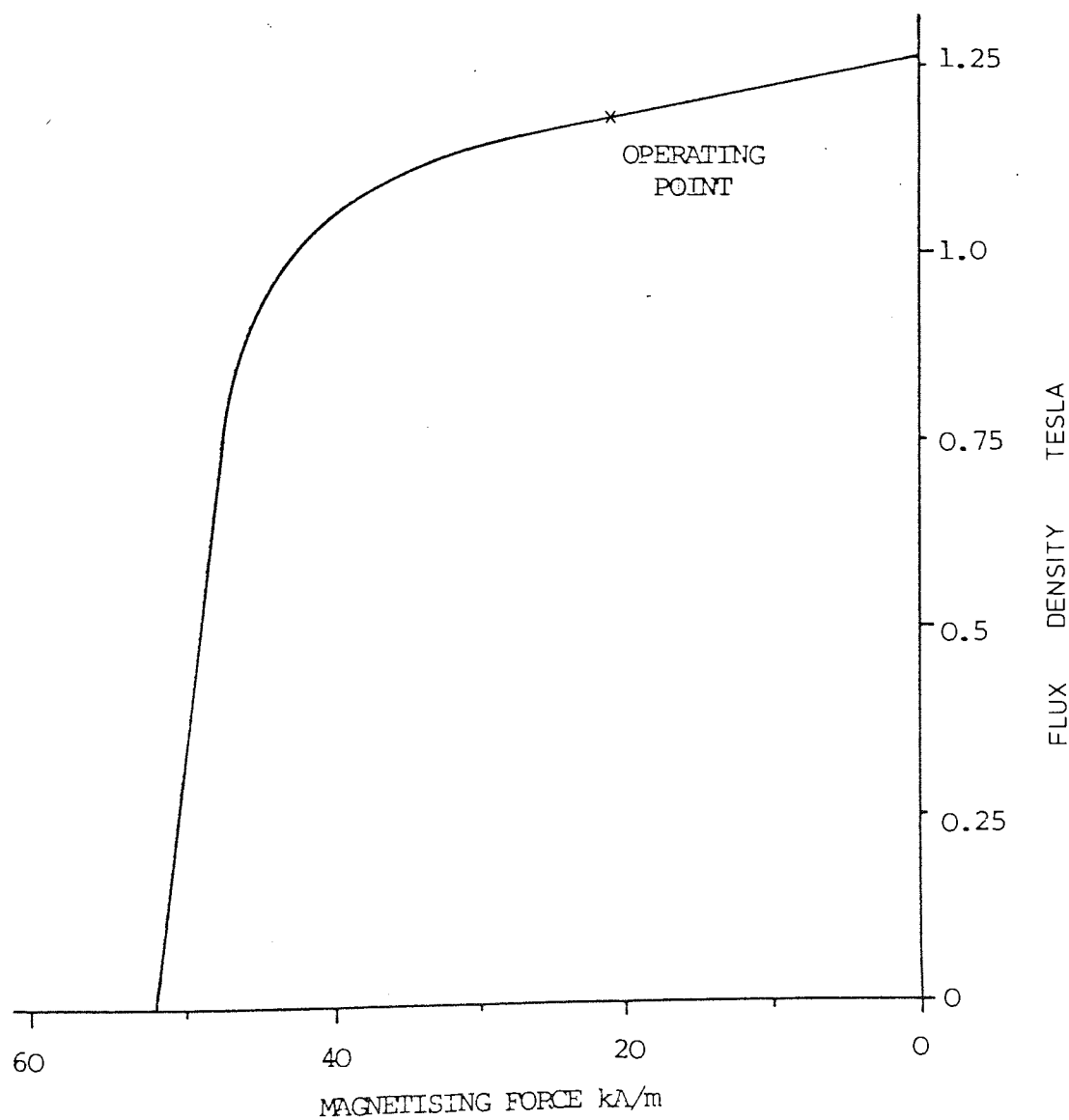


FIGURE 3.17 DEMAGNETISATION CURVE FOR ALCOMAX III

The permeance of the permanent magnet itself however is far more sensitive to flux variation, especially when the flux is in the region 1 to 1.5 mwb. To keep this value correct in the computer programme it was necessary to adapt the demagnetisation curve into a permeance-flux curve as described for the stator and rotor components. Figure 3.18 shows this curve and it can be seen how critical the value of permeance is over certain regions.

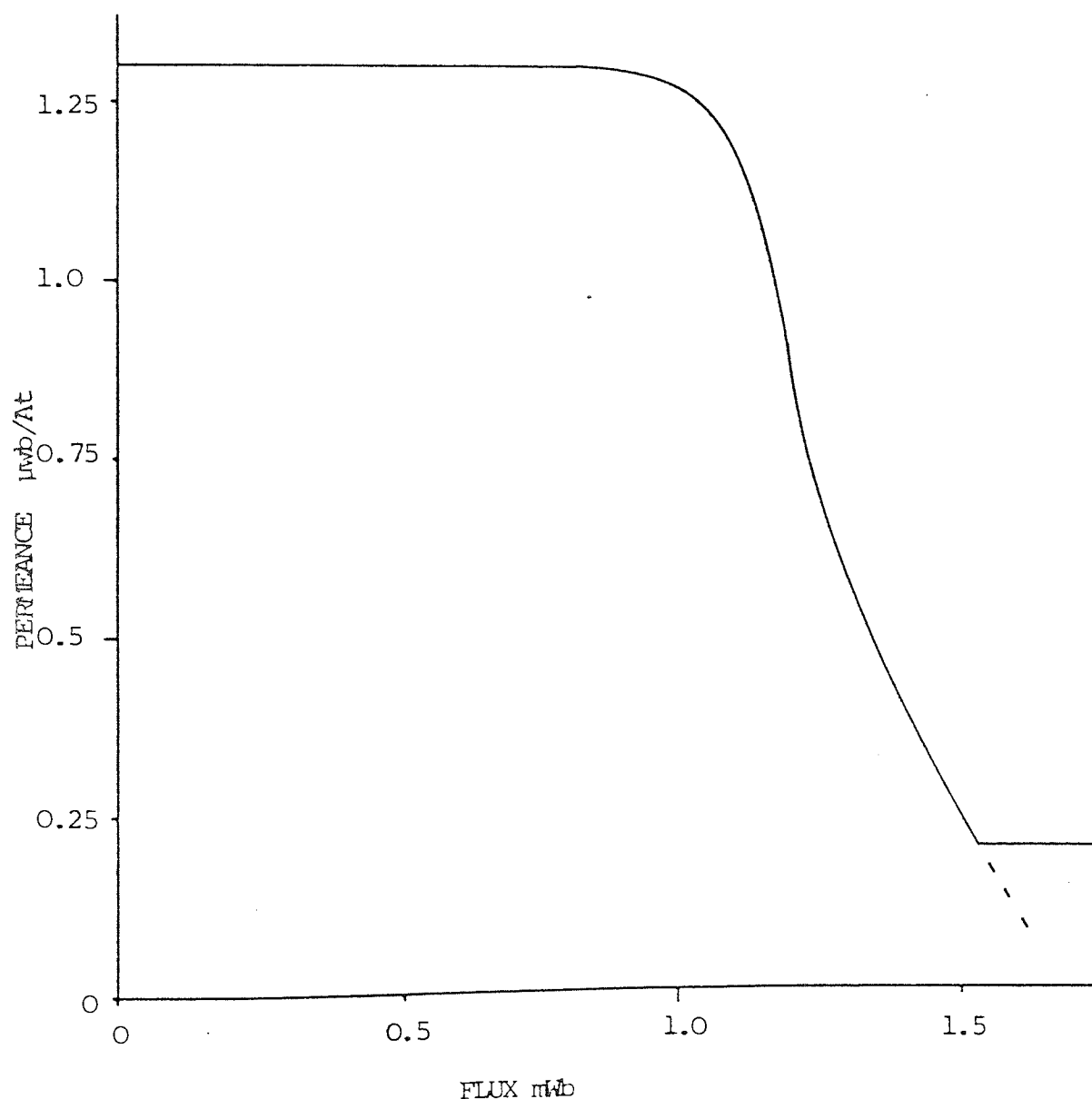


FIGURE 3.18 PERMEANCE-FLUX CHARACTERISTIC FOR THE PERMANENT MAGNET

3.3.4 COMPARISON OF SINGLE PHASE AND DOUBLE PHASE EXCITATION

The calculation of values of permeances for the components of the equivalent magnetic circuit was based on the assumption that both the field windings were to be excited. However, when only one phase is excited, the flux paths within the machine vary. The flux paths for both the two phase and single phase cases are shown in Figures 3.19 and 3.20 respectively.

The nature of the model is such that the calculation of permeance of the stator components holds true for both cases of excitation. However, the flux paths in the rotor change considerably and it is not possible to find one set of parameters which will maintain an accurate representation for both cases. For single phase representation, modifications have to be made to the length of the flux paths in the rotor. Other than this small amendment the model is suitable for both single phase and two phase excitation of the stepper motor.

3.3.5 CONCLUSION

It has been shown how a true representation of the stepper motor magnetic circuit can be devised from a study of the construction of the machine. Each component of the model has been analysed so that its magnetic characteristic may easily be represented and implemented using a digital computer programme. The flux path within

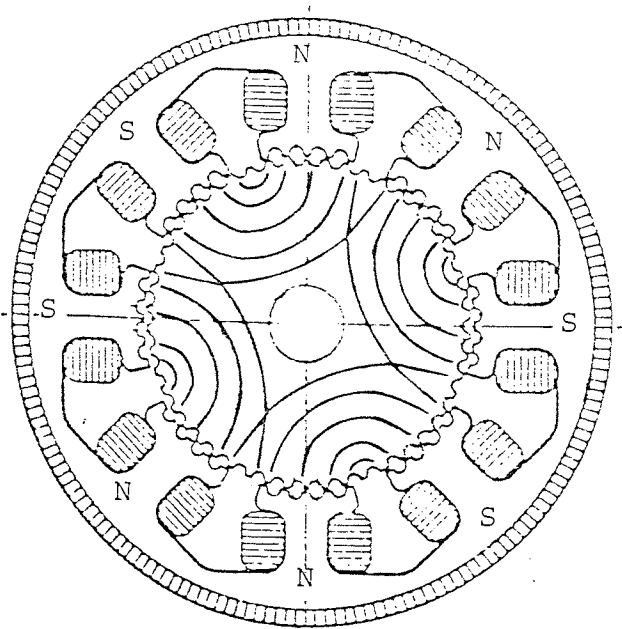


FIGURE 3.19 FLUX PATH FOR TWO PHASE EXCITATION

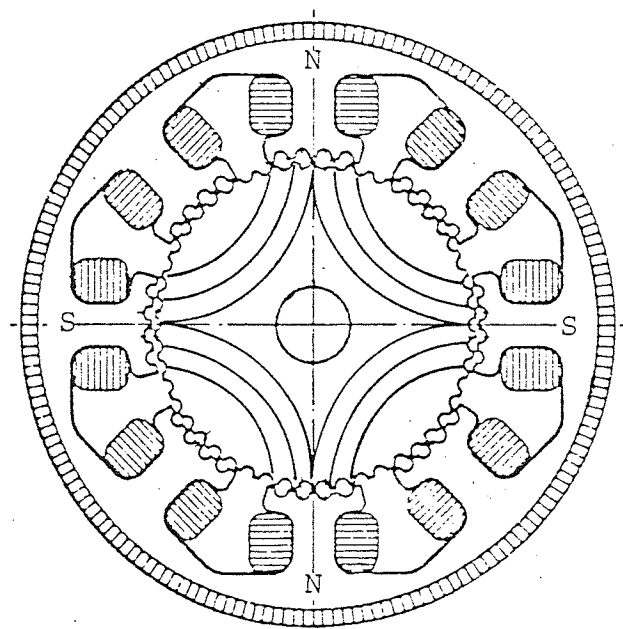


FIGURE 3.20 FLUX PATH FOR SINGLE PHASE EXCITATION

the rotor caps was found to be the most difficult to represent of the magnetic circuit components identified. Some estimation was required to determine the length and active area of these flux paths. It is to this aspect of the model, therefore, that attention must be concentrated in order to produce sufficient accuracy and a means of assessing sensitivity.

3.4 PREDICTION OF THE STATIC TORQUE DISPLACEMENT CHARACTERISTIC

3.4.1 DEVELOPMENT OF THE TORQUE EQUATION

The development of the torque equation into a form suitable for the application to the stepper motor is shown in appendix 2, and an outline is given below.

$$\begin{aligned}
 \text{Torque } T &= \frac{1}{2} \phi^2 \frac{dR}{d\theta_m} \\
 &= \frac{1}{2} \frac{\phi^2}{p} \frac{dP}{d\theta_m} \\
 &= \left[\frac{N_r}{N_r - N_s} \right] \cdot \frac{1}{2} \cdot \left[\frac{\phi}{p} \right]^2 \frac{dP}{d\theta_e} \quad (3.4)
 \end{aligned}$$

provided $N_r \neq N_s$...

where R is Magnetic Reluctance

θ_m is Mechanical Angle

ϕ is Flux in Air Gap

p is Magnetic Permeance

N_r is Number of Teeth on Rotor

N_s is the effective number of teeth of the stator.

The fact that the stator consists of salient poles means that the actual number of teeth on the stator is less than the number suggested by their pitch. Two design strategies exist for the positioning of the stator teeth, therefore the effective number of teeth should not be calculated using the pitch of the teeth. In fact the effective number of teeth may be found from the number of rotor teeth, the number of poles and the number of steps per revolution.

$$N_s = N_r \pm \frac{N_p N_r}{N}$$

where N_p is Number of Salient Poles

N is Number of steps per revolution of the motor.

Equation (3.4) gives the torque produced by any one air gap of the magnetic model. Finding the total torque requires the summation of the torque for all the air gaps.

$$\text{Total Torque} = \frac{N_r}{2(N_r - N_s)} \sum_{n=1}^8 \left[\frac{\phi_n}{P_n} \right]^2 \frac{dP_n}{d\theta_e} \quad (3.5)$$

The permeance and its first derivative are calculated directly from the permeance Fourier co-efficients. The flux, however, has to be computed from the equivalent magnetic circuit.

NOTE on relationship between Mechanical and Electrical angular displacement.

From Figure 3.6 it can be seen that whenever pole number 1 is at a position of maximum permeance of the gap, the gap of pole number 5 is at a similar position, thus the mechanical cycle is effectively repeated twice over one revolution of the rotor. This is due to the fact that the stator effectively has two more teeth than the rotor. The electrical cycle repeats each time the gap at pole number 1 has maximum permeance, and occurs once each rotor tooth pitch. Consideration of these facts enables the following expression to be derived:-

$$\theta_e = \frac{N_r}{N_r - N_s} \theta_m \quad \text{provided } N_r \neq N_s$$

3.4.2 DEVELOPMENT OF THE ALGORITHM

Obtaining the value of flux within the air gaps of each limb of the model requires analysis of the equivalent magnetic circuit. Firstly the parameters MMF FRONT and MMF REAR as defined in Figure 3.8 must be found, and secondly, provided the permeances of all the components are known, the flux in each limb calculated.

The method of reduction used on the equivalent magnetic circuit is based on the Norton and Thevenin equivalent circuits.

Figure 3.21 shows how limb 1 of the model is converted from a limb containing four series elements into a two element parallel circuit. This type of reduction is applied to all eight limbs of Figure 3.8 and the result is shown in Figure 3.22.

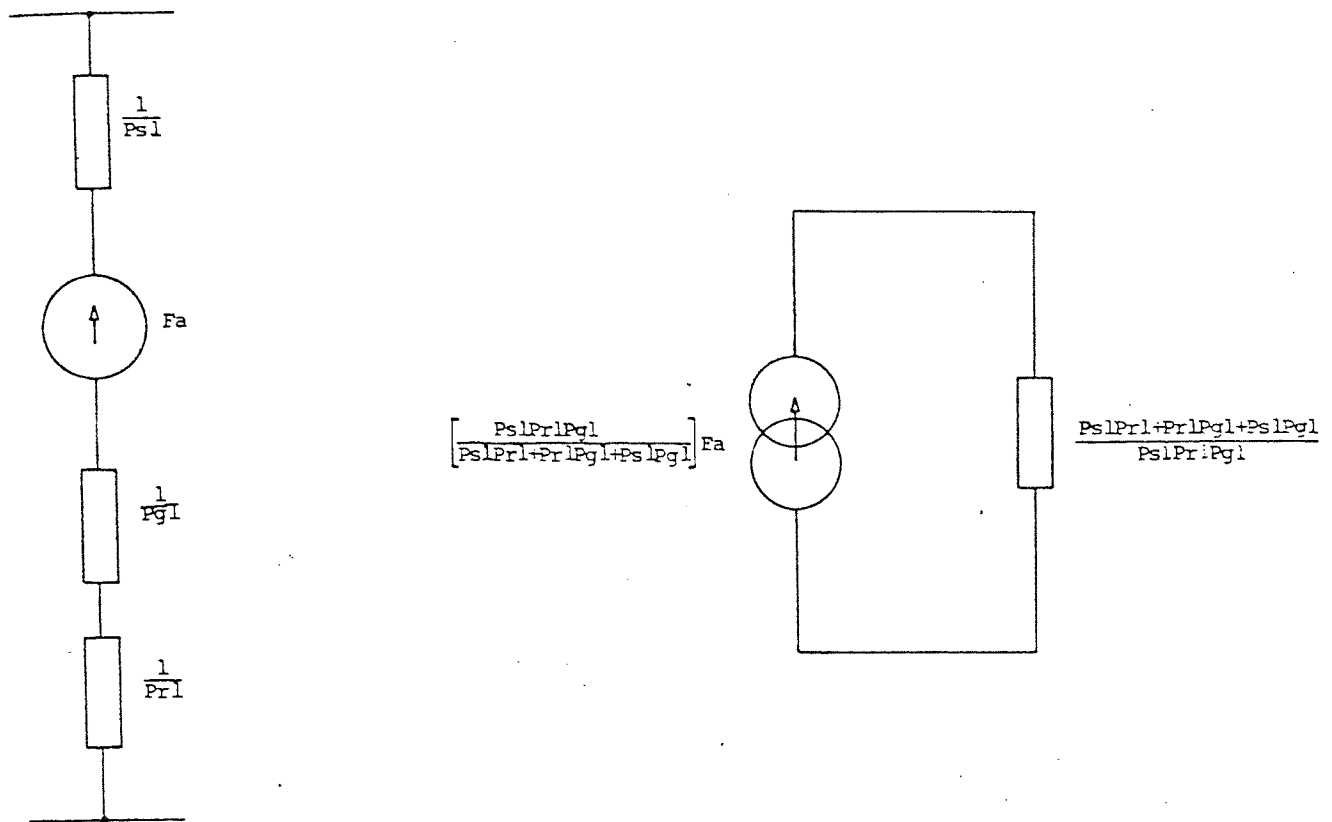


FIGURE 3.21 SERIES TO PARALLEL CONVERSION FOR ONE LIMB

To simplify the notation

$$E_n = \frac{P_{sn} \cdot P_{rn} \cdot P_{gn}}{P_{sn} \cdot P_{rn} + P_{rn} \cdot P_{gn} + P_{sn} \cdot P_{gn}} \quad (3.6)$$

Each group of four equivalent parallel limbs shown in Figure 3.22 may be summed together as simple groups of parallel permeances and flux sources, the result of this step is shown in Figure 3.23.

The final stage of development is to convert the two element parallel circuits into their series equivalent circuits. The result is a circuit containing no parallel limbs at all; as shown in Figure 3.24. This simplified magnetic circuit was used to calculate the two values

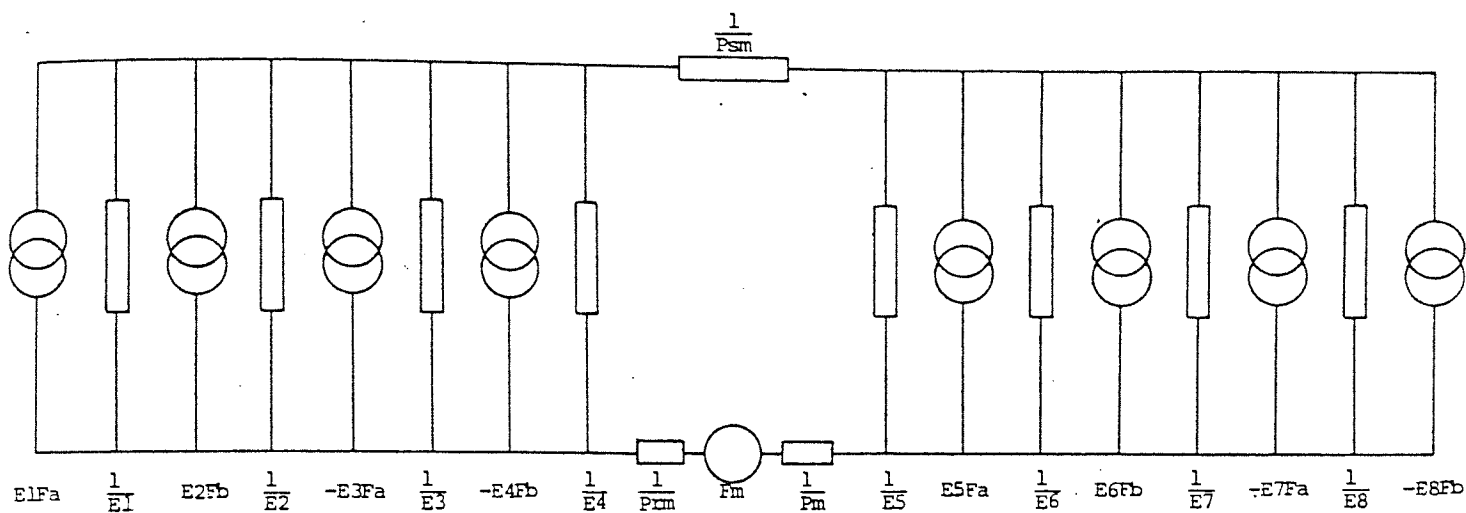


FIGURE 3.22 8 PARALLEL LIMB EQUIVALENT MAGNETIC CIRCUIT

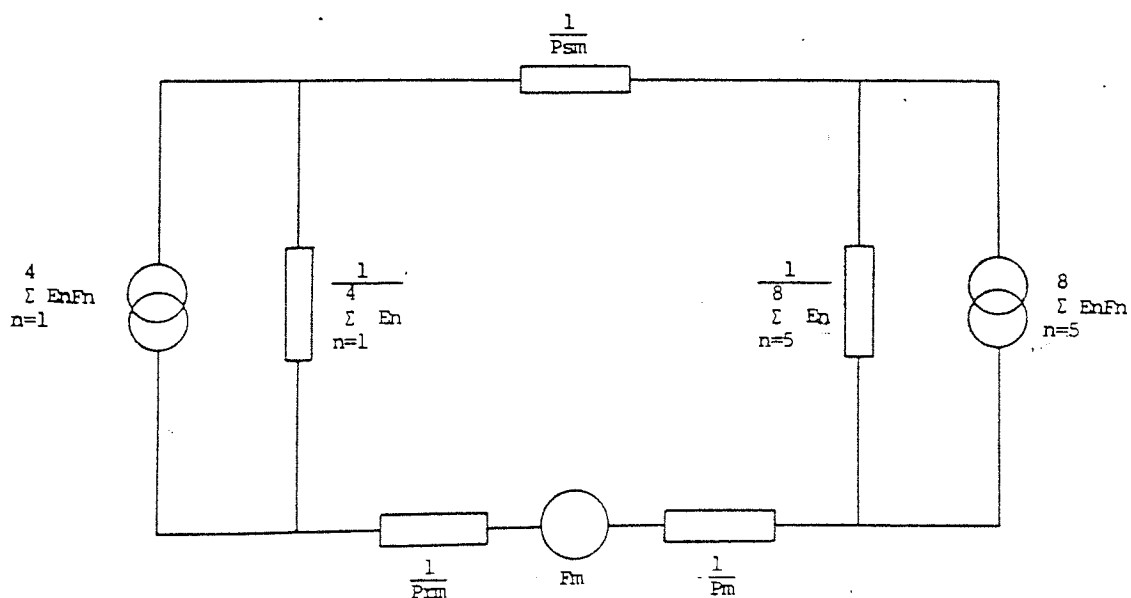


FIGURE 3.23 SUMMED PARALLEL LIMB EQUIVALENT MAGNETIC CIRCUIT

of mm.f required using the equations outlined below.

$$\text{TRANSFLUX} = \frac{\left[F_m \frac{\frac{\sum_1^4 E_n F_n}{\sum_1^4 E_n}}{\frac{\sum_1^4 E_n}{\sum_1^4 E_n}} + \frac{\sum_5^8 E_n F_n}{\sum_5^8 E_n} \right]}{\left[\frac{1}{\sum_1^4 E_n} + \frac{1}{\sum_5^8 E_n} + \frac{1}{P_m} + \frac{1}{P_{sm}} + \frac{1}{P_{rm}} \right]} \quad (3.7)$$

$$\text{MMF FRONT} = \text{TRANSFLUX} \frac{1}{\frac{\sum_1^4 E_n}{\sum_1^4 E_n}} + \frac{\sum_1^4 E_n F_n}{\sum_1^4 E_n} \quad (3.8)$$

$$\text{MMF REAR} = -\text{TRANSFLUX} \frac{1}{\frac{\sum_5^8 E_n}{\sum_5^8 E_n}} + \frac{\sum_5^8 E_n F_n}{\sum_5^8 E_n} \quad (3.9)$$

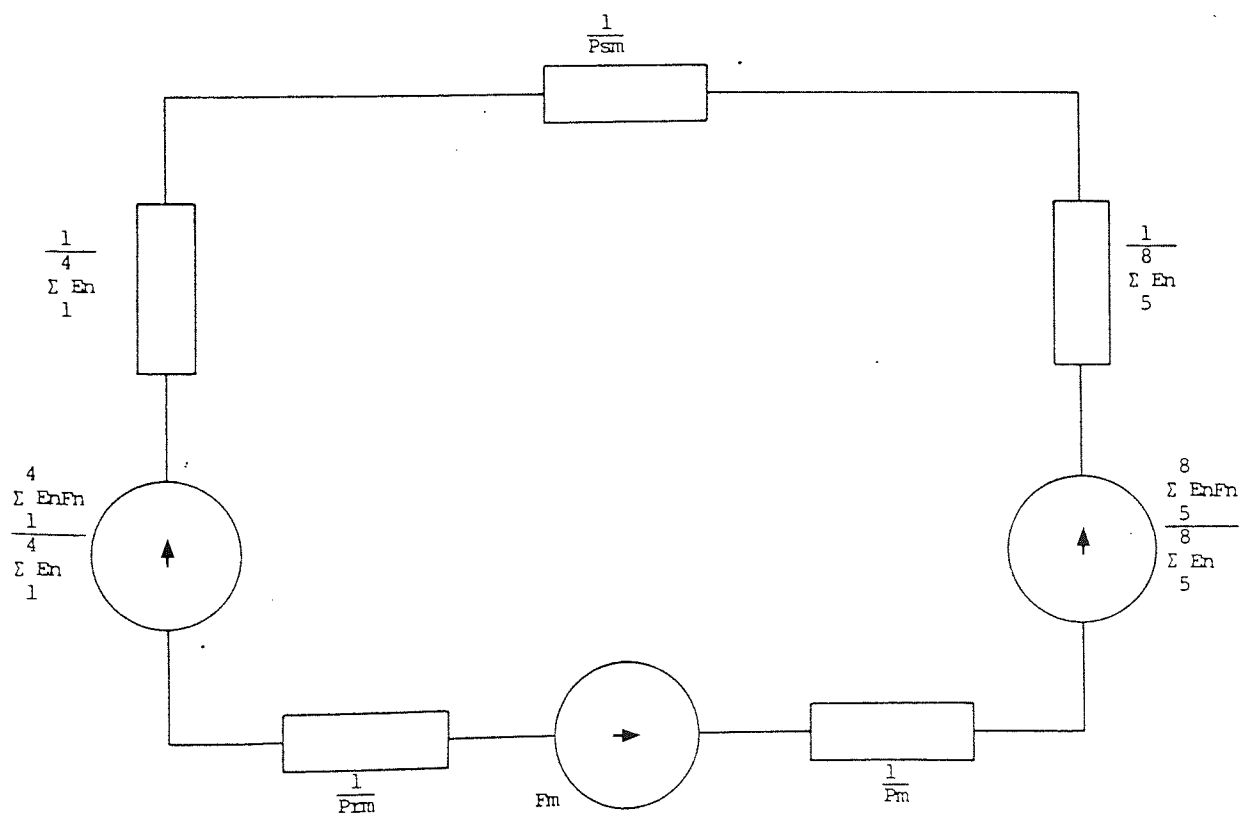


FIGURE 3.24 SERIES EQUIVALENT MAGNETIC CIRCUIT

Referring back to Figure 3.8 the flux in each limb can now be calculated

$$\text{FLUX}_n = [\text{MMF}_n - \text{MMF}_{\text{REAR}}^{\text{FRONT}}] E_n \quad (3.10)$$

Once the flux for each limb is known it may be substituted in equation (3.5) and hence the torque calculated.

Examination of equations (3.8), (3.9) and (3.10) will show that they are not independent and therefore cannot be solved directly. In fact the expression for flux in each limb includes values of E_n which are derived from the permeances of the iron paths. These values of permeance are dependent on the flux in the limb. It is therefore necessary to develop an iterative procedure which first calculates the flux in the limb from estimations of permeances. The estimations of permeances can then be modified using the calculated value of flux in the limb and so on. The programming of iterative loops is a well established computing technique which requires certain precautions to be taken. The function being solved may not produce results which are closer to its solution on each iteration but instead produce successively diverging results. This type of unstable function has to be adapted so that its solution can be found. The method used in this application was to take the new result as an indication of the direction and proportion by which the estimate must be modified. By taking a small proportion the function becomes quite stable and the values of flux

and permeance eventually converge towards their true values. A limit has to be set so that when consecutive values of flux are sufficiently close to each other, the iteration stops and stores the last values of flux and permeance to be calculated.

A similar iterative procedure is required for the calculation of m.m.f. at front and rear of the machine, as these values are also dependent on the permeance of the iron components.

The resultant programme to compute torque contains two iterative loops, one inside the other, the interaction of the two loops and organisation of the programme is shown in Figure 3.25, which is the flow chart of the complete programme.

3.4.3 THE STATIC TORQUE PROGRAMME

CORAL 66 was chosen as the programme language because a structured language was preferred and this language was available on both the University I.C.L. mainframe computer, and also the departmental, Texas Instruments, mini computer.

Eleven procedures were developed for use within the main programme, each procedure was tested independently to establish integrity and check the procedures.

PROCEDURE NAMES AND FUNCTIONS

- | | | |
|-----------------|---|--|
| 1. SINE (ANGLE) | } | The procedures available for SIN and COS required the angle to be in |
| 2. COSE (ANGLE) | | |

radians. The two procedures SINE and COSE return the sine and cosine for an angle defined in degrees.

3. EQUIV (LIMB) Returns the value E_n as defined in equation (3.6) for the limb number specified.

4. SUM(START,END) Returns the summation of E_n over the range specified by START and END.

$$\text{SUM} = \sum_{n=\text{START}}^{\text{END}} E_n$$

5. PROD(START,END) Returns the summation of the product $E_n F_n$ over the range specified by START and END.

$$\text{PROD} = \sum_{n=\text{START}}^{\text{END}} E_n F_n$$

6. TRANSFLUX Returns the value of the transverse flux as defined in equation (3.7).

7. CALCFLUX Returns the value of flux in the limb defined by the variable LIMB in the main programme.

$$\text{CALCFLUX} = \text{MMF} \begin{Bmatrix} \text{FRONT} \\ \text{REAR} \end{Bmatrix} . \text{EQUIV}(\text{LIMB})$$

- | | | | |
|-----|-------------------|---|------------------------------------|
| 8. | CALCROTPERM(FLUX) | } | Return the values of permeance |
| 9. | CALCSTAPERM(FLUX) | | for the rotor and stator using |
| | | | data defined in Figures 3.14 and |
| | | | 3.15. |
| 10. | PERMMAG(FLUX) | | Returns the value of the permeance |
| | | | of the permanent magnet using |
| | | | data defined in Figure 3.18. |
| 11. | TORQUE | | Returns the value of torque as |
| | | | defined by equation (3.5). |

At the start of the programme the initial estimated values for rotor permeances (P_r), stator permeances (P_s), permanent magnet permeance (P_m) and the flux have to be entered. This is followed by the constant values of the permanent magnetic path parameters (P_{sm}) and (P_{rm}) and the currents (I) for which the calculation of torque is required. From the current values, the m.m.f.'s are calculated.

The calculation of torque is carried out separately for each rotor displacement angle required. This is normally over the range from -180 degree to +180 degree. Once the variable angle is set, the gap permeance and its first derivative may be calculated.

In order to test the divergence of each iterative loop, the values of m.m.f. from the previous iteration have to be saved, but for the first iteration, these values are set to zero. The calculations of the values of m.m.f. are carried out by calling the procedure to calculate the transverse flux

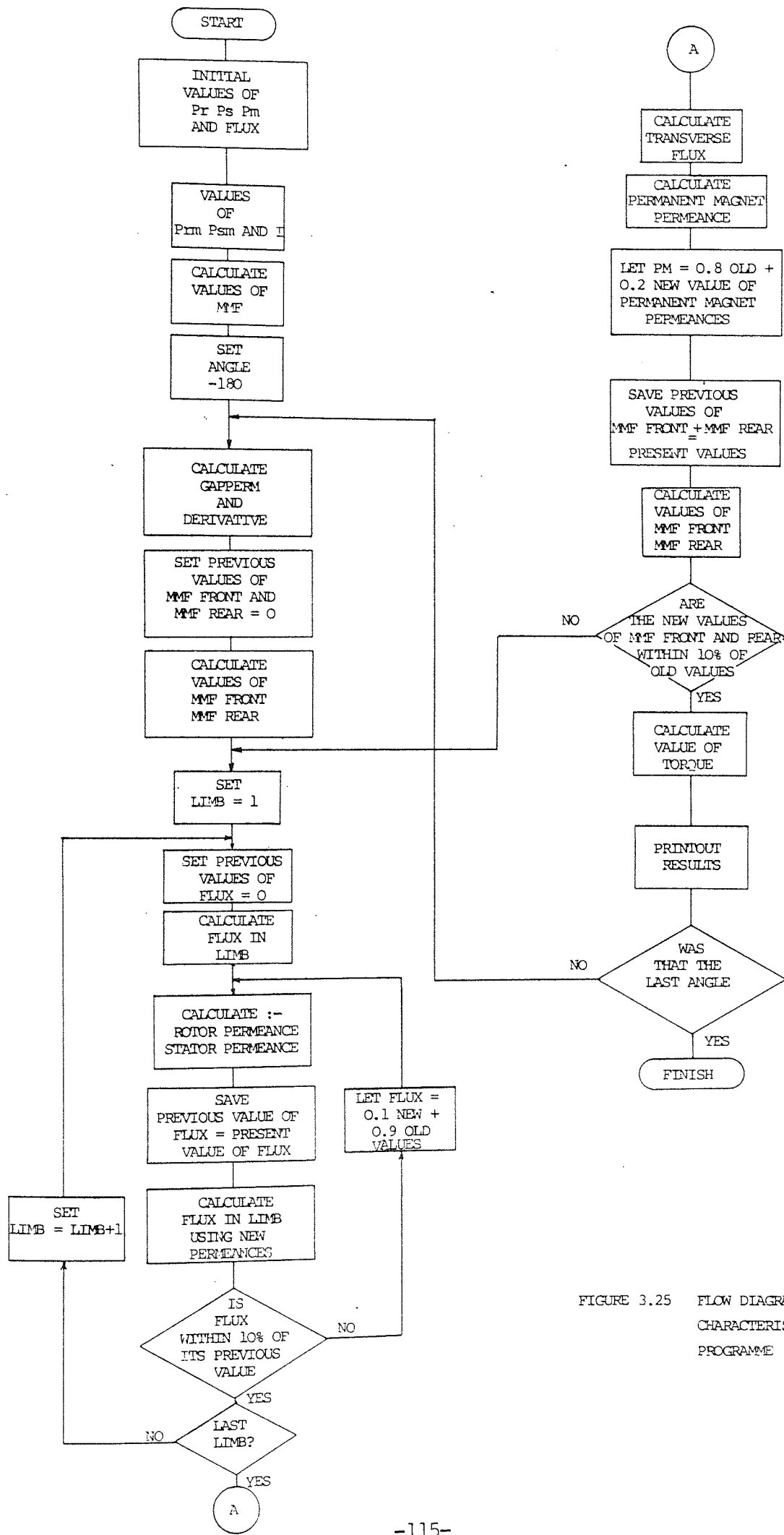


FIGURE 3.25 FLOW DIAGRAM OF STATIC TORQUE CHARACTERISTIC PREDICTION PROGRAMME

and applying equations (3.8) and (3.9). Once the values of m.m.f. are known for each limb, the flux is calculated using the estimated values of permeance, and an iterative procedure is then used to improve the estimates of permeance and flux until values are found which satisfy the calculated m.m.f. Each limb is treated separately in turn. When new values for permeance in all eight limbs have been established, these values are used to re-calculate the transverse flux and the permanent magnet permeance. From these values, new values of m.m.f. are calculated, these values are compared with the saved values to test convergence and if necessary, the procedure is repeated to find new values for the flux and permeances in each limb. When successive values of m.m.f. are found to be sufficiently close to each other, the value of torque is calculated using the most recently calculated values of flux in each limb.

3.4.4 RESULTS OF THE STATIC TORQUE PROGRAMME

The computer programme was developed essentially to predict the torque of the stepper motor accurately under all conditions, including those of magnetic saturation. The best test of accuracy which can be applied to this programme is to compare the results obtained from it with figures for the static torque characteristic measured from physical tests on the motor. A complete set of results was available from work undertaken by Justice⁽²⁴⁾ the reliability of this data was confirmed independently by

Bourne⁽³¹⁾ and so it was felt unnecessary to repeat the tests.

Figures 3.26 to 3.30 compare the results obtained from the programme and from the tests with both windings excited for currents of 0.5, 1, 3, 6 and 7 Amperes respectively. In all cases the gap permeance figures used in the programme were those resulting from the moment method of calculation.

A most useful and often quoted parameter of stepper motors is the peak value of the static torque. This value is referred to as the holding torque of the motor, as this is the maximum torque which the motor can hold in a static position. Figure 3.31 shows the variation of holding torque with current varying from zero to 7 Ampere with both phase windings excited.

Figures 3.32 to 3.34 compare results obtained for 0.5, 3, and 7 Ampere for single phase excitation and Figure 3.35 shows the holding torque characteristic for single phase excitation.

As some of the parameters used in the computer programme to calculate the static torque have been estimated, an assessment must be made to show what effect an incorrect estimate would have on the resulting torque from the programme. It can be seen that an error is most likely to occur in the estimation of the area and length of the flux paths in the rotor iron. Figures 3.36 and 3.37 show the effect of the worst case estimates of this value. Table

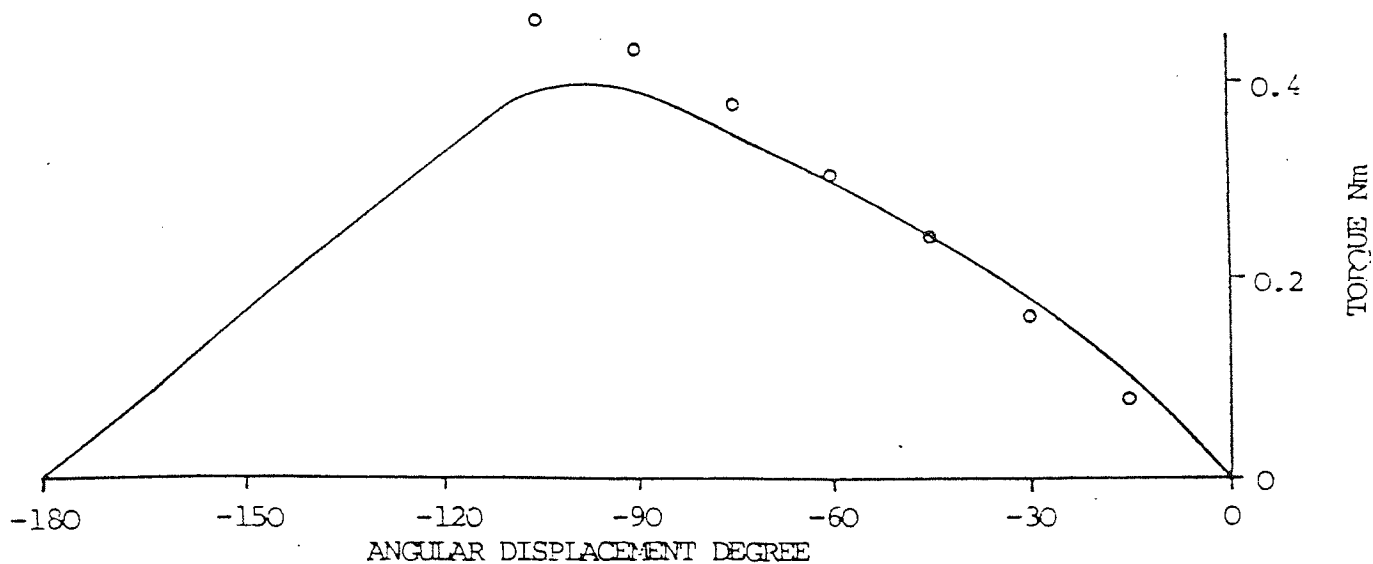


FIGURE 3.26 STATIC TORQUE CHARACTERISTIC PREDICTION. 2 PHASE 0.5A

o REPRESENTS MEASURED VALUES

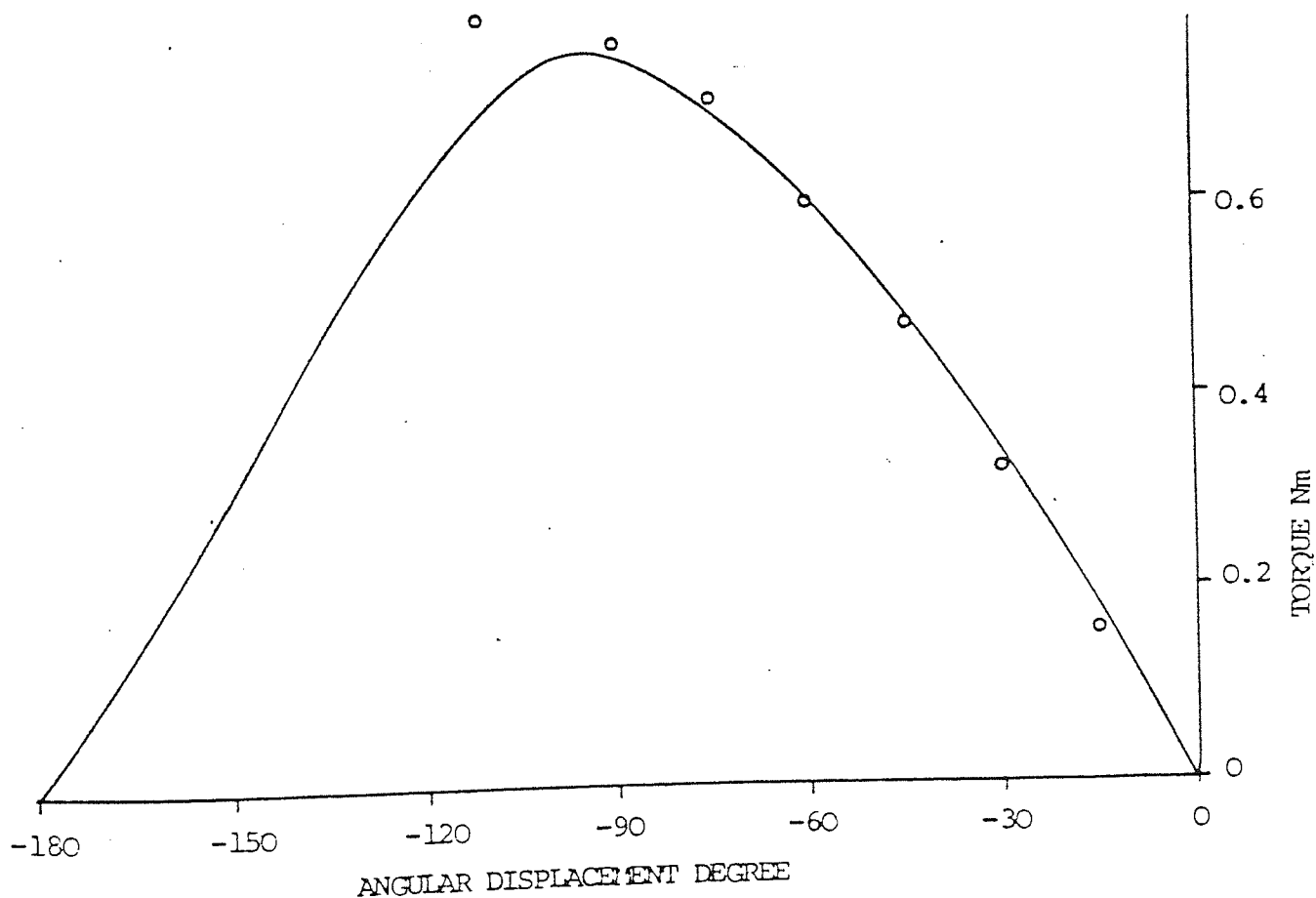


FIGURE 3.27 STATIC TORQUE CHARACTERISTIC PREDICTION. 2 PHASE 1A.

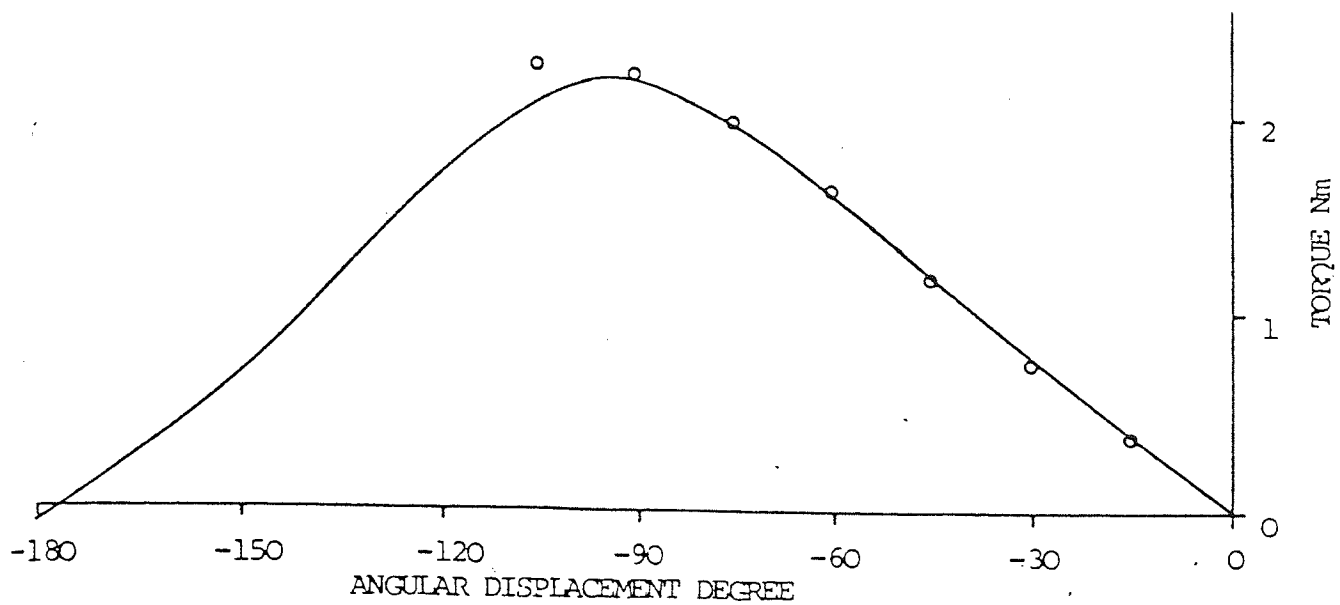


FIGURE 3.28 STATIC TORQUE CHARACTERISTIC PREDICTION. 2 PHASE 3A

o REPRESENTS MEASURED VALUES

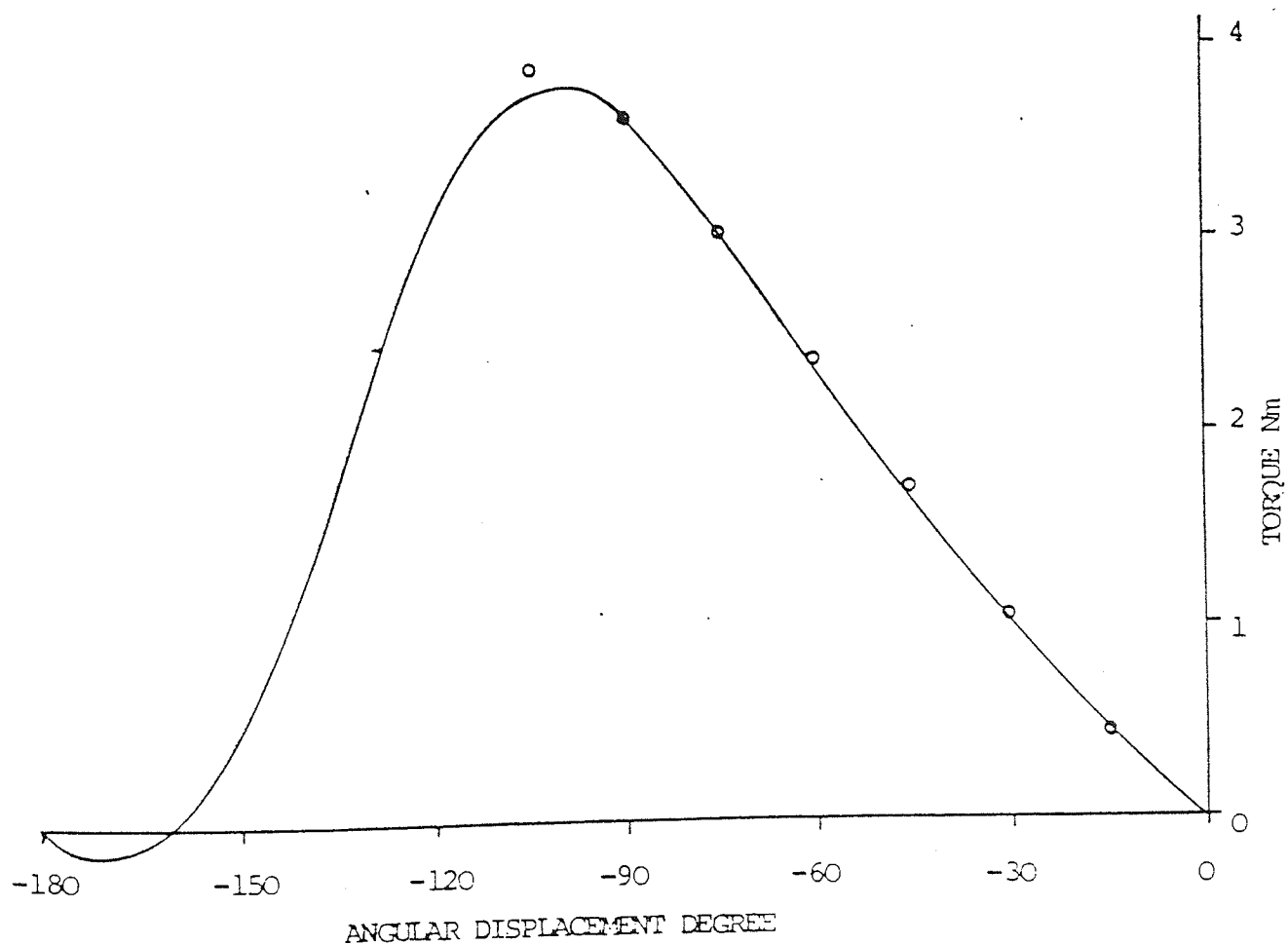


FIGURE 3.29 STATIC TORQUE CHARACTERISTIC PREDICTION. 2 PHASE 6A

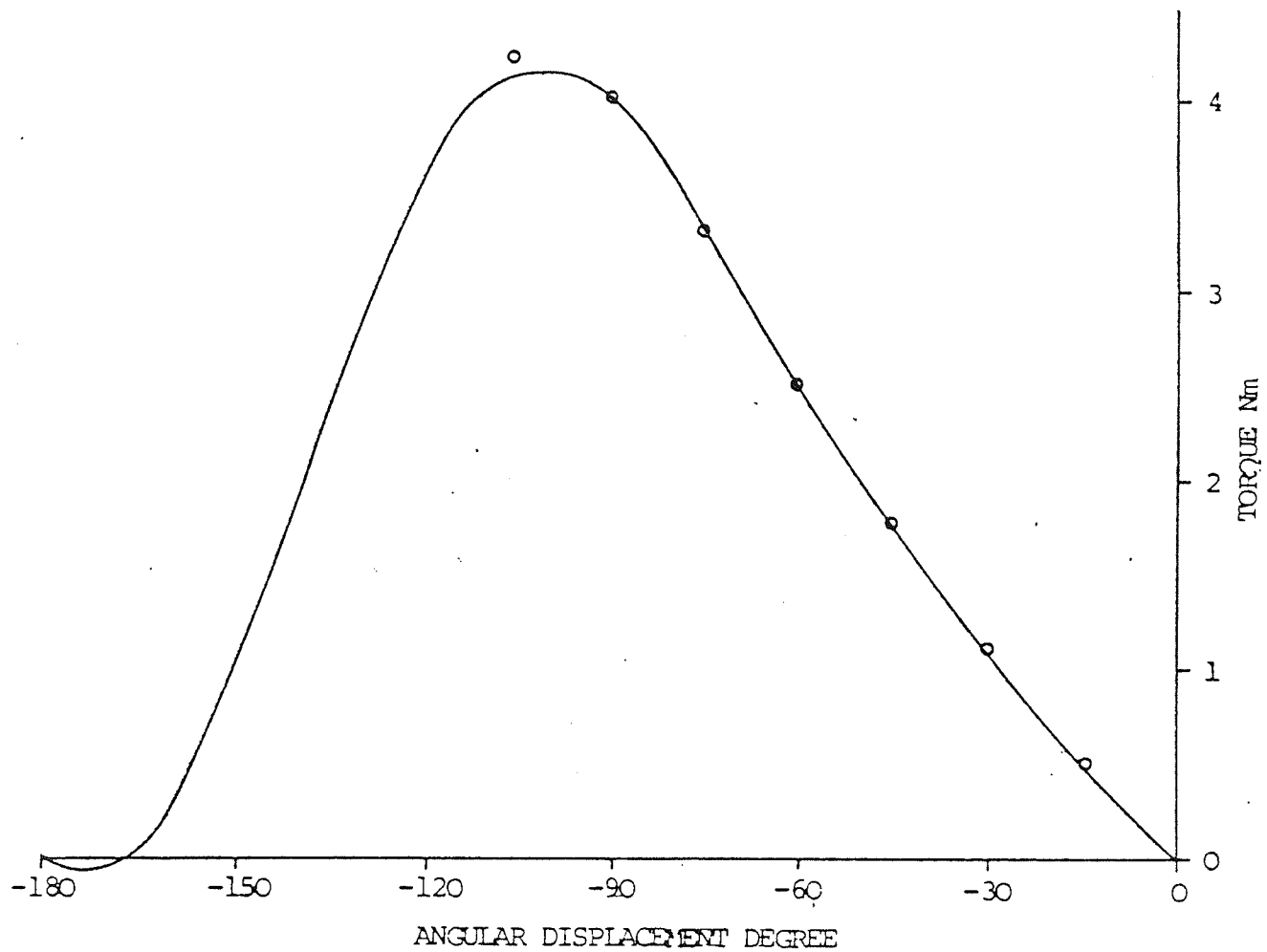


FIGURE 3.30 STATIC TORQUE CHARACTERISTIC PREDICTION. 2 PHASE 7A

o REPRESENTS MEASURED VALUES

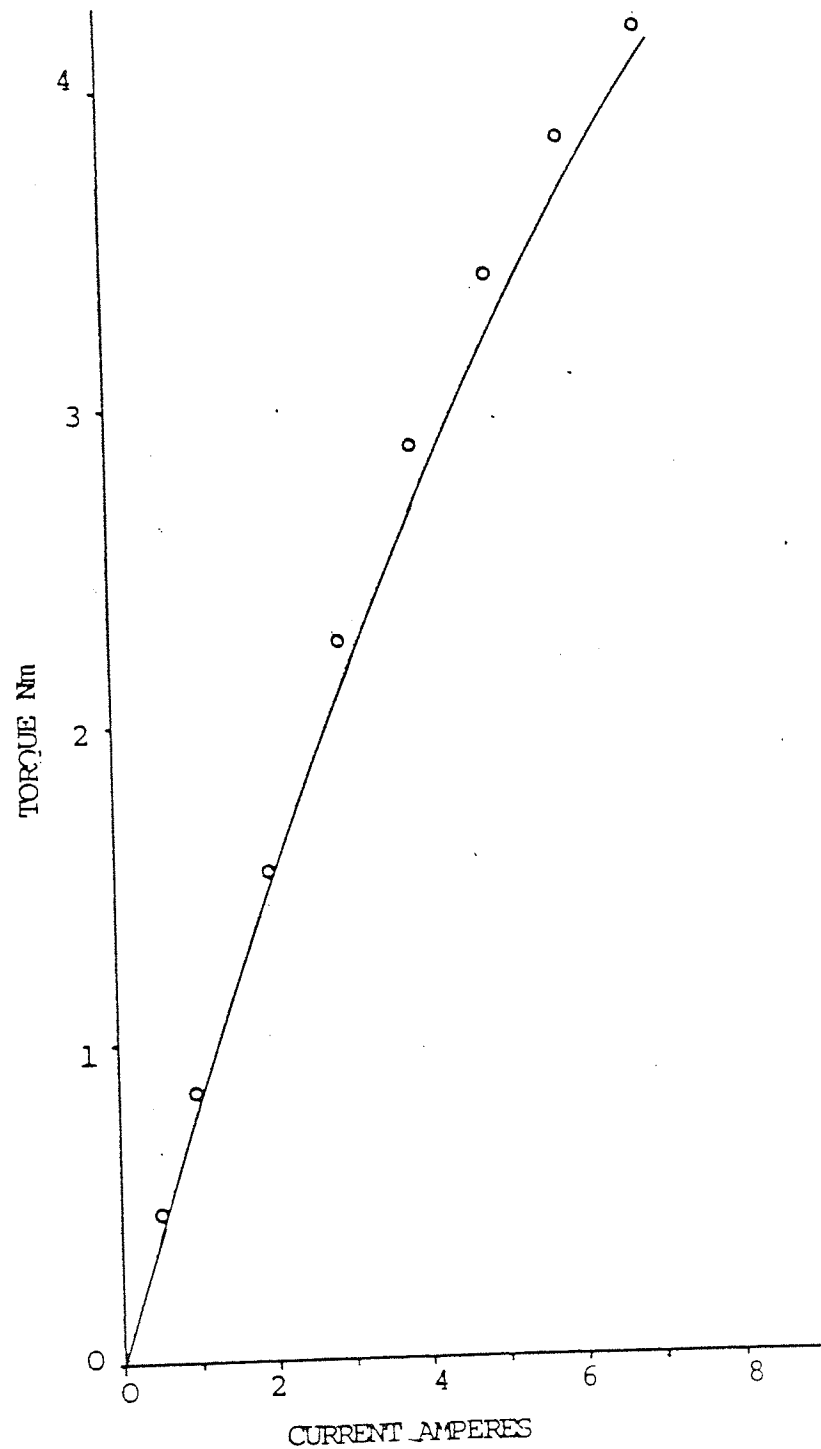


FIGURE 3.31 HOLDING TORQUE CHARACTERISTIC FOR TWO PHASE EXCITATION
o REPRESENTS MEASURED VALUES

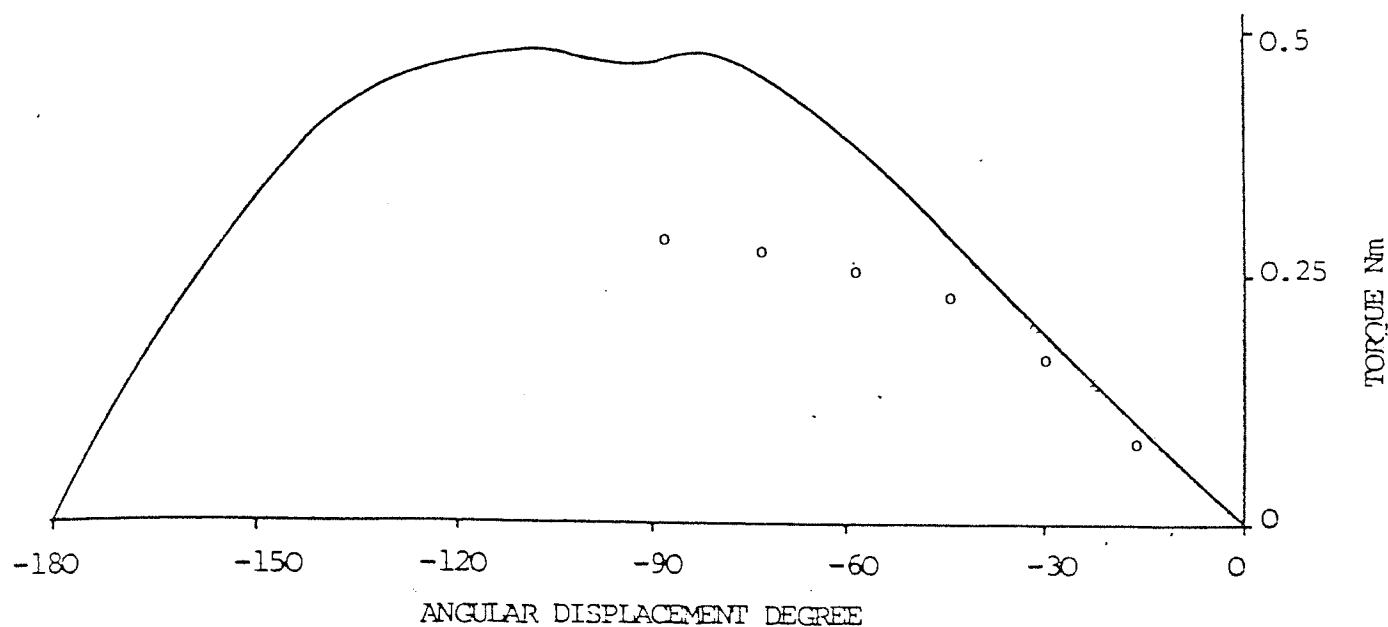


FIGURE 3.32 STATIC TORQUE CHARACTERISTIC PREDICTION. SINGLE PHASE 0.5A

MEASURED VALUES AT 0.5 AMP ARE
AVERAGED FROM SEVERAL MEASUREMENTS

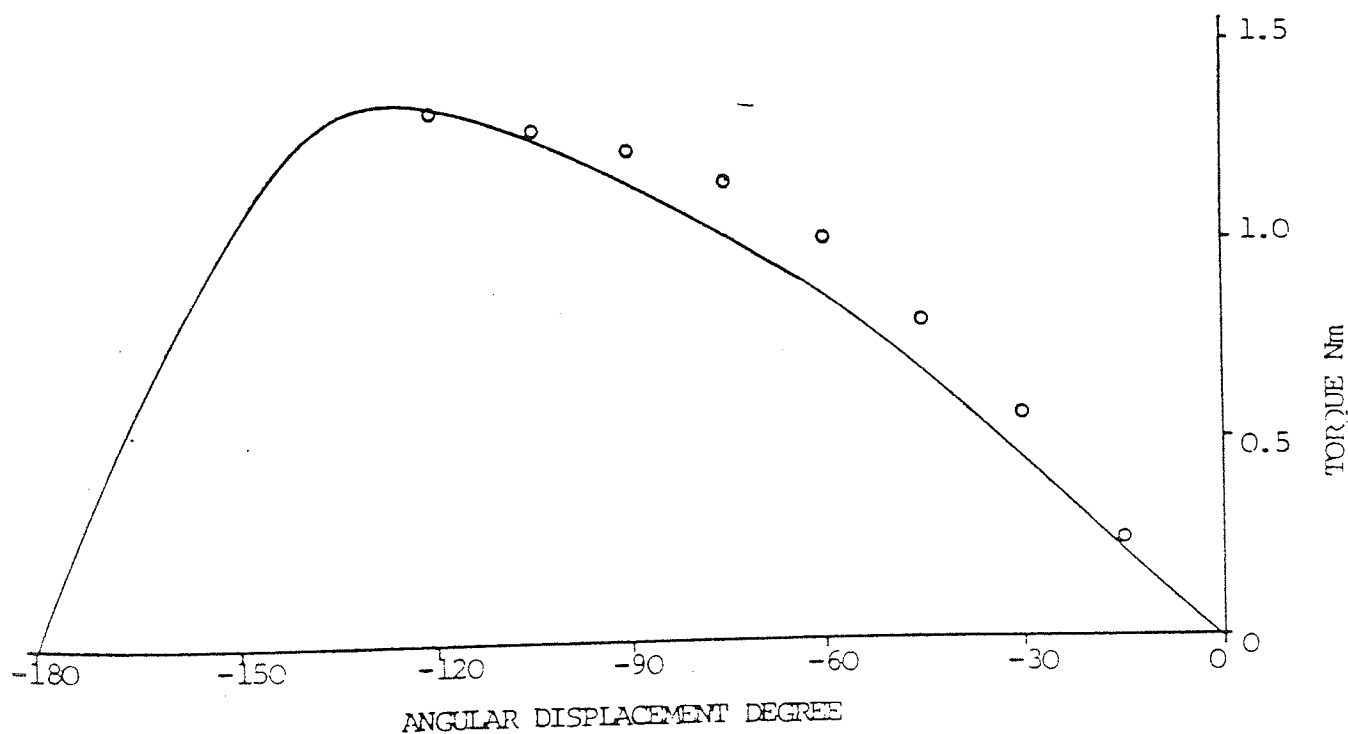


FIGURE 3.33 STATIC TORQUE CHARACTERISTIC PREDICTION. SINGLE PHASE 3A

o REPRESENTS MEASURED VALUES

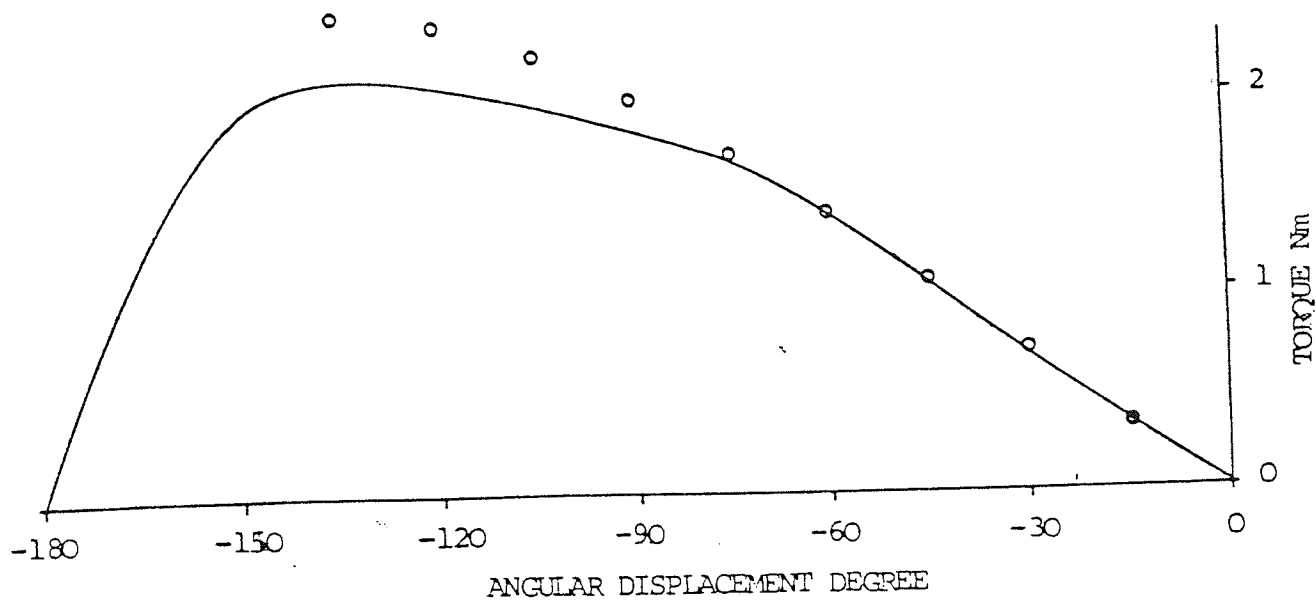


FIGURE 3.34 STATIC TORQUE CHARACTERISTIC PREDICTION. SINGLE PHASE 7A
 o REPRESENTS MEASURED VALUES

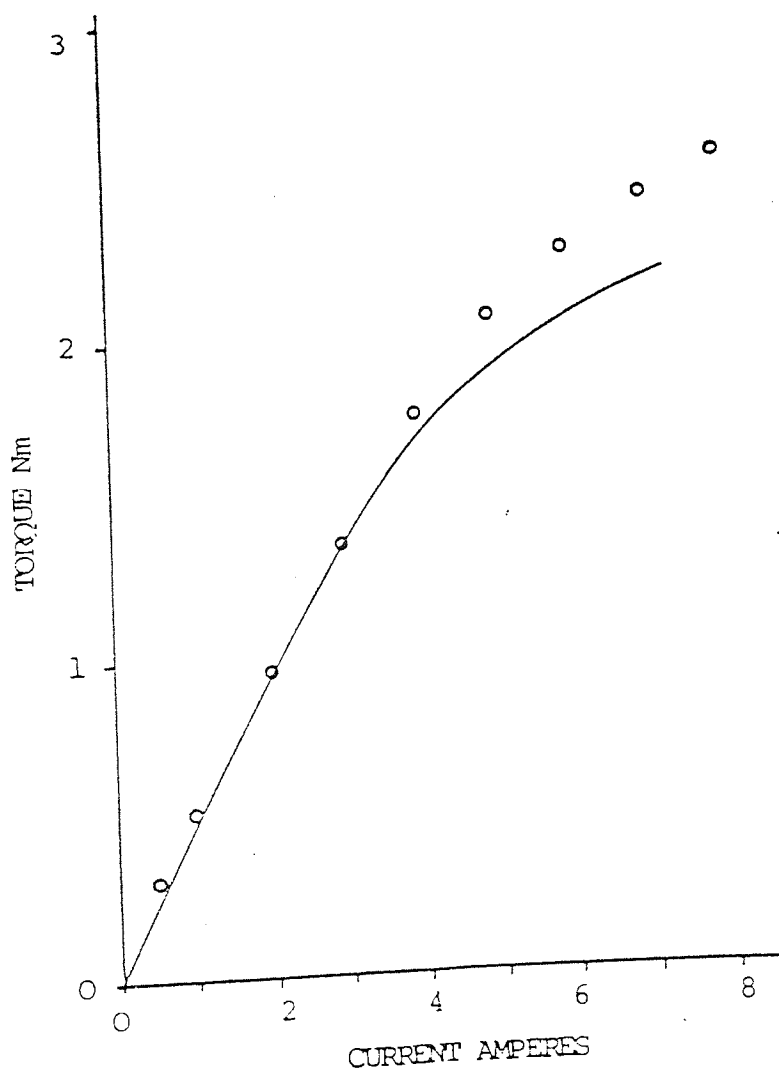


FIGURE 3.35 HOLDING TORQUE CHARACTERISTIC FOR SINGLE PHASE EXCITATION

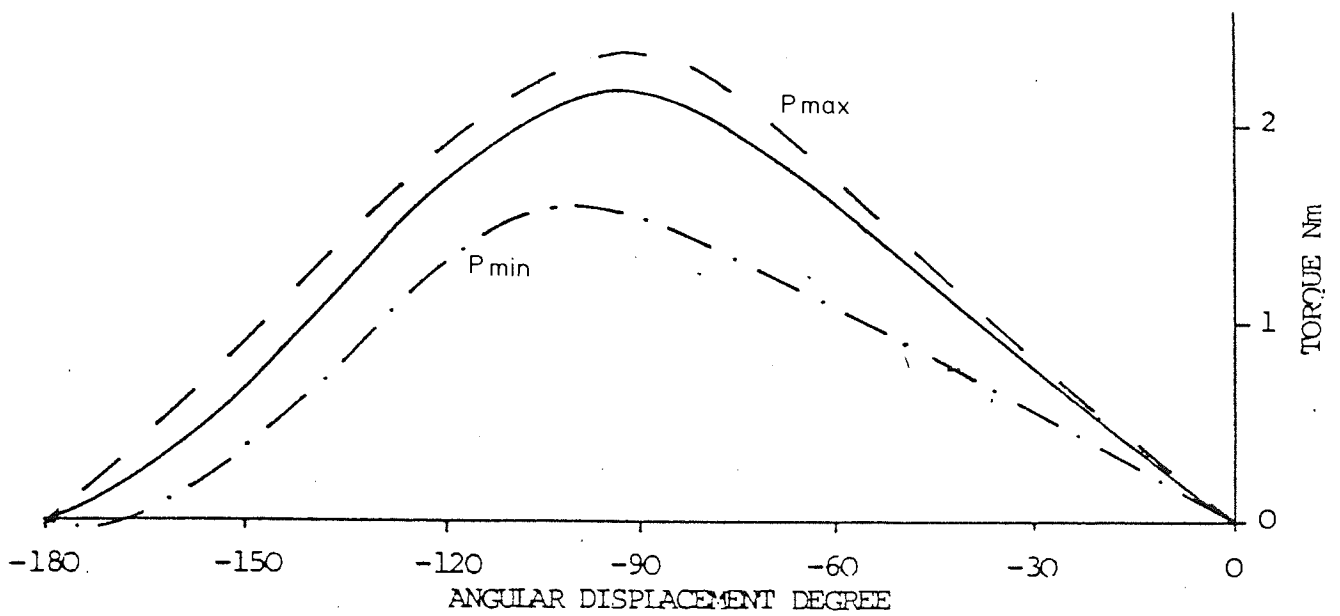


FIGURE 3.36 STATIC TORQUE CHARACTERISTIC PREDICTION. 2 PHASE 3A USING EXTREME VALUES OF ROTOR PERMEANCE

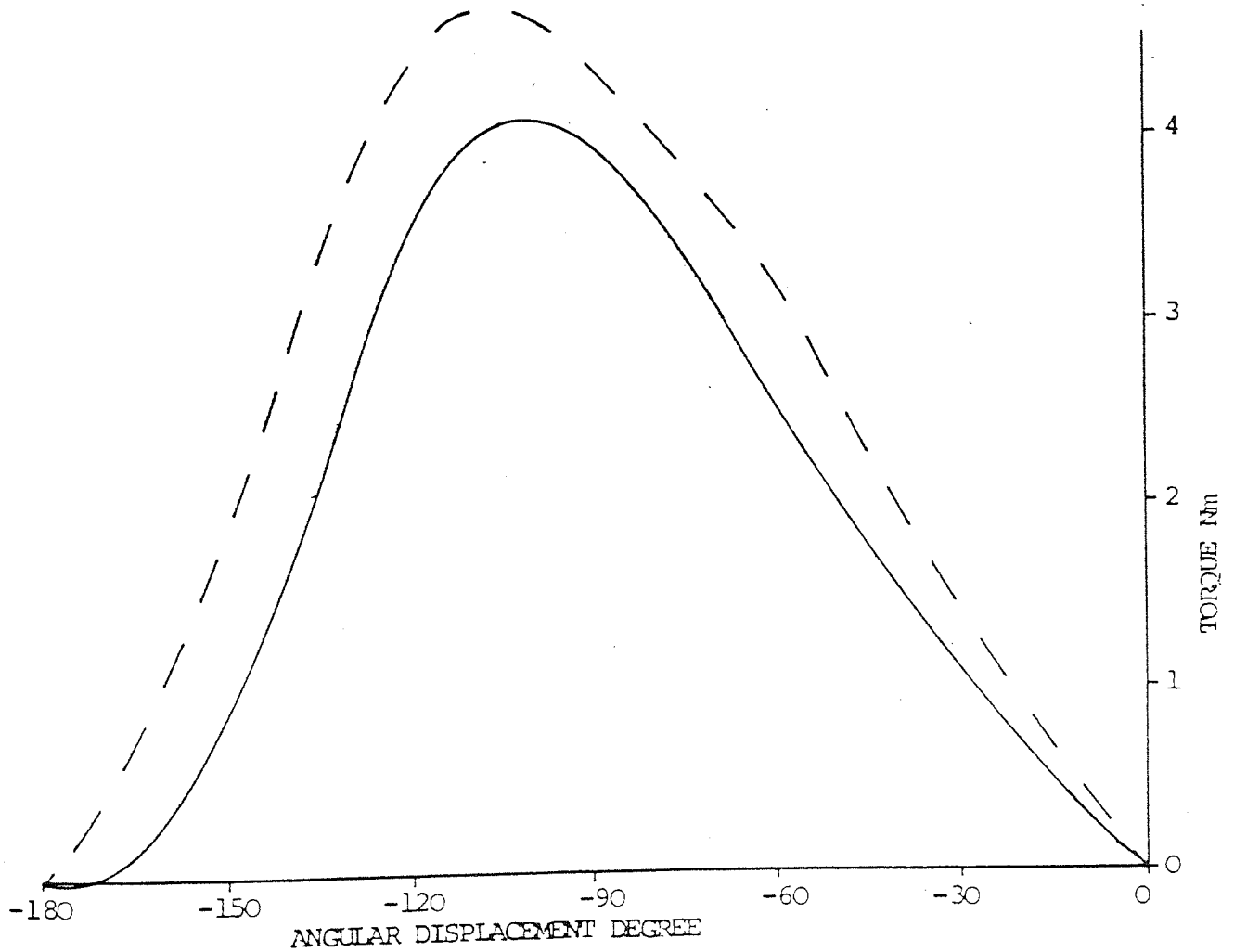


FIGURE 3.37 STATIC TORQUE CHARACTERISTIC PREDICTION. 2 PHASE 7A USING EXTREME VALUES OF ROTOR PERMEANCE

3.3 shows the values used for these extreme estimates.

	LOW	MEAN	HIGH
LENGTH METRE	7×10^{-3}	8×10^{-3}	9×10^{-3}
AREA SQ. METRE	3.2×10^{-4}	5.0×10^{-4}	6.8×10^{-4}

TABLE 3.3 ROTOR FLUX PATH DIMENSIONS

For the estimation of extreme LOW permeance values the active motor path was taken to be the longest path with smallest area, thus producing the worst possible error. For the high estimation the two other extreme values were used to produce the highest possible permeance.

3.5 DISCUSSION

3.5.1 SIMPLIFICATIONS OF THE MODEL

The theory developed in this chapter describes a complex equivalent magnetic circuit of the stepper motor. The complexity of the model must be justified. Possible simplifications to the model have been inspected and the capabilities of the resulting systems assessed.

One simplification which may be introduced is to lump all the non-linearities of the iron components together into one representative parameter. This single parameter may take one of several forms.

1. An iron permeance component for each limb
2. A modifier for permeance of the air gap
3. A modifier for torque.

If the total nonlinearity is to be represented by one permeance value per limb then the resultant equivalent magnetic circuit is as shown in Figure 3.38 and the resulting equation for torque:-

$$\text{TORQUE} = \frac{Nr}{2} \sum_{i=1}^4 \left\{ \frac{[F_i - F_o]}{P_{ai} + P_i} \right\}^2 \frac{dP_i}{d\theta}$$

$$\text{where } F_o = \frac{\sum_{i=1}^4 \left[\frac{P_i F_i}{P_i + P_{ai}} \right] + \frac{P_m F_m}{P_m + P_{a5}}}{\sum_{i=1}^4 \left[\frac{P_i}{P_i + P_{ai}} \right] + \frac{P_m}{P_m + P_{a5}}}$$

P_a is a value of permeance to represent nonlinear effects. Other symbols are as defined for the 8 limb model.

The parameter P_a is a variable which is dependent upon the excitation current in the windings. A series of values for this permeance has been found which, when substituted in the equations result in accurate values of torque. However, the values of P_a were found by solving the torque equations for P_a for known torques and currents. To attempt to calculate true values for P_a from the machine geometry would be very complex as such calculations involve the

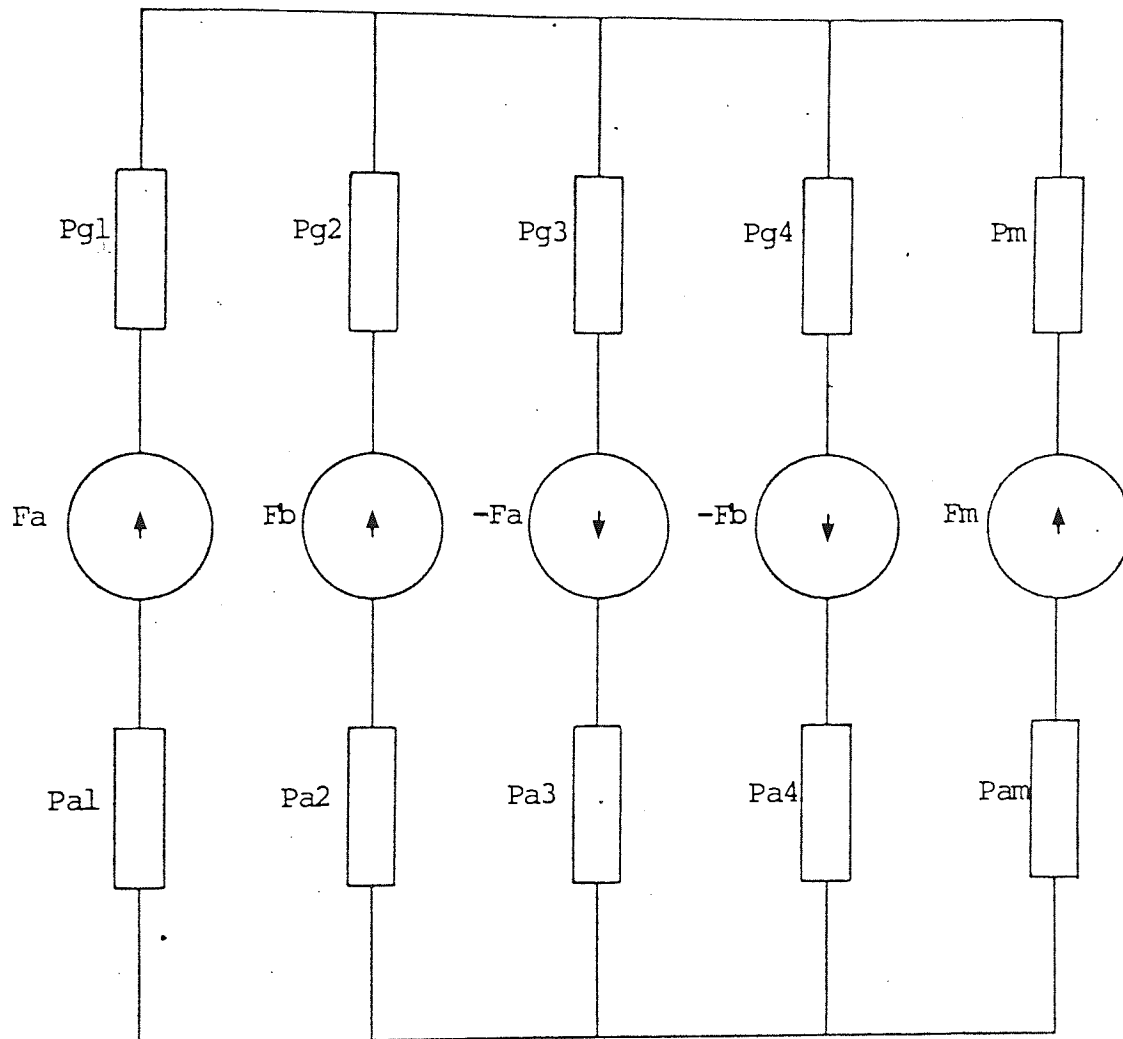


FIGURE 3.38 SIMPLIFIED EQUIVALENT MAGNETIC CIRCUIT USING P_a TO REPRESENT ALL NONLINEAR PERMEANCES

combination of two completely different flux paths, one in the rotor and one in the stator. Not only are the flux paths of incompatible geometry but are also made of different types of iron. Any realistic calculation of P_a would totally negate the simplification which was intended by its use..

A modifying value for permeance of the air gap is a simplification which must be considered, because such a method has two significant advantages. Firstly, the equivalent magnetic circuit becomes perfectly symmetrical and so can be reduced to a four limb model. Secondly, because there are no permeances which are dependent on flux the iterative loops are no longer required in a programme to solve the equations of the resulting model.

This model differs very little from the one proposed by Justice⁽²⁴⁾. In fact Justice does use variations of gap permeance coefficients to produce more accurate torque characteristics. However the values which he used were obtained by the analysis of the measured static torque characteristics.

An attempt to produce modified values for the permeance coefficients directly from the machine geometry becomes complex because estimates must be made of how the permeance in the gap varies as the flux increases. It can be seen that fringing effects and saturation of the iron teeth will tend to decrease the permeance of the air gap. These conditions can best be approximated by calculating the permeance coefficients for gap geometries of varying profiles of teeth. Figure 3.39 shows how the tooth profile was approximated to represent the air gap at conditions of high magnetic flux, and table 3.4 shows the resulting permeance coefficients in terms of C_n and P_n .

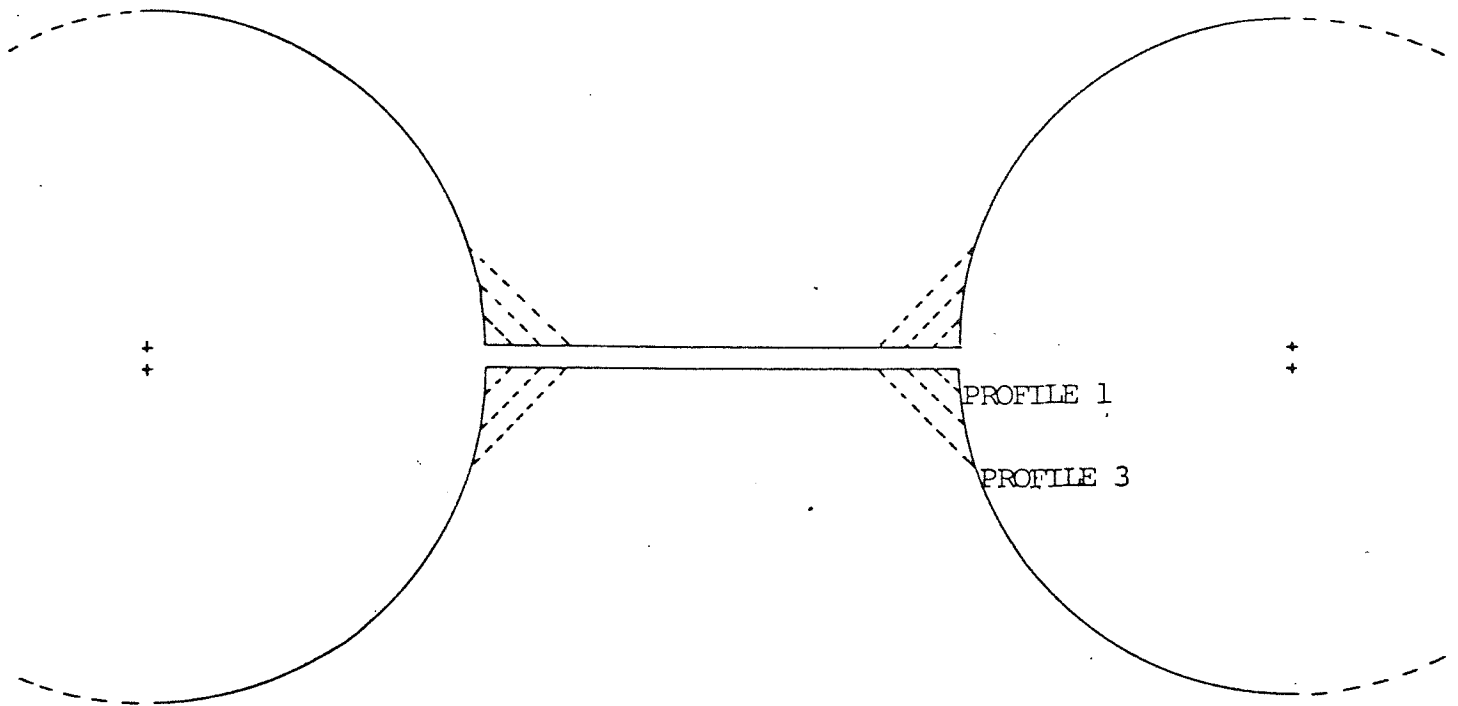


FIGURE 3.39 APPROXIMATION OF MAGNETIC SATURATION BY VARYING TOOTH PROFILE

	PROFILE 1	PROFILE 2	PROFILE 3
C_0	11.635	10.39	9.125
C_1	5.783	5.311	4.646
C_2	0.3087	0.5785	0.8624
C_3	0.248	0.07476	0.02987
C_4	0.1404	0.1601	0.07995
	μ_{wb}/At	μ_{wb}/At	μ_{wb}/At
P_0	2.34	2.09	1.83
P_1	1.09	1.00	0.877
P_2	0.478	0.896	0.133
P_3	0.0261	0.0787	0.0315
P_4	0.0706	0.0805	0.0402

TABLE 3.4 PERMEANCE COEFFICIENTS FOR SATURATED TOOTH PROFILES

Results obtained for torque using these modified tooth profiles are given in Figures 3.40 and 3.41 and the results show that the saturating type profiles indicate a small increase in torque at small angles. However for the 7 Amp case the peak value of torque reduces slightly compared with that obtained using a model which ignores magnetic saturation (Fig. 3.4). Modifying the pole profile sufficiently to obtain a good value for peak torque would result in the shape of the characteristic being unacceptable.

Finally, the method of simplification which applies a modifier to the torque equation returns to the method described by Chai⁽²⁶⁾. This system will produce very accurate results providing that the correct modifier is chosen. This is due to the fact that the shape of the characteristic is determined by the harmonics introduced by the permeance of the air gap. The modifying value serves only to scale the curve to produce the correct values of torque.

Derivation of the modifier is, however, a matter of using known values of torque for a particular design of motor. Using the model with this type of simplification, it is not possible to predict the torque during the design of a motor.

3.5.2 EXTENSIONS TO THE USE OF THE MODEL

Although the model of the step motor was developed to accurately predict the static torque characteristic, it is

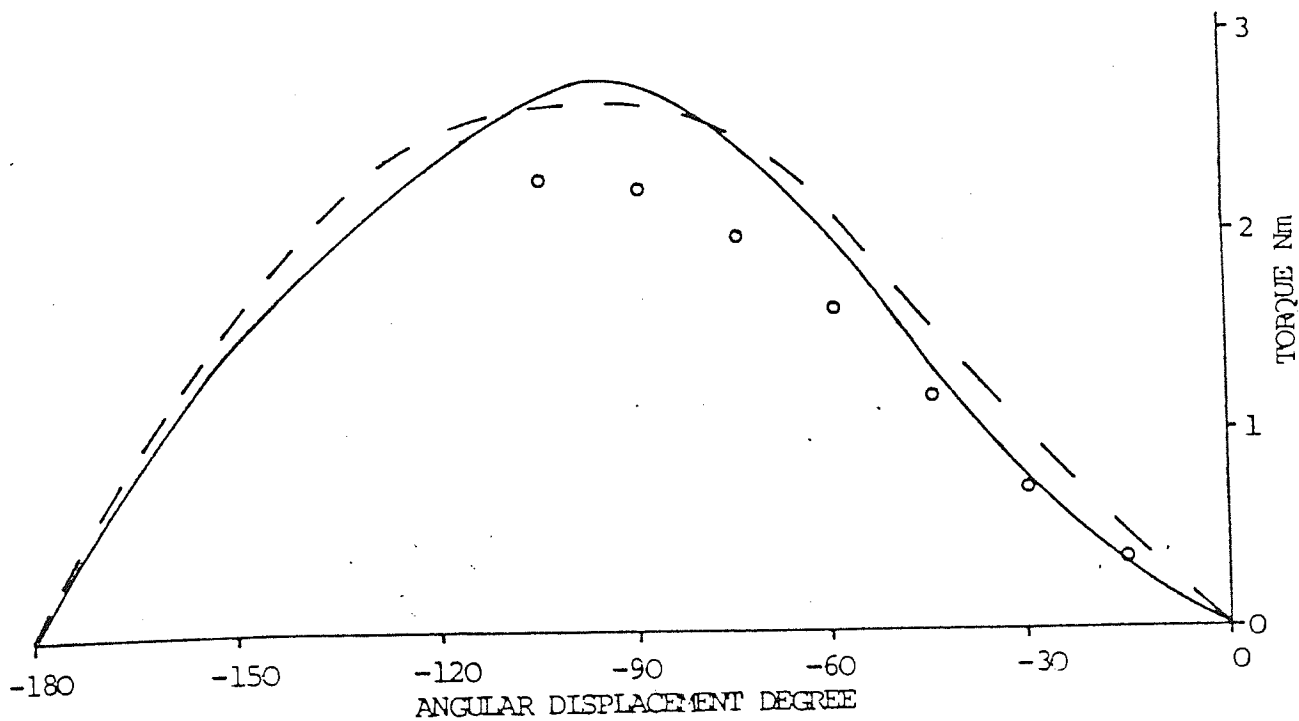


FIGURE 3.40 STATIC TORQUE CHARACTERISTIC PREDICTION. 2 PHASE 3 AMP
USING TOOTH PROFILES 1 AND 3

o REPRESENTS MEASURED VALUES

— PROFILE 1
- - PROFILE 3

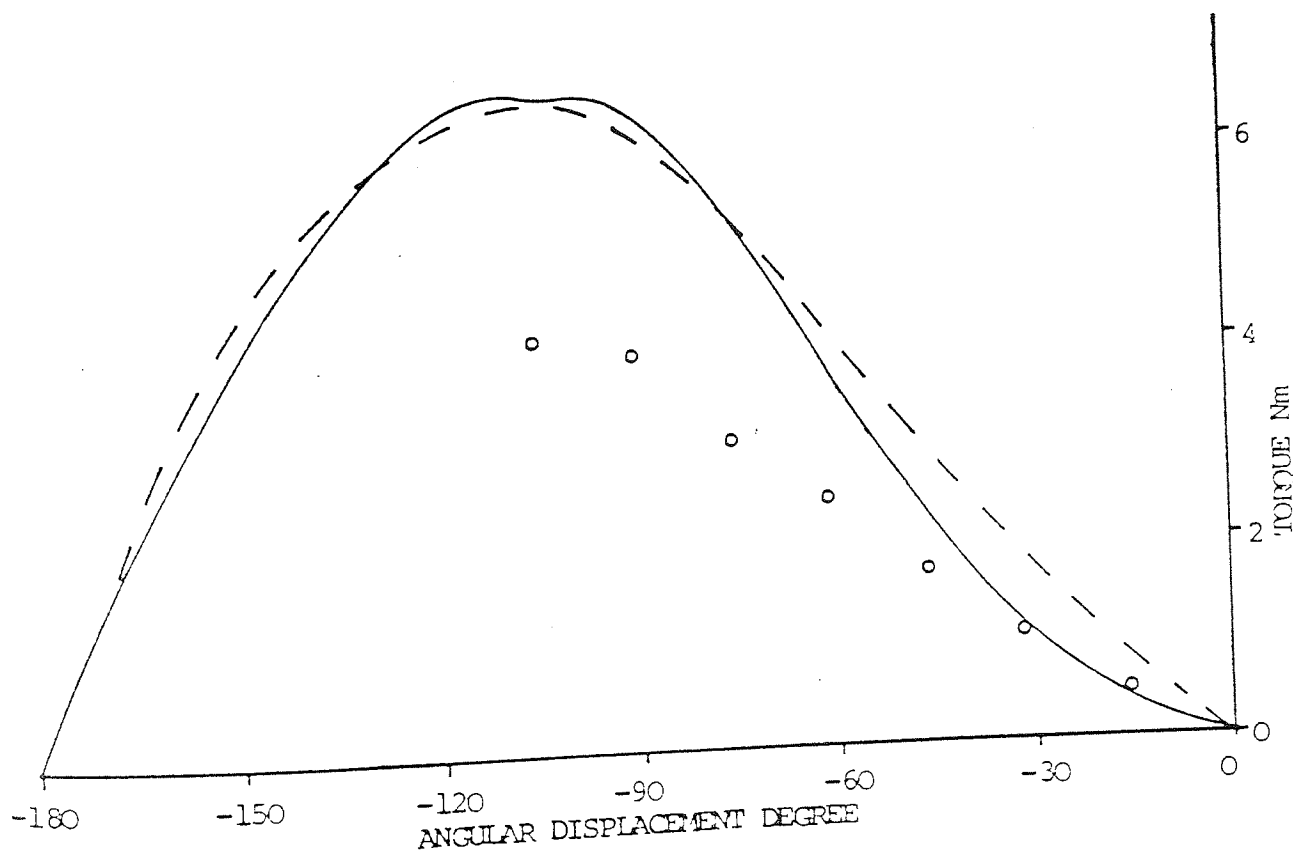


FIGURE 3.41 STATIC TORQUE CHARACTERISTIC PREDICTION. 2 PHASE 7 AMP
USING TOOTH PROFILES 1 AND 3

also useful for a full investigation of the magnetic circuit of the motor. The computer programme used to calculate the torque also calculates the permeance of each iron component and the fluxes within them, hence values of the magnetic fluxes within the motor can easily be obtained from the programme. One useful exploitation of this data is to ascertain which portions of the iron are most severely saturated. A further use is to observe how the flux varies within the limbs over one electrical cycle of the machine. Such information is shown in Figure 3.42 which shows that in this particular case of 6 Ampere, saturation tends to occur only in the poles where the permanent magnet flux adds to the field winding flux. There is quite a significant difference in the other limbs, in which these fluxes oppose each other.

The computer may be programmed to output many different parameters for any angle and current combination. Also dimensions and characteristics of the machine's component parts may be easily changed within the programme. Therefore, the programme will be of assistance in future research as an aid to the magnetic circuit design of step motors.

It has already been shown how different tooth geometries may be substituted in the computer programme to approximate magnetic saturation. This may be extended so that different designed profiles of pole pieces may be investigated, without the need for expensive fabrication of a machine.

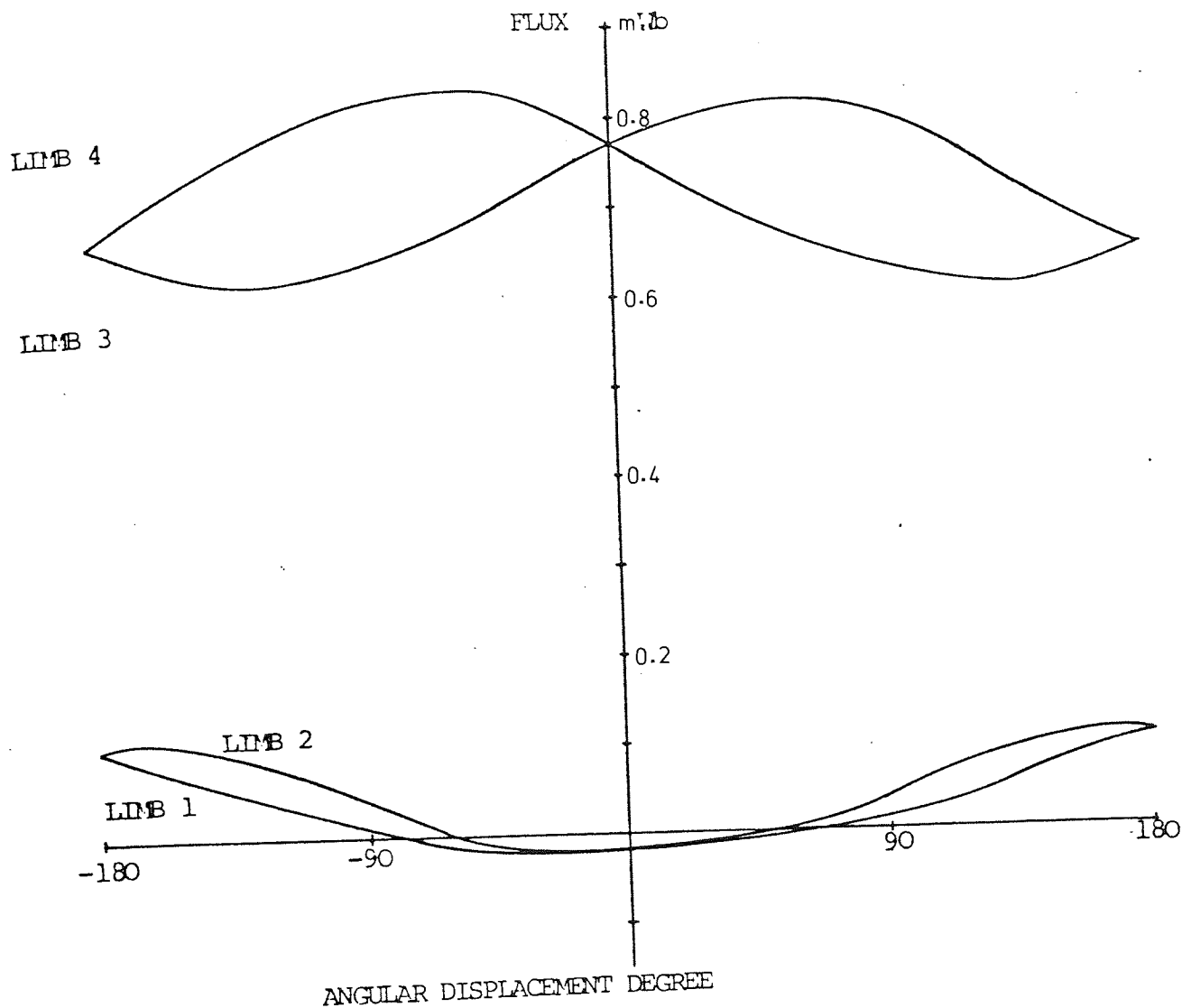


FIGURE 3.42 VARIATION OF FLUX OVER ONE CYCLE 2 PHASE 6 AMP.

As an example, the two popular strategies of stator pole design have been investigated. The first method of design is to make the pitch of the stator teeth equal to $2\pi/N_s$, this results in the pole profile as shown in Figure 3.12. The alternative is to make the pitch of the stator teeth equal to the pitch of the rotor teeth. This results in the point of maximum permeance for all the teeth of one pole occurring at the same instant. The relationship between tooth and pole permeance coefficients now becomes

$$P_n = 4\mu_o t C_n \text{ tooth}$$

Symbols as defined in equation (3.3), and the table of

permeance co-efficients becomes

Coefficient	Permeance Using Moment Method μ_{wb}/At
P_0	2.55
P_1	1.22
P_2	0.0223
P_3	0.0820
P_4	0.00456

TABLE 3.5 PERMEANCE COEFFICIENTS FOR ALTERNATIVE STATOR DESIGN

Substituting these values of permeance coefficients in the computer programme results in a torque characteristic as shown in Figures 3.43 and 3.44 for the 3 Amp and 7 Amp cases respectively. Comparing these figures with those for the other design strategy figures, 3.28 and 3.30, shows an overall increase in peak torque of up to 20 per cent.

It is generally accepted that the 'Moment Method' of permeance calculation produces more accurate results than either the Straight Line Arc or Conformal Transformation Methods. The loss of accuracy of torque prediction which is incurred by using the simple methods, can be assessed by substituting the appropriate permeance coefficients in the computer programme. Figures 3.45 and 3.46 show the results obtained for torque by using the coefficients

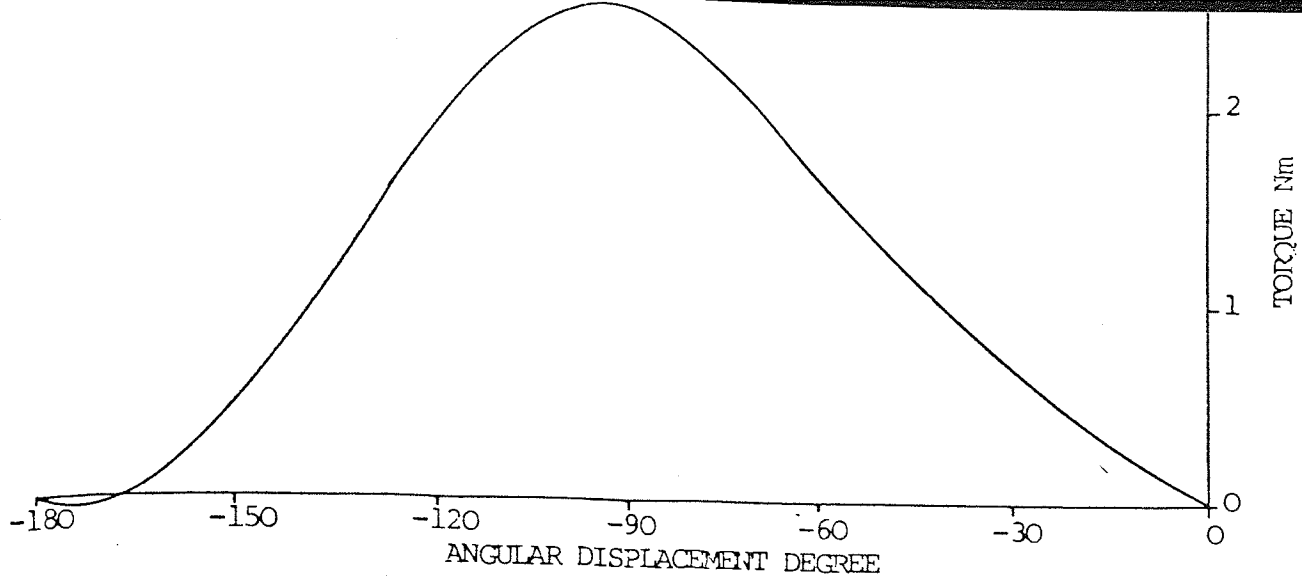


FIGURE 3.43 STATIC TORQUE CHARACTERISTIC PREDICTION. 2 PHASE 3A FOR ALTERNATIVE POLE DESIGN

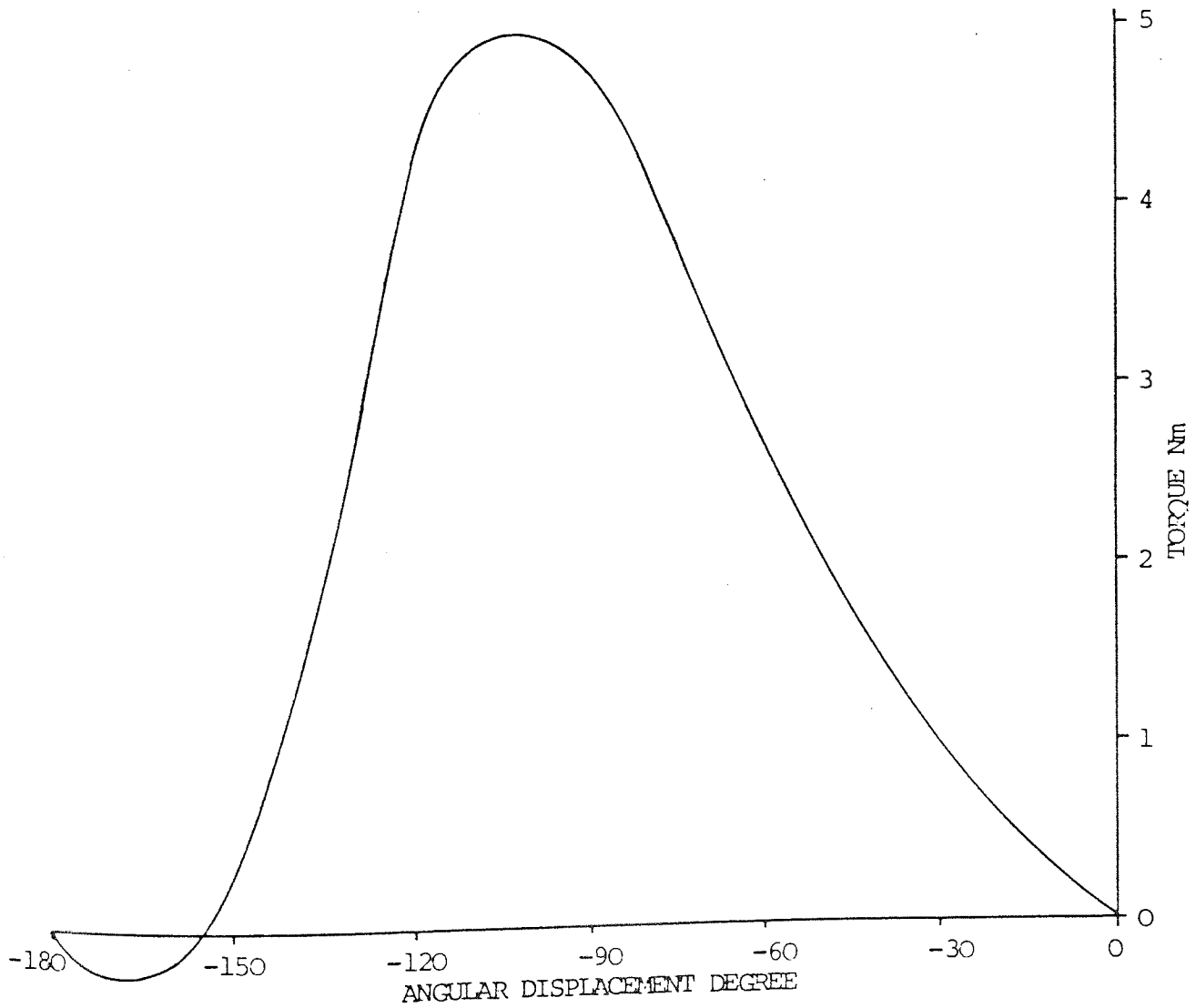


FIGURE 3.44 STATIC TORQUE CHARACTERISTIC PREDICTION. 2 PHASE 7A FOR ALTERNATIVE POLE DESIGN

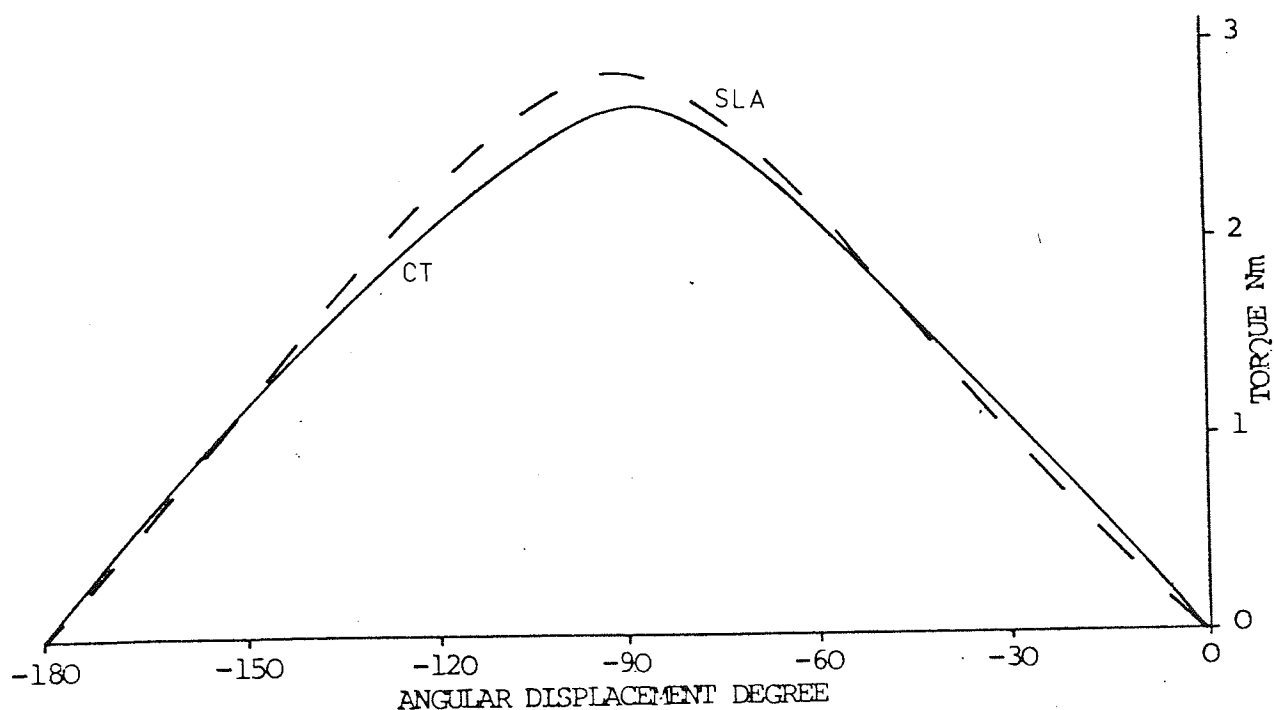


FIGURE 3.45 STATIC TORQUE CHARACTERISTIC PREDICTION. 2 PHASE 3A AIR GAP PERMEANCES CALCULATED BY STRAIGHT LINE ARC METHOD AND CONFORMAL TRANSFORMATION METHOD.

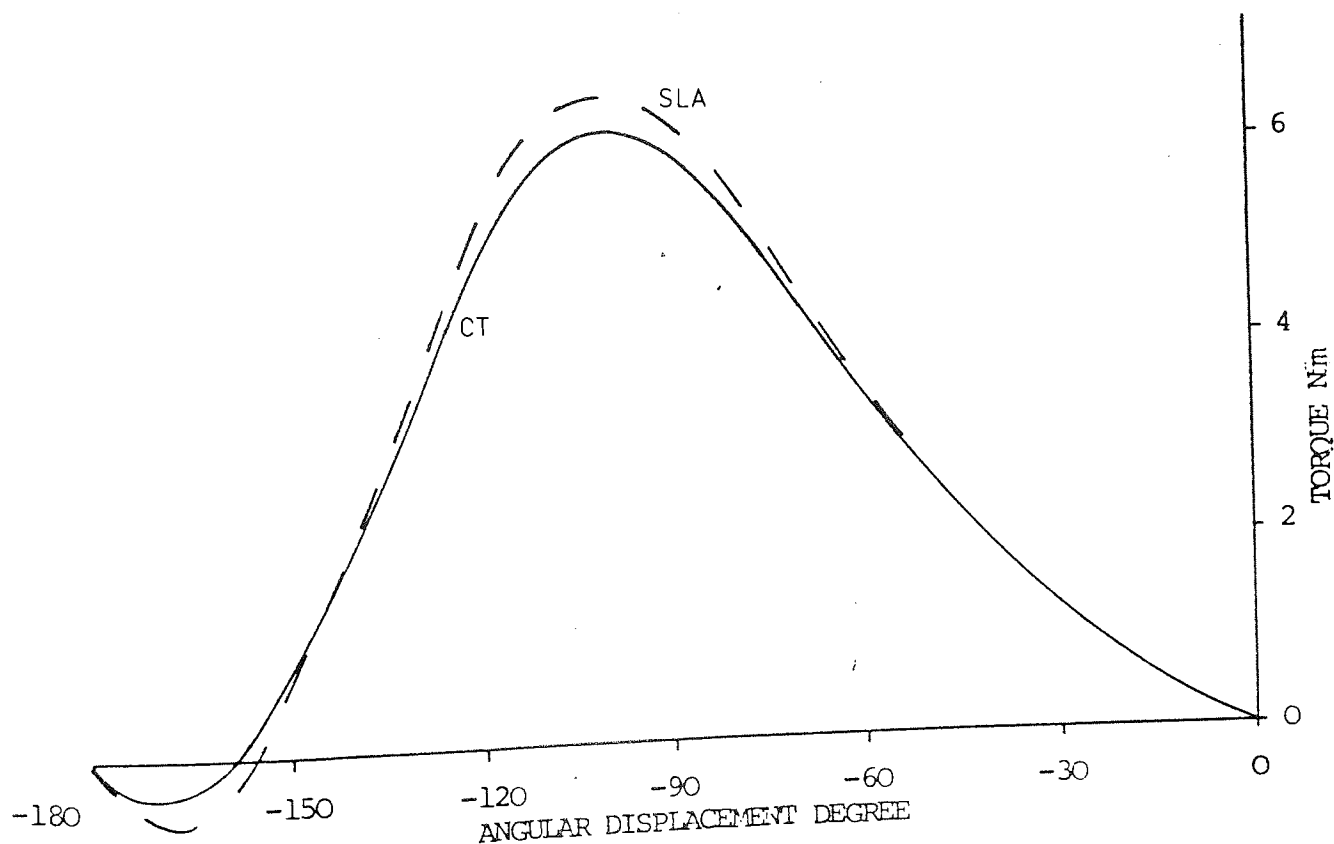


FIGURE 3.46 STATIC TORQUE CHARACTERISTIC PREDICTION. 2 PHASE 7A AIR GAP PERMEANCES CALCULATED BY STRAIGHT LINE ARC METHOD AND CONFORMAL TRANSFORMATION METHOD.

detailed in Table 3.2. These results show that an accuracy of about 10 per cent may be maintained when the simpler forms of permeance calculations are used.

Other uses of the model include investigating the variable reluctance type motor by equating P_m to zero, and predicting the cogging torque of the machine by entering values of zero phase current into the programme. Both these cases are discussed by Chai⁽²⁷⁾ but as they do not involve magnetic saturation no further explanation is given here.

3.5.3 THE DYNAMIC TORQUE CHARACTERISTIC

The static torque characteristic indicates the torque developed by the motor for constant excitation with the motor held stationary. During each step of the motor both the excitation current and the rotor position are varying simultaneously. With the aid of the static torque computer programme a characteristic has been produced which combines these varying parameters for a single step of the motor. Figure 3.47 shows that when the current is changed from 6A to -6A in one phase, it takes 11 mS to reach the final value. Figure 3.48 shows the single step response of the machine and it can be seen from this that during the first 11 mS the rotor passes its settling position and goes into the overshoot region. The static torque programme has been applied to these changing conditions of current at 1 mS intervals and Table 3.6 shows the values of current used to

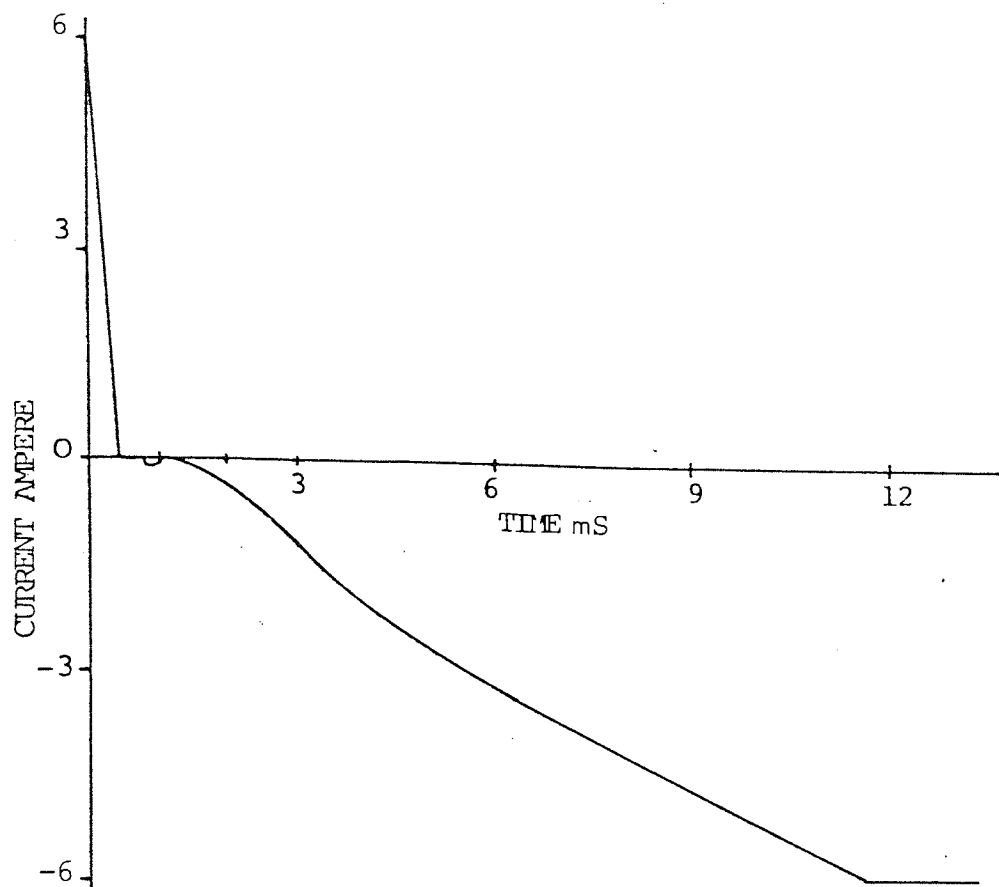


FIGURE 3.47 TWO PHASE, SINGLE STEP TIME CURRENT CURVE

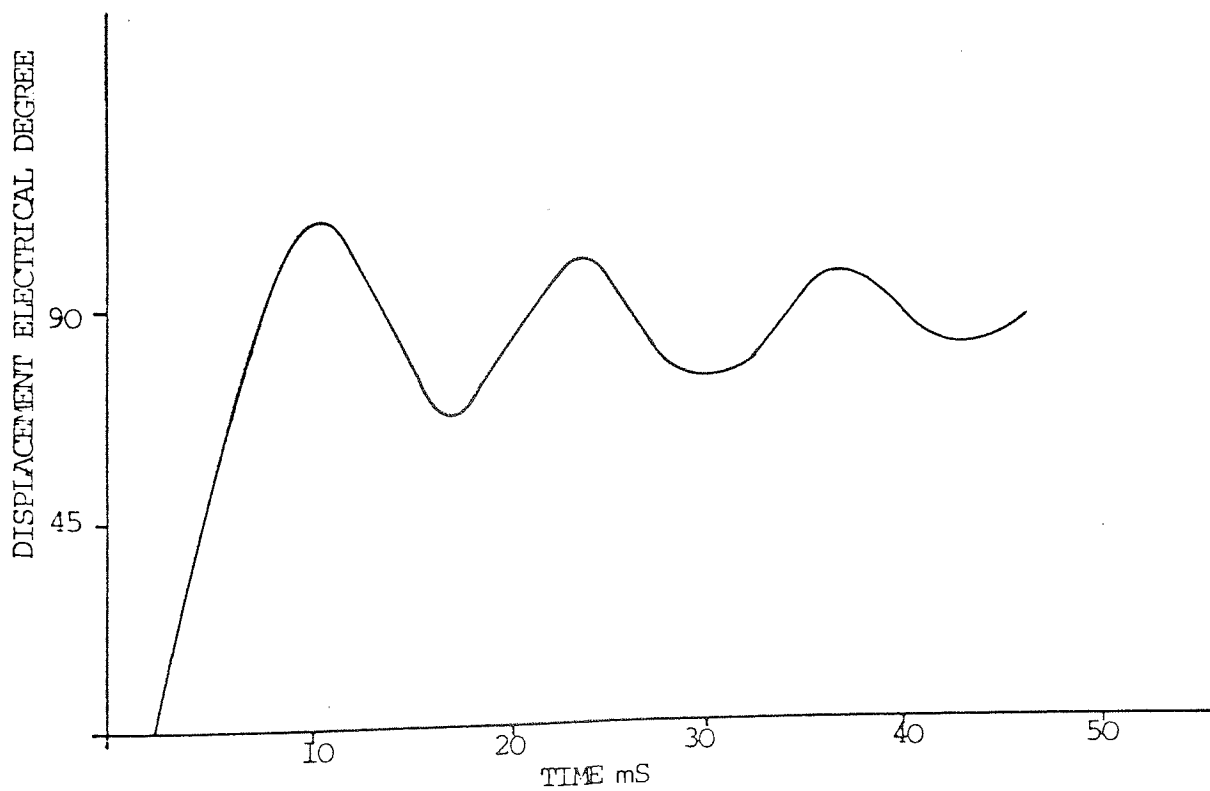


FIGURE 3.48 TWO PHASE, 6A. SINGLE STEP RESPONSE

TIME mS	CURRENT 1 A	CURRENT 2 A	POSITION DEGREE
0	6	6	0
1	6	0	0
2	6	-0.396	0
3	6	-1.18	13
4	6	-1.98	30
5	6	-2.71	44
6	6	-3.22	58
7	6	-3.62	88
8	6	-4.07	95
9	6	-4.53	100
10	6	-5.09	
11	6	-5.55	
12	6	-6.0	100

TABLE 3.6 TWO PHASE SINGLE STEP RESPONSE TIME-CURRENT
AND POSITION

calculate each static torque characteristic.

Figure 3.49 shows the results obtained over the range -10 to 130 degrees.

From the dynamic response (Figure 3.48) the position of the motor at each time interval may be found, these values are also shown in Table 3.6. Applying each position to its respective torque-angle curve on Figure 3.49 results in a new curve being obtained, this curve shows how the torque varies with angle during the single step of the machine.

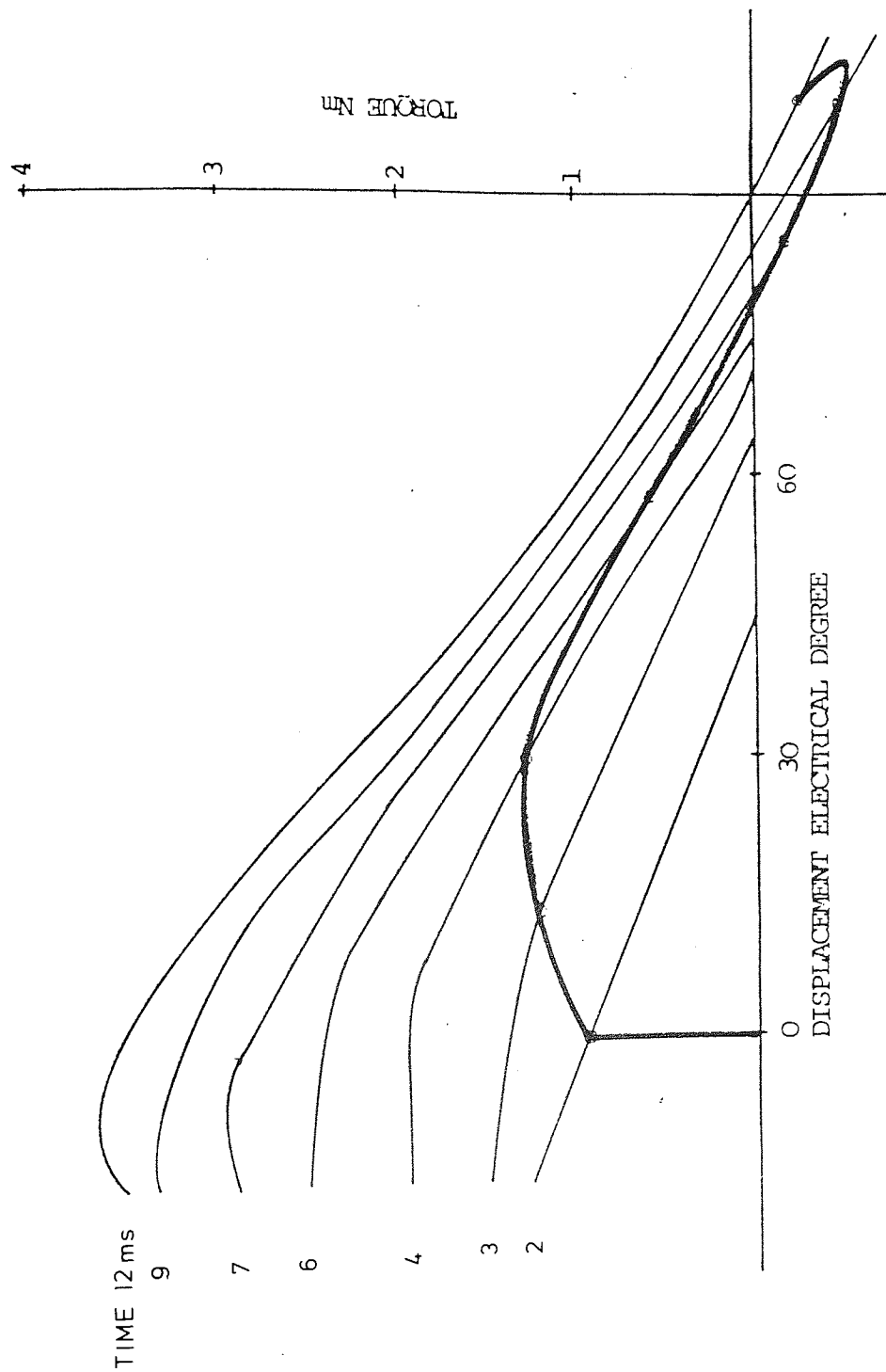


FIGURE 3.49 THE DYNAMIC TORQUE CHARACTERISTIC

This curve of torque generated against rotor angle enables further estimation of the effects of current forcing to be made. If the rate of change of current is not increased but the current is forced beyond the required value before settling to a constant current then little advantage is to be gained. This is because the increase in torque will only be effective after the rotor has passed the required position. A more advantageous system of current forcing would be to increase the rate of change of current. This would result in an increase of torque during the early stages of rotor movement.

3.5.4 SINGLE STEP RESPONSE

The accurate calculation of the single step response of a stepper motor requires that many complex variables be brought together into one function. One method of simplifying this task is to use the static torque characteristic which, if accurately known, reduces many of the independent variables into one function. As already shown the static torque curve involves many of the design variables of the machine and also the current at which the machine is excited. Many of the recent proposals for step response prediction have proved to be complex functions, even when the torque characteristic is known. Although these predictions result in accurate data the requirement of the system design engineer is for a simple method of calculating system response so that natural frequencies and step overshoot may be reasonably estimated.

Figure 3.50 shows the single phase, single step response for the stepper motor. From this figure it can be seen that the motor gives very little movement over the first 15 ms. This period of time is ample for the excitation current to reach its full value. The motor can therefore be approximated to a control system with a step input of torque. The system includes the inertia of the rotor and the friction associated with its movement. For simplicity the torque characteristic can be approximated to a linear relationship between torque and angle. The motor may now be represented by the system shown in Figure 3.51 and the equation of position found in terms of its Laplace Transformation with respect to time.

$$\theta(s) = \frac{T_m}{(Js^2 + k_1s + k_2)s}$$

where s Laplace operator

T_m Maximum Torque

J Inertia of Rotor

k_1 Frictional Constant

k_2 Constant of Proportionality for Torque/Angle

Such a system is simple to solve in terms of time providing the appropriate constants are known. The following values were measured from the machine.

Inertia of Moving parts	$J = 0.000448 \text{ kg m}^2$
Friction	$k_1 = 0.028 \text{ Nms}$

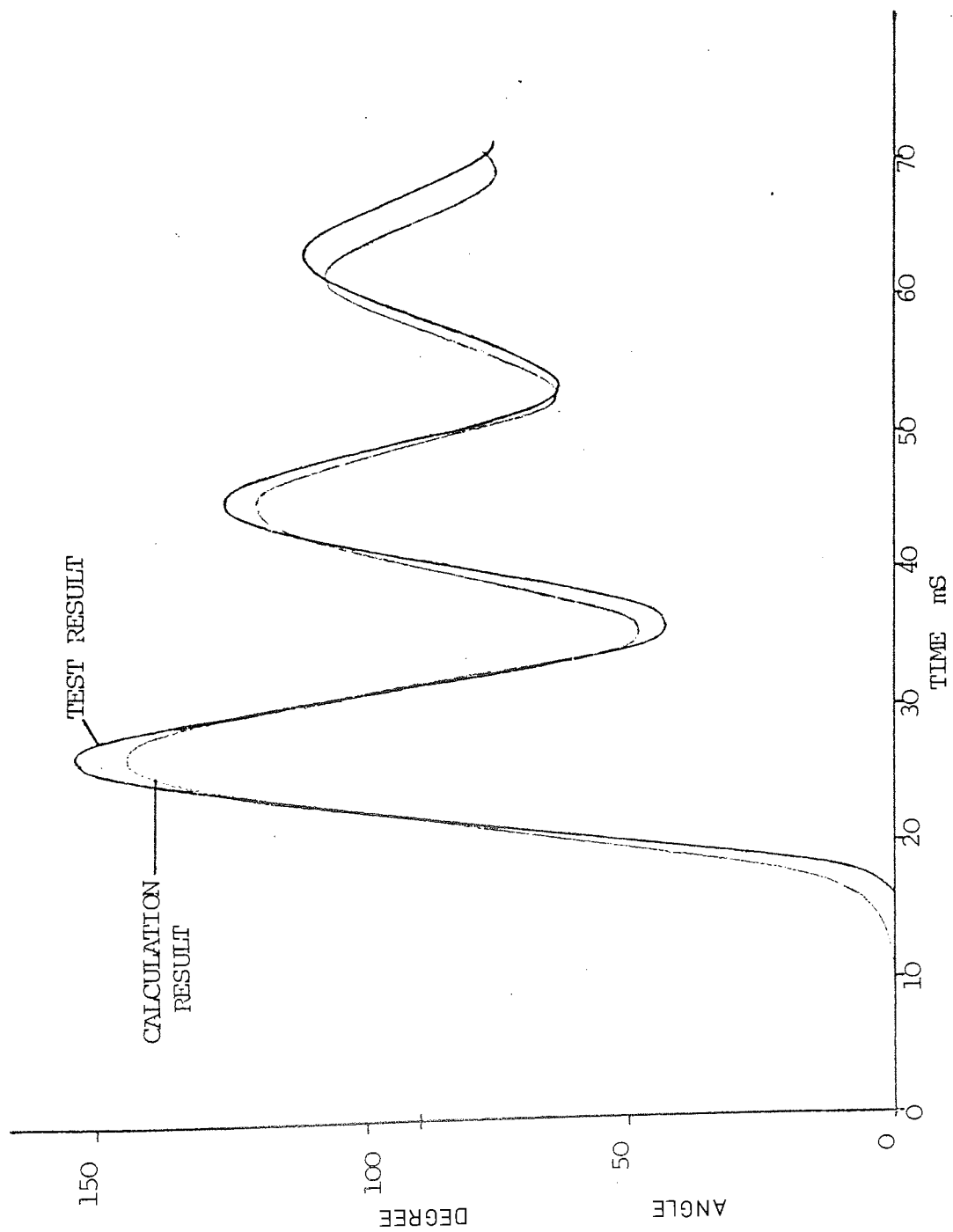


FIGURE 3.50 SINGLE PHASE, 6A. SINGLE STEP RESPONSE

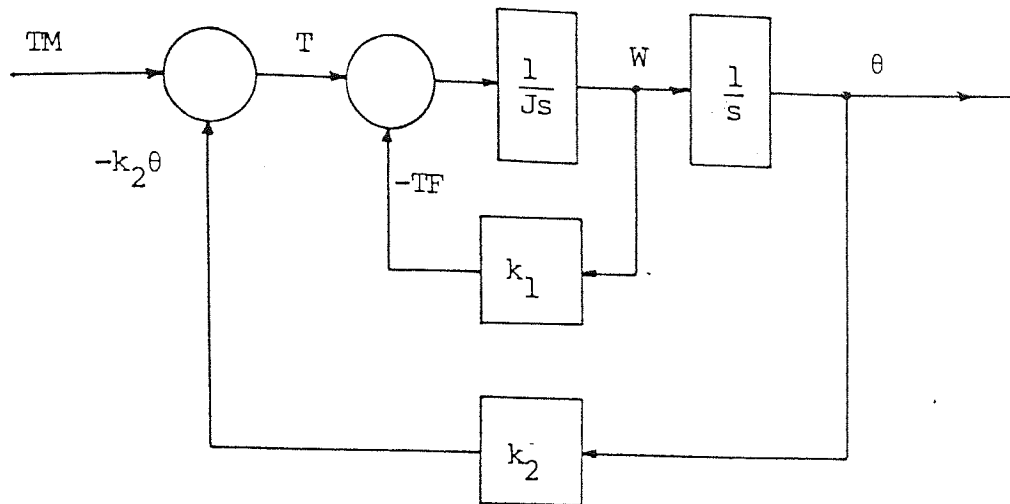


FIGURE 3.51 CONTROL SYSTEM REPRESENTATION OF THE STEPPER MOTOR

The torque-angle relationship was approximated from Figure 3.34 with the following results

Maximum Torque

$$T_m = 2 \text{ Nm}$$

Constant of Proportionality $k_2 = \frac{2}{\pi} \times 84 \text{ Nm/mech rad.}$

The resulting equation for displacement with respect to time is:-

$$\theta = \frac{\pi}{84} [1 - e^{-31.25t} [\cos 344t + 0.09 \sin 344t]]$$

The resulting response is shown in Figure 3.50 to compare with the response recorded from the machine.

The accuracy of the results obtained are sufficient to give an insight into the behaviour of the system. The main advantage of this method is its simplicity. The simple solution is applicable only if the current rise time is short compared to the step response. It can be seen from the dynamic torque characteristic for the two phase response that the torque producing mechanism becomes too complex to be represented by this simple model when the position response is fast.

The method of calculating the step response discussed here may be extended to include more accurate representations of the static torque characteristic, and it is hoped that future work may include extending the idea of representing a stepper motor as a control system. The use of a more complex control system may improve the resulting data while keeping the system simple enough to allow rapid calculation of the main parameters of the system by established control system methods.

3.6 CONCLUSION

It has been shown that the static torque characteristic for the stepper motor is a parameter which contains much information about the machine. To be able to predict accurately the torque developed by a motor under certain conditions would be of great use in both the prediction of the dynamic behaviour of the motor and also in the early stages of motor design. The present methods of static

torque prediction have been reviewed and it was concluded that the shortcomings of most methods are due to the fact that they require tests to be carried out on the machine and are therefore of little use to the machine designers.

A new method has been proposed which is based on the equivalent magnetic circuit of the motor and this equivalent circuit was analysed in terms of its permeances to produce a solution to the torque equations of the motor. The numerical solutions to the torque equations have been implemented on a digital computer and the result verified against the known performance. The model has been examined and its main weaknesses thoroughly investigated to establish reliability.

Methods of simplifying the model have been investigated and their advantages and disadvantages discussed, showing that such simplifications do not represent the stepper motor adequately.

A brief assessment was made of other data which could easily be obtained from the computer programme, showing how a greater understanding of the magnetic actions and reactions may be gained by fully exploiting such a programme.

Finally, examples of the uses of the static torque programme were given which show how the data obtained from it may be applied to simplify further calculations into the behaviour of stepping motors.

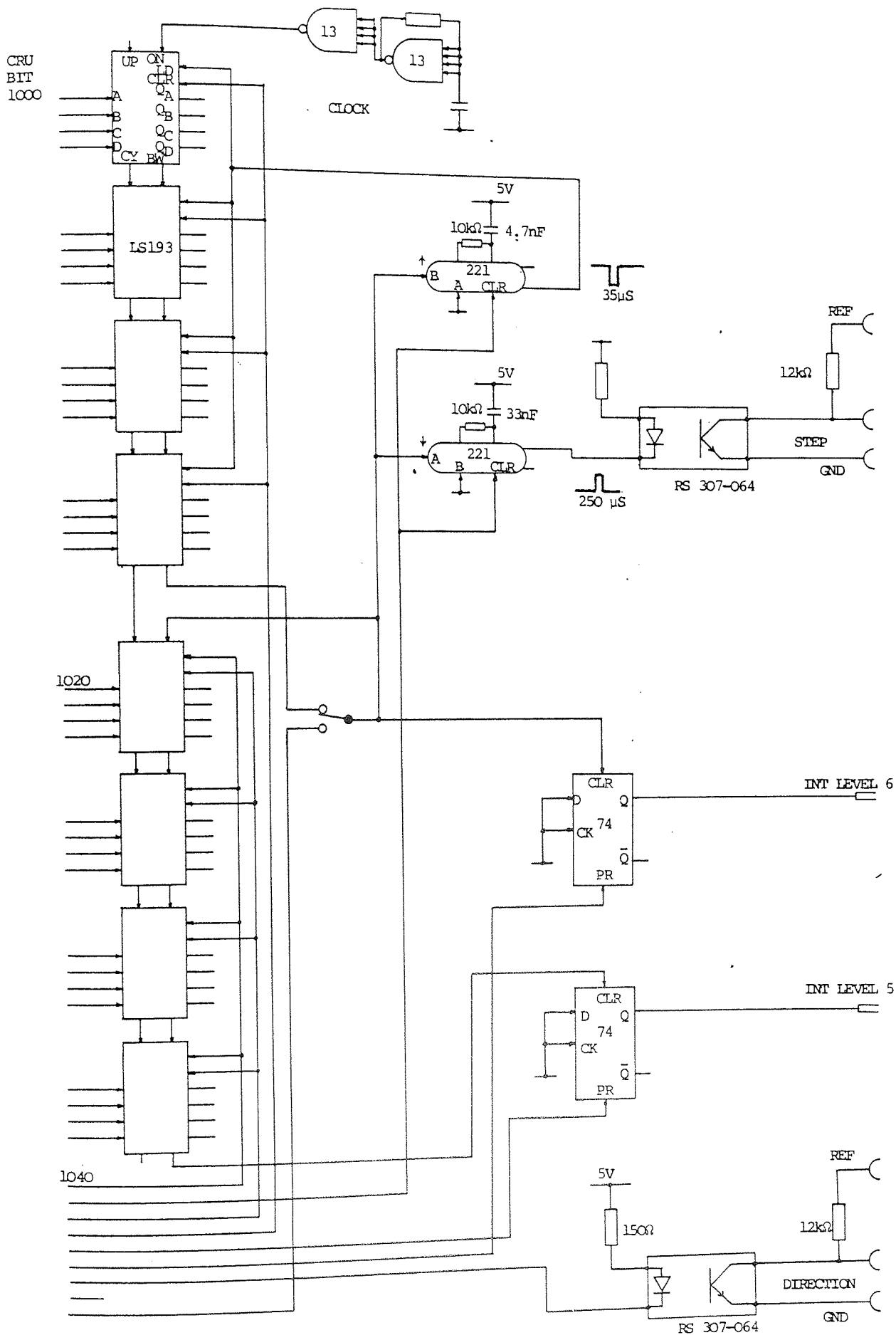
APPENDIX

CIRCUIT DIAGRAM OF MICROPROCESSOR
TO STEPPER MOTOR INTERFACE

APPENDIX 1

CIRCUIT DIAGRAM OF STEPPER MOTOR INTERFACE

The circuit diagram included in this appendix does not include the standard CRU interface circuit.



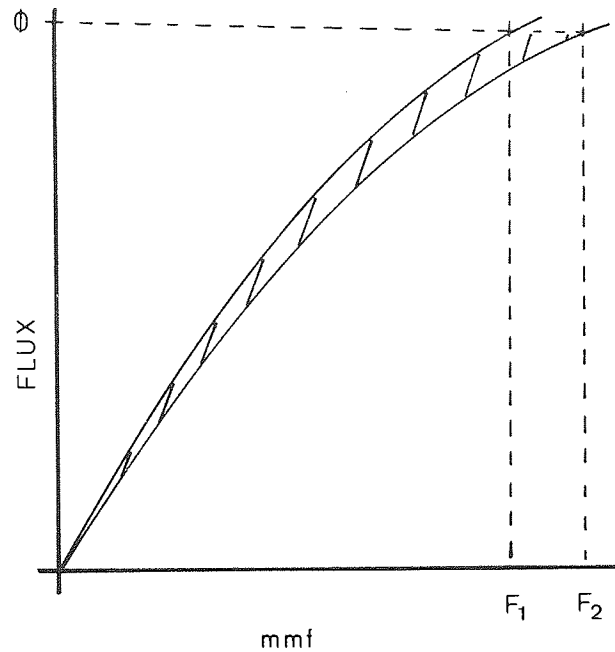


FIGURE A.2.1 ILLUSTRATING VIRTUAL WORK

The torque acting upon a rotor of a variable reluctance type machine^p may be found from the principle of virtual work (Ref. A1). It can be shown that the mechanical work achieved for an incremental rotor movement $d\theta$ is equal to the change in the magnetic field energy with constant flux:-

$$\text{i.e. } W_{\text{mech}} = T d\theta = -dW_{\text{fld}} \quad \text{with } \phi \text{ constant}$$

where W_{mech} Mechanical work

T Torque

$d\theta$ increment of angular displacement

dW_{fld} increment of field energy

ϕ magnetic flux

The change of field energy dW_{fld} is represented by the shaded area of Figure A2.1, and it can be shown that for the linear case this area is

$$\begin{aligned} dW_{fld} &= \frac{1}{2} \phi (F_2 - F_1) \\ &= \frac{1}{2} \phi^2 dR \end{aligned}$$

where dR is increment of magnetic reluctance

In order to justify the application of these linear equations to the case of the saturated stepper motor the assumptions are made that the distribution of flux and leakage does not change during the increment of movement $d\theta$. Also it is assumed that the volume of magnetic material in the field remains constant.

If these two assumptions are met then the only changes in magnetic conditions caused by the displacement $d\theta$ occur in the immediate vicinity of the air gap and the problem reduces to one involving changes in only the linear portion of the field.

These conditions are well satisfied by the stepper motor under static conditions and hence the linear equations may be used to calculate the static torque. These conditions however are not true for larger movements of the rotor and hence the linear equations would not apply to the dynamic case of torque calculation.

Ref. A1. FITZGERALD, A. E., and KINGSLEY, C.: "Electric Machinery", second edition, Pub. McGraw-Hill, 1961.

LIST OF REFERENCES

1. MORREALE, A., and IRANI, R.: "Stepping Devices, Introduction, Types and Variations", Proceedings of the International Conference on Stepping Motors and Systems, University of Leeds, England, 1974, pp. 1-12.
2. KENT, A. J.: "The Variable Reluctance Step Motor", *ibid.*, 1974, pp. 13-30.
3. NIJDAM, L. M., and KING, D. S.: "Basic Principles of Permanent Magnet Stepper Motors", *ibid.*, 1974, pp. 31-36.
4. KORDIK, K., and SENICA, K.: "Step Motor Selection", *ibid.*, 1974, pp. 37-55.
5. SPRACKLAN, S. G.: "Standardisation of Stepper Motor Terminology, Configuration and Test Data", *ibid.*, 1974, pp. 56-66.
6. BISCOE, G. I., and MILLS, A. S.: "The Rationalisation and Standardisation of Stepping Motors and Their Test Methods", Proceedings of the Incremental Motion Control Systems and Devices Symposium, University of Illinois, U.S.A., 1977, pp. 331-342.
7. HUGHES, A., LAWRENSON, P. J., STEELE, M. E., and STEPHENSON, J. M.: "Prediction of Stepping Motor Performance", Proceedings of the International Conference on Stepping Motors and Systems, University of Leeds, England, 1974, pp. 67-76.

8. BORMAN, M. D.: "Optical Shaft Angle Encoders for the Measurement and Control of Incremental Motion-Practcial Design Considerations", Proceedings of the Incremental Motion Control Systems and Devices Symposium, University of Illinois, U.S.A., 1976, pp. A1-A6.
9. ALFORD, A.: "Design and Analysis of a Modern Step Motor Control System", M.Sc. Thesis, University of Aston in Birmingham, England, October 1976.
10. "TMS 9900 MICROPROCESSOR DATA MANUAL", Published by Texas Instruments Limited, 1975.
11. "TMS 9900 MICROPROCESSOR ASSEMBLY LANGUAGE PROGRAMMER'S GUIDE", Published by Texas Instruments Limited, 1978.
12. LAFRENIERE, B. C.: "Interactive Microprocessor-Controlled Step Motor Acceleration Optimisation", Proceedings of the Incremental Motion Control Systems and Devices Symposium, University of Illinois, U.S.A., 1978, pp. 97-110.
13. KUO, B. C., and SINGH, G.: "Closed-Loop and Speed Control of Step Motors", *ibid.*, 1974, pp. C1-C32.
14. HUGHES, J. L.: "Computer Lab. Workbook", Published by Digital Equipment Corporation, 1969, pp. 115-116.
15. RADULESCU, M. M. and STOIA, D.: "Microprocessor Closed-Loop Stepping Motor Control", Proceedings of the International Conference on Stepping Motors and Systems, University of Leeds, England, 1979, pp. 106-112.

16. BAILEY, S. J.: "Incremental Servos", Control Engineering, 1960, 7, November pp. 123-127 and December pp. 97-102.
17. O'DONOHUE, P. J.: "Transfer Function for a Stepper Motor", *ibid*, 1961, 8, November pp. 103-104.
18. KIEBURTZ, R. B.: "The Step Motor - The Next Advance in Control Systems", IEEE Trans., 1964, AC-9, pp. 98-104.
19. ROBINSON, D. J., and TAFT, C. K.: "A Dynamic Analysis of Magnetic Stepping Motors", *ibid*, 1969, IECI-16, pp. 111-125.
20. SNOWDON, A. E., and MADSEN, E. W.: "Characteristics of a Synchronous Inductor Motor", Trans. AM. Inst. Elec. Eng., 1962, 81, pp. 1-5.
21. PICKUP, I. E. D., and RUSSELL, A. P.: "Nonlinear Model for Predicting Settling Time and Pull-in Rate in Hybrid Stepping Motors", Proc. IEE, Vol. 126, No. 4, April 1979, pp. 307-312.
22. STEPHENSON, J. M., and CORDA, J.: "Computation of Torque and Current in Doubly Salient Reluctance Motors From Nonlinear Magnetisation Data", Proc. IEE, Vol. 126, No. 5, May 1979, pp. 393-396.
23. CHAI, H. D.: "Magnetic Circuit and Formulation of Static Torque for Single Stack Permanent Magnet and Variable Reluctance Step Motors", Proceedings of the Incremental Motion Control Systems and Devices Symposium, University of Illinois, U.S.A., 1973, pp. E1-E18.

24. JUSTICE, M.: "Simulation and Control of a Stepping Motor", Ph.D. Thesis, University of Aston in Birmingham, England, October 1977.
25. HARRIS, M. R., HUGHES, A., and LAWRENSON, P. J.: "Static Torque Production in Saturated Doubly-Salient Machines", Proc. IEE, Vol. 122, No. 10, October 1975, pp. 1121-1127.
26. CHAI, H. D.: "A Simple Model for Representing Saturation Effects in Step Motors", Proceedings of the Incremental Motion Control Systems and Devices Symposium, University of Illinois, U.S.A., 1976, pp. G1-G8.
27. KENJO, T., and ICHIKAWA, M.: "Torque Analysis of Saturated Step Motors in Term of Stieltjes Integral", *ibid.*, 1977, pp. 271-282.
28. CHAI, H. D.: "Permeance Model and Reluctance Force Between Toothed Structures", *ibid.*, 1973, pp. K1-K12.
29. JONES, A. L.: "Permeance Model and Reluctance Force Between Toothed Structures", *ibid.*, 1976, pp. H1-H8.
30. CHAI, H. D.: "Technique for Finding Permeance of Toothed Structures of Arbitrary Geometry", Proceedings of the International Conference on Stepping Motors and Systems, University of Leeds, England, 1976, pp. 31-37.
31. BOURNE, R.: "The Steady-State Performance of the Salient Pole Permanent-Magnet Vernier Stepping Motor", M.Sc. Thesis, University of Aston, 1972.